KTH Industrial Engineering
and Management

District Heating-Driven Membrane Distillation for Water Purification in Industrial Applications

DANIEL MINILU WOLDEMARIAM

Doctoral Thesis, 2017

KTH Royal Institute of Technology

Energy Technology Department

SE-100 44 Stockholm, Sweden

This doctoral research has been carried out in the context of an agreement on joint doctoral research supervision between KTH Royal Institute of Technology, (Stockholm, Sweden), and Politecnico di Torino − PoliTo, (Turin, Italy). The research was partially funded by the European Commission through the SELECT+ (Environomical pathways for sustainable energy services) program, an Erasmus Mundus Joint Doctorate.

Printed by Universitetsservice US-AB Drottning Kristinas väg 53B SE-114 28 Stockholm Sweden

ISBN 978-91-7729-414-6

Trita KRV Report 17-02

ISSN 1100-7990

ISRN KTH/KRV/17-02-SE

Academic Dissertation which, with due permission of the KTH Royal Institute of Technology, is submitted for public defense on Tuesday the 13th June 2017, at 9:00 a.m. in Sal M235, Brinellvägen 68, Stockholm.

Abstract

Domestic and industrial water demands are growing globally due to population growth and rapid economic development, placing increasing strains on water resources. Wastewater effluents generated from these and other activities impact the environment and are thus subject to tightening regulation. The focus of research and development in water treatment processes aims at both pollutant removal efficiency and cost of purification.

Membrane distillation (MD) is a developing thermally driven technology capable of achieving extremely high environmental performance utilizing renewable energy sources to a high degree. District heating networks, and in particular those driven by biomass, represent an ideal heat supply for MD systems.

This thesis presents a technoeconomic assessment of district heating driven MD for water purification in selected industrial applications. The study covers analysis of MD separation performance and the related costs from different district heating integration scenarios. The analyses are based on three types of semi-commercial MD modules, with experiments conducted at laboratory and pilot scales. The case studies include pharmaceutical residue removal from effluents of municipal wastewater treatment plant, wastewater purification in pharmaceutical industry, and ethanol concentration in bioethanol production plant. Full-scale simulation studies were carried out for the identified case studies based on the experimental data obtained from MD module along with process information gathered from the industries. Results from the pharmaceutical residue removal pilot trials showed very good to excellent separation efficiency for 37 compounds at feed concentrations ranging from ng/L to mg/L. From alcohol-water feeds, ethanol concentrations were increased from 5% to nearly 90%. Simulation studies revealed that district heating

integration of MD systems is feasible. Costs per unit volume of purified water are higher than competing technologies, however the configurations enable enhanced environmental performance that would be difficult to achieve otherwise.

Keywords

Membrane Distillation, District Heating, Wastewater Purification, Heat demand, Technoeconomy

Sammanfattning

Kommunala och industriella vattenkrav växer globalt på grund av befolkningstillväxt och snabb ekonomisk utveckling, vilket ökar belastningen på vattenresurserna. Avloppsvatten från alla verksamheter påverkar miljön och är därmed föremål för tilltagande reglering. Fokus i forskning och utveckling av vattenreningsprocesser syftar till att både öka effektiviteten i avlägsnandet av föroreningarna och att minska kostnaderna för detta. Membrandestillation (MD) är en ny termiskt driven teknik som kan uppnå extremt hög miljöprestanda genom att den är effektiv och i hög grad kan drivas av förnybara energikällor. Fjärrvärmesystem, särskilt de som drivs av biomassa, utgör en idealisk värmeförsörjning för ett MD-system. Avhandlingen presenterar en teknoekonomisk bedömning av fjärrvärmedriven MD för vattenrening i utvalda industriella applikationer. Studien analyserar MD-systemets separationsprestanda och kostnader i olika fjärrvärmeintegrationsscenarier. Analyserna baseras på tre typer av semi-kommersiella MD-moduler, med experiment utförda på laboratorie- och pilotskala. Fallstudierna innefattar: borttagning av läkemedelsrester från avloppsvatten från kommunalt avloppsreningsverk; avloppsvattenrening i läkemedelsindustrin; och uppkoncentrering i bioetanolproduktionsanläggning. Fullskaliga simuleringsstudier har utförts för fallstudierna baserat på experimentella data erhållna från MD-modulen och med processinformation som samlats in från industrin. Resultaten från försöken med läkemedelsrester visade mycket god till utmärkt separationseffektivitet för 37 föreningar vid föroreningskoncentrationer som sträckte sig från ng/liter till mg/liter. Vid uppkoncentrering av alkohol ökades etanolhalten från 5 % till nära 90 %. Simuleringsstudier visade att fjärrvärmeintegration av MD-system är möjlig. Kostnader per volym renat vatten är högre än konkurrerande teknik, men konfigurationerna möjliggör förbättrad miljöprestanda som skulle vara svår att uppnå på annat sätt.

Nyckelord

Membrandestillation, Fjärrvärme, Avloppsvattenrening, Värmebehov, Teknoekonomi

Acknowledgments

Foremost I would like to express my sincere gratitude to my advisor Professor Andrew Martin for his continuous support, guidance and motivation from my first day at KTH to the completion of this dissertation. I would like to thank my co-advisor at PoliTo Professor Massimo Santarelli for hosting me and his guidance during my stay in Turin. Special thanks to my industrial mentor, Aapo Sääsk (Scarab Development AB.) for the enlightening discussions with him throughout my study. I appreciate the feedback and comments offered by Dr. Alaa Kullab. I thank Uwe Fortkamp for the permission to participate in a research project with IVL and to use the Membrane Distillation pilot plant at Hammarby Sjöstadsverk. I am grateful for the constructive comments, suggestions and technical support from Henrik Dolfe (Scarab) and Miriam Åslin (Xzero). Advice and comments given by Anders Holmbom (Agroetanol) and Peter Gruvstedt (AstraZeneca) has been a great help for the industrial case studies during the Fjärrsyn project.

My Ph.D. study was partly funded by the European Commission through the European Joint Doctoral Program- SELECT+ which I am grateful to. I am thankful for the financial support from European institute of Innovation and Technology EIT through InnoEnergy Ph.D. School for participating in innovation courses. I would also like to express my gratitude to the Swedish Energy Agency, the Swedish Environmental Protection Agency (Naturvårdsverket), the Swedish District heating Association (Svensk Fjärrvärme) and Xzero for their financial support for the projects. I owe a very important debt to Associate Professor Joachim Claesson for his comments and suggestions as internal reviewer of this dissertation. I want to thank also Anders Malmquist, Justin Chiu, and Vera Nemanova for acting as members of the internal reviewing committee and their feedbacks.

I would like to offer my special thanks to Chamindie Senaratne for facilitating all activities involving SELECT+ mobility and the joint doctoral issues. I appreciate the technical support from the laboratory engineers: Lief, Mikael and Göran at Heat and Power Technology Division (HPT) laboratory. Thank you all friends and colleagues in the department who contributed to my study and personal life.

And finally, to my caring wife Mimi and our lovely sons Aman and Sim, you are my encouragement and hope, Thank you.

Daniel M. Woldemariam

May 2017, Stockholm

List of publications incorporated into this dissertation

Journal Publications

1. D. Woldemariam, A. Kullab, U. Fortkamp, J. Magner, H. Royen, A. Martin, Membrane distillation pilot plant trials with pharmaceutical residues and energy demand analysis, *Chemical Engineering Journal,* Volume 306, 15 December 2016, pp 471–483.

2. D. M. Woldemariam, A. Kullab, A. R. Martin, District heat-driven water purification via membrane distillation: New possibilities for applications in Pharmaceutical Industries, *Industrial Engineering Chemistry Research,* 2017, 56 (9), pp 2540−2548.

3. D. Woldemariam, A. Kullab, E. U. Khan and A. Martin, District heating-driven membrane distillation in industrial-scale bioethanol production: Technoeconomic study, (under review in *Renewable Energy*).

4. D. Woldemariam, A. Martin, and M. Santarelli, Exergy analysis of air-gap membrane distillation systems for water purification applications, *Applied Sciences,* 2017, 7 (3), 301.

Conference publications

5. D. Woldemariam, A. Martin, District heating powered membrane distillation system for industrial applications, International Scientific Conference on Pervaporation, Vapor Permeation and Membrane Distillation, September 21−24, 2014, Torun, Poland.

6. D. Woldemariam, A. Martin, District heating-powered membrane distillation for industrial applications: Wastewater treatment in

Pharmaceutical industries, The 2015 Annual meeting of the North American Membrane Society NAMS, May 30–June 3, 2015, Boston, MA, USA.

7. D. Woldemariam, A. Kullab, E. U. Khan and A. Martin, District heating-driven membrane distillation in industrial-scale bioethanol production: Technoeconomic study, Proceedings of ECOS 2016 – The 29th International Conference on Efficiency, Cost, Optimization and Environmental Impact of Energy Systems, June 19–23, 2016, Portoroz, Slovenia.

Other Publications

Technical reports

8. D. Woldemariam, E. Khan, A. Kullab, A. Martin, District heat-driven water purification via membrane distillation, 2016, Rapport 2016:229, Energiforsk AB, Stockholm. http://www.energiforsk.se/program/fjarrsyn/rapporter/district-heat-driven-water-purification-via-membrane-distillation-2016-229/

9. U. Fortkamp, H. Royen, M. Klingspor, Ö. Ekengren, A. Martin, D. M. Woldemariam, Membrane Distillation pilot tests for different wastewaters: Separation of pharmaceutical residues and treatment of flue gas condensate with Xzero Membrane Distillation in Pilot Scale at Hammarby Sjöstadsverk, October 2015, Report No. B 2236, IVL Svenska Miljöinstitut, Stockholm. http://www.ivl.se/english/startpage/pages/publications/publication.html?id=5172

Author's contributions to the papers

The author of this dissertation is the lead-author of the papers from 1 to 8 where the author performed experiments, analyses and writing of the papers. In journal paper 1, the author performed the MD experiments, the energy analyses and the paper writing. In journal paper 2, the author performed collecting the industrial data, analyzing, doing the simulation studies and writing of the paper. In journal paper 3, the author performed the data collecting from the industry, analyzing, doing simulation studies and writing of the paper. In journal paper 4, the author performed the experiments, analyzed the data and wrote the paper. In conference papers 5 to 7, the author wrote and held the oral presentations. In technical report paper 8, the author performed data gathering from the industries, full-scale simulation studies and writing of the report. In technical report paper 9, the author did the MD experimental tests, energy analysis, and writing the energy related chapters of the report. All work was done under the advice and guidance of Prof. Andrew Martin.

Nomenclature and Abbreviations

Symbols

n	amortization time, years
A	area of membrane, m^2
C	cost, USD
m	degression coefficient
ρ	density, kg/m^3
H	enthalpy, J/kg
S	entropy generated, J/K
ψ	exergy destruction, %
ε	exergy efficiency, %
Ex	exergy flow rate, kW
R	gas constant, J/mol K
φ	heat recovery factor
h	heat transfer coefficient, W/m^2K
$\dot{Q}$	heat transfer rate, kW
z	interest rate, %
M	large-scale flux
$\dot{m}$	mass flow rate, kg/s
N	molar flow rates, mol/s
X	mole fraction
t	period of time
J	permeate flux, kg/m^2h
P	pressure, bar
K	production capacity, m^3/h
μ	pump efficiency, %
c	specific heat, J/(kg K)
T	temperature, °C
η	thermal efficiency, %
v	Volume, m^3
$\dot{v}$	volume flowrate, m^3/h

W	Power requirement, kW

Subscripts

a	annual
I	anticipated capacity
∞	atmospheric air
b	bottom
ch	chemical
col	column
j	component of stream
cd	condenser
cv	convecion heat transfer
0	dead state
ρ	density
dest	destruction
el	electricity
f	feed
gen	generated
i	input
l	*loss*
min	minimum
o	output
ph	physical
p	product or permeate
r	reboiler
ref	reference unit
sp	specific
T	thermal
vap	vaporization

Acronyms

ABE	Acetone–Butanol–Ethanol
AC	Activated Carbon
AGMD	Air Gap Membrane Distillation
BP	Bioethanol Production
BOD	Biological Oxygen Demand
CAPEX	Capital Expenditure
COD	Chemical Oxygen Demand
CHP	Combined Heat and Power
CL	Confidence Limit
DMM	Digital Multi Meter
DCMD	Direct Contact Membrane Distillation
DH	District Heating
ED	Electrodialysis
EPA	Environmental Protection Agency
EDTA	Ethylenediaminetetraacetic acid
FAS	Fluoroalkylsilane
GOR	Gained Output Ratio
HR	Heat Recovery
HPLC	High Performance Liquid Chromatography
KTH	Kungliga Tekniska Hökskolan (also known as Royal Institute of Technology)
LEP	Liquid Entry Pressure
LGMD	Liquid Gap Membrane Distillation
MS	Mass Spectrometer
MGMD	Material Gap Membrane Distillation
MEDINA	Membrane based Desalination: an Integrated Approach
MBR	Membrane Bioreactor
MCr	Membrane Crystallization
MD	Membrane Distillation
MEDIRAS	Membrane Distillation in Remote Areas
MF	Micro-Filtration

MEMD	Multi-Effect Membrane distillation
MSF	Multi-stage Flash
NF	Nanofiltration
OPMEX	Operational and Maintenance Expenditure
OMD	Osmosis Membrane Distillation
PPCPs	Pharmaceutical and Personal Care Products
PV	Photovoltaic
PE	Polyethylene
PP	Polypropylene
PTFE	Polytetrafluoroethylene
PVDF	Polyvinylidene fluoride
RO	Reverse Osmosis
MEDESOL	Seawater Desalination by Innovative Solar-Powered Membrane-Distillation System
SWRO	Seawater Reverse Osmosis
SPE	Solid-Phase Extraction
SED	Specific Energy Demand
IVL	Svenska Miljöinstitutet (Swedish Environmental Research Institute)
SGMD	Sweeping gas Membrane Distillation
TN	Total Nitrogen
TOC	Total Organic Carbon
UFLC	Ultra-Fast Liquid Chromatography
UF	Ultrafiltration
VMD	Vacuum Membrane Distillation
V-MEMD	Vacuum Multi-Effect Membrane Distillation
WWTP	Wastewater Treatment Plant

Table of Contents

List of Figures

List of Tables

1 Introduction

Access to clean water is a fundamental human right, however its provision is far from universal. Globally over 780 million people do not have access to clean water, and nearly 2.5 billion do not have adequate water for sanitation [1]. Water quality and availability affect human health and also influences economic development, since nearly all economic sectors rely directly on a clean water supply. On a worldwide basis the industrial sector has a water demand second only to agriculture, and exhibits a demand that is increasing at a greater rate [2]. Thermal power plants represent the main industrial user of water, however many other industrial processes follow closely behind. The amount of water used in industries varies widely from one to another depending on the type of water utilization and scale. Water is commonly employed in industrial processes such as pulp and paper, textile, and semiconductor manufacturing; to enable steam-driven electricity production; and is used in various productions processes including cooling and cleaning [3]. In other industries, notably the food, beverage and pharmaceutical sectors, water is an ingredient in finished products for human consumption [4]. Examples of such products include dairy products, soups, beverages and medicines. Environmental regulations such as the EU Water Directive [5] and other national and local statutes have led industries to recycle more water and to raise standards of effluents, thus adding more complexity and cost to the water treatment methods employed. Various types of large-scale water treatment technologies are in use to supply the quality of water required for the specific industrial purpose. Most of these water treatment methods involve a number of sequential processes like filtration, biological or chemical reaction, adsorption and related procedures. Advanced treatment technologies such as reverse osmosis (RO) are necessary for achieving high separation efficiency and are often used in ultrapure water applications (e.g. boiler make-up water, and rinse water in semiconductor manufacturing). Drawbacks of RO and other related

pressure-driven separation processes are their susceptibility to membrane fouling and high specific electricity demand.

Advanced water treatment alternatives featuring similar or improved separation efficiency as compared to RO but with lower energy impact are of great interest for industrial applications, in particular those technologies that can utilize renewable energy sources. Membrane distillation (MD) is one such technology. MD combines the benefits of membrane separation, as in RO, with reduced electricity needs. The technology was first conceived several decades ago, mostly for desalination, and is yet to be fully commercialized. High heat demand is one of the major hindrances towards seeing a more widespread deployment of MD technology. In order to overcome this obstacle, it is imperative to focus on thermal integration issues, which means that thermal energy supply in combination with heat dissipation – all within the context of the specific application – must be given careful consideration. Integration with district heating (DH) networks represents an overlooked opportunity in this context, which is somewhat surprising since both concepts operate broadly within the same temperature span (40–90^{o}C or so). In the Nordic countries and other locations, DH networks are largely renewables based. Therefore the pairing of the two concepts can enhance the overall sustainability of industrial processes requiring advanced water treatment. Progress in this area strongly depends upon the identification of specific industrial applications for MD technology, including verification of actual performance for a given set of parameters.

1.1 Objectives

The main objective of this investigation is to evaluate district heating-driven membrane distillation for water purification in selected industrial applications. Specific objectives include the following:

- Survey of industries in Sweden in order to find the most promising applications;

- Identification of specific ways in which MD technology can be integrated to district heating networks;
- Evaluation of separation efficiency of relevant aqueous feedstocks;
- Analysis of MD energy demand and exergy efficiency for systems integrated to district heating networks;
- Technoeconomic feasibility in comparison with competing technologies for the selected applications – water purification in municipal wastewater treatment and in the pharmaceutical industry, and ethanol concentration and water recovery in bioethanol production.

1.2 Outline of the Thesis

This thesis is divided into the following nine chapters:

Chapter 1 states the motivation and background for this work and also formulates the objectives and methodology.

Chapter 2 contains a review of literature on the primary developments of membrane distillation along with a description of the specific applications under consideration.

Chapter 3 presents a background on district heating and potential integration with membrane distillation systems.

Chapter 4 describes the experimental setups and methods used for providing input to simulations of large-scale processes.

Chapter 5 investigates the performance of an MD pilot plant for removal of pharmaceutical residues in municipal wastewater treatment plants.

Chapter 6 is dedicated to MD's technoeconomic performance for applications in the pharmaceutical industry.

Chapter 7 explores the competitiveness of MD versus conventional distillation process for ethanol concentration and water recovery in a bioethanol production plant.

Chapter 8 presents an exergy analysis of the investigated MD equipment.

Chapter 9 provides conclusions and future outlook.

The major contributions of the thesis are linked to the published articles, listed on page vii, as follows:

- Demonstration and quantification of separation efficiency and thermal demand for an MD pilot facility utilizing feedstocks containing pharmaceutical residues at a wide range of concentrations (Paper 1).

- Feasibility studies of novel concepts involving district heating-driven MD technology for wastewater treatment in the pharmaceutical industry (Paper 2) and in bioethanol production (Paper 3).

- Exergy analysis of MD technology with focus on heat source/heat sink matching (Paper 4).

1.3 General methodology and delimitation of the Thesis

Extensive experimental investigations were conducted for all the applications considered. The experimental studies were performed using two laboratory scale MD units and one pilot scale MD system. For samples with questionable safety to test at large scale, such as ethanol-water separation described in Chapter 7, only bench-scale experiments were considered. To identify a potential application and then simulate the full-scale process, the following methodologies were employed: literature survey of water purification and other separation technologies in relevant industrial processes; experimental MD investigations; and system analyses (mass and energy balance calculations) with input obtained from experiments and the selected industry. Full-scale simulation studies

include a comparison of economic gains of the MD integrations over the current practices in each industrial case study under consideration.

Certain aspects were omitted in order to make the investigation tractable. For example, practical issues related to membrane fouling or scaling along with the fate of MD concentrate are not included in this dissertation. Some MD feedstocks were reproduced synthetically as treatment of the actual sources was impractical. Finally, thermal integration with district heating networks considered a simplified approach, neglecting seasonal variations.

2 Membrane Distillation

Membrane Distillation (MD) is a separation process driven by an imposed vapor pressure gradient across a hydrophobic microporous membrane. The MD process is able to produce ultrapure water in a single step, separates high concentration feeds and takes place at temperatures below 100°C and ambient pressure [6]. An imposed temperature difference across the membrane causes a water vapor pressure gradient, resulting in water vapor transport through the pores from the feed to the cooling side of the membrane. The technology was introduced in the 1960s [7, 8] and is still being developed with possibilities of overcoming some limitations of the already established and widespread membrane-based separation technologies. Key advantages of membrane distillation processes over conventional separation technologies are: relatively lower energy costs and reduced vapor space compared to conventional distillation; a complete rejection of dissolved, non-volatile species to produce ultrapure water (electrical conductivity of 5 µS/m); reduced membrane fouling as compared with microfiltration, ultrafiltration, and reverse osmosis; lower operating pressure than pressure-driven membrane processes [9, 10] and lower operating temperature (60°C–90°C) as compared with conventional evaporation [11, 12]. Low-grade heat sources such as waste heat can drive the MD process, and these types of heat sources are advantageous in large-scale industrial applications where heat is a byproduct. Hence, recently much attention is given to MD processes driven by waste heat [13] and solar energy [14]. These possibilities of integrating MD with low-grade heat sources facilitate its use at small scales, e.g. provision of purified drinking water and hot water in a single-family house [15] – and at large scales e.g. water purification in biomass-fired combined heat and power plants [16]. These and other examples illustrate the benefits of good thermal integration: however, in cases where internal heat recovery is not possible MD's specific energy

demand can be much higher as compared to conventional membrane processes.

2.1 Membrane distillation configurations

Membrane distillation modules are designed in various ways depending on how the permeate vapor is collected and condensed. There are four common types of MD module configurations as shown in Figure 2.1. In all of the four configurations, the hot feed is always maintained in direct contact with one side of the membrane, with different schemes employed on the opposing membrane side.

A Direct Contact Membrane Distillation (DCMD) module is designed so that the membrane is cooled by the permeate. This type of module has the simplest design and is capable of producing a reasonably high permeate flux [8, 14, 18]. DCMD is best suited for applications such as desalination [19–21], concentration of aqueous solutions [22], boron removal [23], concentration of juice products [24], MF pretreated wastewater purification from olive mill [25], and removal of radioactive elements [26]. DCMD has limitations in that heat recovery by using feed as coolant is not possible [27] and also exhibits high heat loss via conduction [6].

Air Gap Membrane Distillation (AGMD) is the second type of MD module design in which a thin layer of air is interposed between the membrane and the condensation surface, which in turn is cooled on the opposite side. The inclusion of an air gap and condensation plate prevents a direct contact between permeated vapor and cooling water, which limits the rate of heat transfer from the hot feed side to the cooling water. Therefore, this internal heat recovery in AGMD module leads to higher energy efficiency than DCMD [28] and limits heat loss due to conduction [6]. However the presence of an air gap hinders mass transfer, leading to lower permeate flux [29, 30]. AGMD has module been considered for many membrane distillation applications, particularly where thermal energy availability is limited [29, 31, 32] and for applications such as ethanol separation [33, 34], purification of arsenic contaminated water [35] and desalination [36, 37].

Vacuum Membrane Distillation (VMD) is the third type of MD module design in which the permeate side is maintained under reduced pressure, as low as 0.1 kPa [38]. The vacuum creates a driving force for transmembrane flux [39] by increasing the vapor pressure difference across the membrane [40, 41]. The technique also enhances the process by removing air from membrane pores [6] and lowering conductive losses [42, 43]. This combination enables VMD to produce a higher permeate flux than DCMD and AGMD [21, 44]. Limitations of VMD include an increased risk of membrane wetting (i.e. loss of hydrophobicity), requirement of membranes with sufficient mechanical strength [45], and additional energy requirement for the vacuum pump [6]. VMD is most commonly applied to remove volatiles from an aqueous solution such as ethanol-water separation [46], recovering volatile aromas from fruit juices [47], volatile organic compounds removal from water [48], desalination [44], and ammonia removal from aqueous solutions [49].

The fourth configuration, Sweep Gas Membrane Distillation (SGMD), involves blowing a stripping gas (e.g. air or nitrogen) on the permeate side, serving as a carrier for the produced vapor. This configuration has greater mass transport rate than AGMD, however the additional cost for the sweep gas and requirement of an external condenser are disadvantages [50, 51]. Even though this process configuration is the least investigated, it has been mostly tested for separation of volatiles such as ammonia gas from wastewater [52], ethanol-water separation [53], desalination of sea water [40, 54–56] and recovering of fruit juice aromas [47].

From these four commonly investigated MD configurations, DCMD is the most widely applied configuration in laboratory MD research for its simplicity of design and assembly, whereas AGMD has received more attention for commercial applications, because of its improved energy efficiency and capability for latent heat recovery [57, 58].

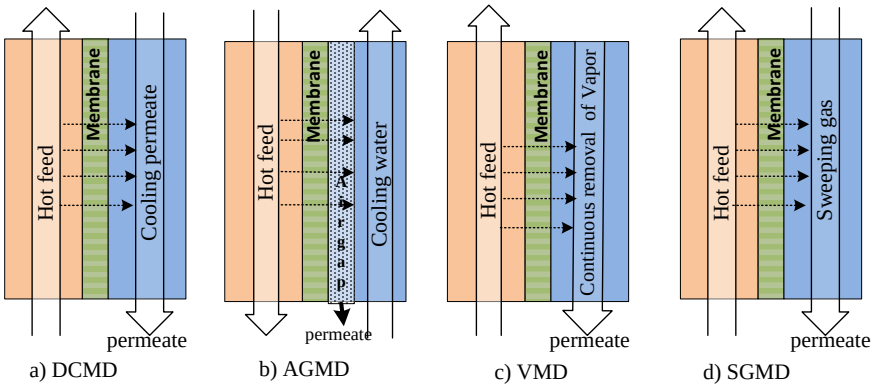

Figure 2.1. The four types of membrane distillation module configurations.

In general, when compared to other pressure driven water purification technologies, the commercialization of MD has been limited mostly due to its low thermal efficiency and challenges related to module design [59]. In the context of making MD process more thermally efficient and economical, there have been efforts aiming at maximizing the flux and minimizing the heat demand. Some of the recently developed MD configurations include liquid or material gap MD, osmotic MD, and multi-effect or multi-stage MD configurations.

Material Gap Membrane Distillation (MGMD) is a modified form of AGMD in which the air gap is replaced by a material other than air. MGMD is intended to improve the lower permeate flux from AGMD. Francis *et al.* [60] investigated the performance of MGMD by filling up sand and deionized water in the air gap. The authors reported that introducing these materials increased the permeate flux 200–800%. However, other materials like polyurethane and PP mesh did not show any effect on the flux. The effect of these materials on the heat transfer and so thermal efficiency of the module was not assessed.

Osmotic membrane distillation (OMD), which is also called isothermal membrane distillation, osmotic evaporation, gas membrane extraction or osmotic concentration by a membrane, is an isothermal MD process in which the driving force is the vapor pressure difference and uses similar

modules (Figure 2.2) as in DCMD [61]. However, the driving force generated in OMD is because of the difference in a concentration gradient across the membrane caused by a stripping solution at the permeate side [6]. In OMD process the temperatures of the feed and the stripping or absorbing liquids are kept almost at the same temperature, and transmembrane mass transfer takes place at much lower temperature than MD or even at ambient temperature. Water vapor and volatile components are absorbed by a salt solution flowing continuously on the permeate side of the porous hydrophobic membrane. Due to its low process temperature, OMD is preferred for the concentration of volatile components of fruits and aromatic extracts. Applications investigated using OMD include: juice concentration [62–64], reconcentration of sugar solution [65] and brine purification in the chloralkali industry [66].

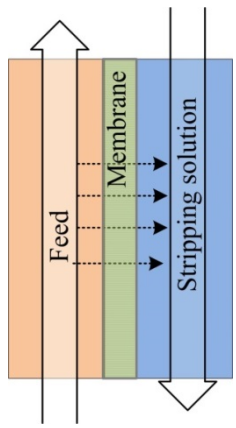

Figure 2.2. Osmotic membrane distillation OMD module configuration

Multi-effect membrane distillation (MEMD) is based on one of the basic MD configurations but combining two or more modules so that the thermal efficiency is significantly increased through internal heat recovery [59]. MEMD configuration (Figure 2.3) is designed to recover heat from permeate through a heat exchanger with or without being heated by an external heat source. MEMD composed of DCMD was reported to have higher recoveries of up to 60% from a single pass due to the reconcentration of the brine in a series of three or more MD modules

and Gained Output Ratio (GOR*) of up to 20 [67]. Another four-staged MEMD configuration based on vacuum MD module is developed by memsys GmbH, aiming to achieve higher efficiency of heat recovery [68]. Memsys claims that the specific heat demand of this V-MEMD is as low as 175 –350 kWh/m^3 and GOR of up 3.6 [69].

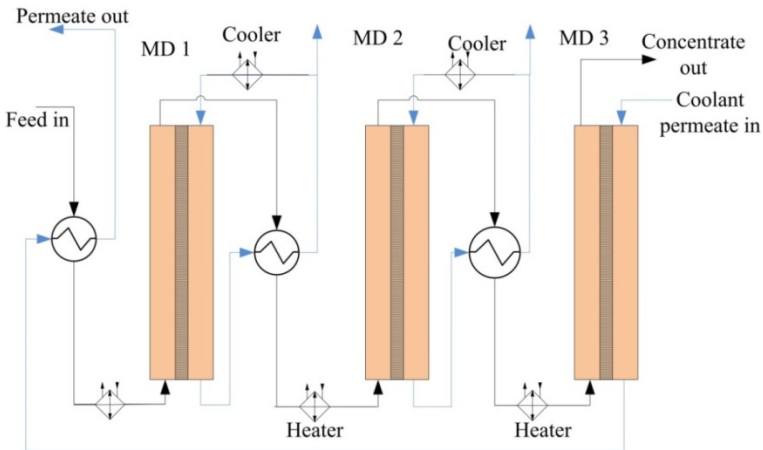

Figure 2.3. An MEMD configuration based on DCMD module where heat exchangers are introduced to reclaim heat from permeate with additional inter-stage brine heating and permeate cooling.

2.2 Developments in membranes for MD applications

The membrane is key component in MD module that determines the separation efficiency of the MD process. In MD hydrophobic microporous membranes are widely used materials. The common membrane properties required in MD processes are as follows: a hydrophobic layer (contact angle > 90^o and liquid entry pressure, LEP of > 2.5 bar), appropriate pore size (0.1–0.3 μm), high porosity (80%), optimum thickness (30–60 μm), minimum thermal conductivity, thermally stable, chemically resistant to acids and bases during membrane cleaning, and

* GOR refers to the ratio of the amount of latent heat required for the evaporation of the purified water to the amount of heat input to the MD. $GOR = \frac{\dot{m}_p * \Delta H}{\dot{Q}_{in}}$, where $\dot{m}_p$ is the permeate rate, ΔH is the latent heat of evaporation of water, and $\dot{Q}_{in}$ is the specific rate of heat input to the MD.

durability [70, 71]. However there are no commercially available membranes fulfilling all these basic requirements, which have contributed to MD not being a widely applied separation process among industries [19].

Studies on synthesis and modification of membrane materials suitable for MD process are still in progress. The two most commonly used membrane materials in MD are hydrophobic polymers polytetrafluoroethene (PTFE) [72–75] and polyvinylidene fluoride (PV-DF) [43–45, 76]; and other materials such as polypropylene (PP) [76–78] and polyethylene (PE) are also widely employed for different MD applications. Synthesis of hydrophobic membranes is usually done in two ways: by stretching technique [59] where the polymer is melted and extruded; or by phase inversion method [79, 80] in which a dissolved polymer is separated and precipitated to form a solid phase of specific morphology. Hydrophilic materials such as acetate and nitrate salts of cellulose are used after modifications with polystyrene and plasma respectively [81] to give them a hydrophobic layer. Fluoroalkylsilane (FAS) grafted ceramic alumina hollow fiber membranes were also tested for water desalination applications in MD and showed comparable performance with hydrophobic membranes regarding salt rejection [82, 83]. However, these ceramic materials are more expensive and reported to have higher heat loss than the hydrophobic membranes due to their thermal conductivity [71, 83]. Even though all the different types of membranes used in MD fulfill the criterion of having a hydrophobic layer, membrane fouling is still a major problem [84].

2.3 Mass and heat transfer in AGMD

In the AGMD process both mass and heat transfer takes place simultaneously across the membrane. Several theoretical studies on mass and heat transfer in AGMD process have been developed by many researchers. The focus of these investigations is mainly on the effects of parameters such as membrane properties, nature of condensing surface, and air gap thickness.

The mass transfer starts when a heated feed for separation is pumped to the feed side of MD module, with a fraction evaporating at the feed-membrane interface. The evaporated water from the hot liquid-vapor interface permeates through membrane pores and emerges from the air-vapor interface at the cooling side of the module where it is condensed. Liquid water is prevented from entering the pores by the liquid-vapor interface which is maintained by a microporous hydrophobic membrane. Different transport phenomena and driving forces may contribute to the overall mass transfer across the membrane and air gap. The trans-membrane mass transfer rate depends on vapor pressure difference between the two sides of the membrane. The permeate mass flux ($\dot{m}$) collected from the cooling side is the mass of water (m) produced in a particular period of time (t) from the unit surface area (A) of the membrane.

$$\dot{m} = \frac{m}{A*t} \tag{2.1}$$

The transmembrane flux (N) in general is usually expressed as a function of the vapor pressure difference across the membrane (ΔP) [85]:

$$N = C * \Delta P \tag{2.2}$$

where C is the net mass transfer coefficient which is dependent on the membrane properties, temperature, pressure and other parameters. The mass transfer coefficient is estimated by applying different mass transport models for the given transport mechanism or combination thereof: Knudsen flow (K), Poiseuille flow (P) and Molecular diffusion (M). Understanding the balance between these transport mechanisms depends on an understanding of membranes' morphology [70, 86]. Knudsen flow applies if the mean free path of the water molecules is greater than the pore size and hence the molecule-pore wall collisions have larger rate than intra-molecular collisions. Then the net mass transfer coefficient C_k is,

$$C_K = 1.064 \frac{r\varepsilon}{\delta\tau}\sqrt{\frac{M}{RT}} \tag{2.3}$$

where r is the pore size, ε is the fractional void volume, δ is the membrane thickness, τ is the tortuosity, R is the gas constant, M is the molecular mass of water and T is the absolute temperature. When the pore size of the membrane is larger than the mean free path of water molecules, the intramolecular collisions are dominant over the molecule-pore wall collisions and the mechanism is called Poiseuille flow. The mass transfer coefficient C_p is described as,

$$C_P = 0.125 \frac{r^2\varepsilon}{\delta\tau}\frac{MP_m}{\lambda RT} \tag{2.4}$$

where λ is the water viscosity and P_m is the average gas pressure inside the membrane. If the molecular diffusion is the dominant resistance by the air in the membrane pores, the mass transfer coefficient C_D will be,

$$C_D = \frac{1}{Y_{lm}}\frac{D\varepsilon}{\delta\tau}\frac{M}{RT} \tag{2.5}$$

AGMD's transmembrane vapor flow can still be described by the general equation (2.2) but the additional air gap presents extra resistance for the vapor flow. The water flux through the air gap can be described as

$$C = \frac{\Delta P}{R_{ag}} \tag{2.6}$$

where R_{ag} is the air gap resistance coefficient

In AGMD process three mechanisms of heat transfer occur. These are latent and conductive heat transfer through the membrane together with radiant heat transfer through the thin air gap that comes after the membrane. Conductive heat transfer depends mainly on properties of the membrane, such as thickness, pore size, the heat conductivity of the

membrane material and also thermal conductivities of the air gap and gasses involved. The latent heat transfer is due to the mass transport of vapor across the membrane. The heat content carried away with the vapor across the module is a function of the total flux and the air gap, whereas, radiative heat transfer occurs from the radiation heat exchange across the air gap between the membrane surface and the condensation plate's surface. The rate of radiative heat transfer is temperature dependent and is comprised of emissivity from the membrane surface, air gap spacer (which affects the effective cross-sectional area), and condensing plate. Even though the radiative heat transfer is usually neglected in large-scale AGMD, one study investigated its effect in AGMD via heat transfer modeling [87].

The primary heat transfer processes in AGMD can be described in the following mechanisms as depicted in Figure 2.4:

a) Heat transfer from bulk feed into membrane surface by convection
b) Heat transport across the membrane by conduction
c) Conductive heat transfer through the air gap
d) Conductive heat transfer through the condensation plate
e) Heat transfer from the cooling plate to the cooling water through convection

The total heat transfer rate across AGMD module can be determined according to the following equation [88]:

$$Q = \frac{k}{b}\left(T_{hm} - T_{mfm}\right) + J_v h_g \tag{2.6}$$

where h_g is the enthalpy of water vapor, J_v is the vapor flux, b is the membrane thickness, T_{hm} the feed temperature near the membrane surface, T_{mfm} is the temperature at the air gap membrane interface, k is the thermal conductivity through the membrane. The first term describes the sensible heat transfer through conduction whereas the second term describes the sensible heat transport via water vapor.

The temperature is slightly lower at the interface between the feed and membrane than in the bulk due to temperature polarization effect, as shown in the AGMD schematic diagram (Figure 2.4). The temperature

polarization effect can be minimized by increasing the feed flow to a high rate. Insertion of spacers can help to increase the turbulence near the membranes so that the temperature polarization could be reduced. The measure of temperature polarization can be described with T_p as in the following equation:

$$T_p = \frac{T_2 - T_3}{T_1 - T_4} \tag{2.7}$$

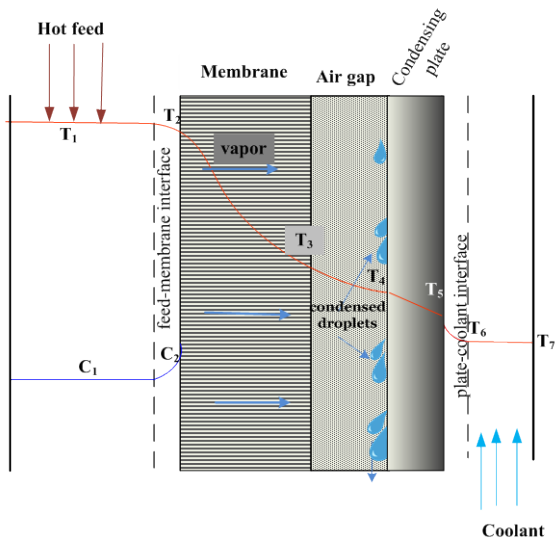

Figure 2.4 Mass and heat transfer scheme across air gap membrane distillation module.

2.4 Applications of MD

Despite MD being not yet a fully mature technology for full-scale commercialization, quite many applications have been investigated both in academic studies and by innovation companies all over the world. New applications are continuously being added, including those relating to the most common categories: desalination and drinking water provision; and water purification. Some examples of these developments are listed below.

2.4.1 Desalination and drinking water purification

Desalination of seawater or brackish water is the most explored application for MD technology. The vastly abundant sea water is a huge potential for pure water supply if sustainable and economic desalination technologies are applied. The conventional desalination technologies such as multi-stage flash (MSF) distillation and reverse osmosis (RO) are mature and widely commercialized even though there have still been studies to improve the technologies so that the cost of desalination is reduced. One of the reasons for the high cost of desalination plants is the high energy demand, which leads to high operating cost. Hence studies looking for technologies with minimal energy demand and use of cheaper alternative energy sources are still undergoing. MD has been extensively studied for desalination applications mostly for drinking water [30, 89–91] and also for treatment of high salinity brines [92, 93]. Among the different configurations of MD, AGMD and DCMD have been widely applied for desalination purposes.

2.4.2 Wastewater treatment and industrial water purification

Wastewater treatment is a complex process and is ultimately governed by environmental regulations or purity requirements in the case of reuse. The process usually includes a series of procedures from filtration of coarse solid matters to decomposition of organic pollutants and reduction or elimination of biological elements including pathogens. The selection of a specific procedure and its complexity depend on the nature and composition of the wastewater to be treated. Dye-contaminated textile wastewater for example requires oxidation, coagulation or flocculation followed by adsorption and NF or UF [94]. Membrane-based wastewater treatment technologies mostly include membrane bioreactor (MBR), nanofiltration (NF), reverse osmosis (RO), and electrodialysis (ED). However in recent years, there are growing concerns on the limitation of these technologies to remove some trace substances such as pharmaceutical residues [95–97]. Gethard *et. al* [98–100] investigated an MD module enhanced by carbon nanotubes for purifying pharmaceutical wastewater and producing pure water for use at the same time. MD has been investigated for wastewater purification and recovery of useful

elements from process water. For example, Hou *et al.* reported DCMD's removal efficiency of boron to be greater than 99.8% [23, 101] which was very high in comparison to RO's performance of 30–40% and ED's 42–75% [101]. VMD was investigated for removing colors of a dyed-aqueous solution [102–104]. Other water purification applications applied in MD include pure water supply for thermal-power cogeneration plants [16], for semiconductor industry [105], and arsenic removal from well-water for drinking [35, 106]. Removing oil from produced water during fracturing process in oil and gas or mining practices is another application for MD, and has shown promising performance [76, 107, 108]. Concentration of juices [47, 62, 64, 109]; concentration of acids [22, 110, 111] and removal of ammonia [52, 59, 112] are some other applications where MD technology has been investigated.

Food processing such as in dairy plants [113, 114], juice concentration [24, 47, 115, 116], ethanol-water separation [34, 46, 117, 118] and concentration of acids [119–121].

2.5 Major MD module developers and suppliers

Even though membrane distillation has gained significant interest from an industrial and academic perspective in recent years, there still exist challenges towards achieving commercialization. This is mainly due to the issues in module design and membrane development. At present there are only a few companies that develop and supply MD modules or units.

Scarab Development AB is a Swedish company which has been developing MD modules under different investment projects: Xzero, HVR and Elixir MD modules. All the three types of MD modules developed by Scarab AB are based on air gap configuration but are different with each other with regard to the type of cooling plate and capacity. The Xzero module is constructed from a stack of ten cassettes each containing two membranes with a total membrane area of 2.6 m^2 and the membrane material is polytetrafluoroethylene (PTFE) with polypropylene (PP) support. A pilot plant of Xzero's AGMD for research and demonstration was installed in 2011 in Stockholm (Figure 2.5 a). The MD system is

driven by heat from district heating network and has a production capacity of 5–10 m^3 pure water per day.

A Fraunhofer spin-off company, Solarspring GmbH (Germany) has developed solar powered MD pilot test facility based on spiral wound AGMD (Figure 2.5. b) for desalination applications. The solar driven MD desalination plants have capacities from 0.1 to 5 m^3/day and are located in areas with high solar intensity, such as Canary Islands in Spain, Pantelleria in Italy and Amarika, Namibia. The modules can be configured to operate as DCMD, LGMD, or AGMD and feature PTFE membrane inserts with PP backings; total membrane area ranges from 5 – 14 m^2 per module [76].

In February 2014 Aquaver, a Dutch cleantech company commissioned and installed the first full-scale commercial MD facility for desalination in a Maldivian Island of Gulhi [58]. The membrane distillation system is supplied by memsys GmbH (Germany) and is based on Vacuum Multi-Effect Membrane Distillation (V-MEMD) configuration (Figure 2.5 c). This module called memDist consists of PTFE membranes and is a modified form of VMD so that thermal efficiency and GOR are improved through four or six stages modules in series with a total membrane area of 6.4 or 52 m^2 respectively [122]. The MD unit installed at Gulhi utilizes waste heat of a local power generator and has a production capacity of 10 m^3 drinking water per day.

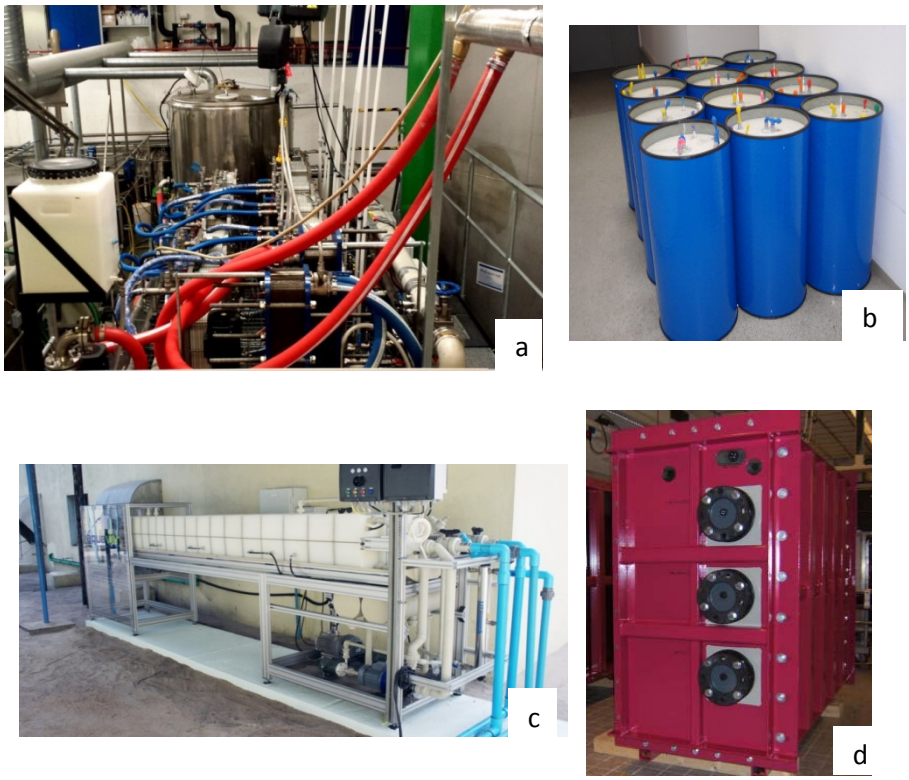

Figure 2.5. Semi-commercial MD modules from different suppliers. a) Xzero's AGMD pilot plant in Stockholm, b) Solarspring's spiral PGMD module [123], c) Memsys' VMD unit in Maldives [58], d) Memstill MD unit for a pilot system [124].

Memstill is an MD system developed by a consortium of nine partners including Keppel Seghers (Singapore) and TNO (The Netherlands Organisation for Applied Scientific Research), who have established Aquastill bv. (Netherlands) for commercialization of the technology (Figure 2.5 d). The Memstill MD system is designed for internal heat recovery to be applied in applications having access to low-grade heat or industries with waste heat [124]. Three pilot plants have been tested since 2008, one in Johor, Malaysia for seawater desalination and the other two in Rotterdam for brackish water distillation by using heat from a coal-

fired power plant [125]. The pilot plants had design capacities of 5 m^3/day based on 24 h operation [126].

3 Energy Sources Driving Membrane Distillation

The membrane distillation process requires a heat source to enable evaporation of the feed, a heat sink to dissipate thermal energy from the cold side, and electricity to drive the pumps. Even though low-grade heat is sufficient for the MD process to occur, the high specific thermal energy demand and the low permeate flux brings challenges for the technology to be used in large-scale applications. Heat sources considered for MD include solar and waste heat in combined heat and power plants (CHP) and other industries. International desalination projects including EU funded initiatives on solar powered membrane distillation: MEDIRAS (MEmbrane DIstillation in Remote Areas) [127], MEDESOL (Seawater Desalination by Innovative Solar-Powered Membrane-Distillation System) [89], and MEDINA (Membrane based Desalination: an Integrated Approach) [128]. Other investigations have linked MD to CHP. The Memstill MD pilot plant in Pantelleria island of Italy is an example of desalination driven by waste heat (temperatures of 70–80°C) from a diesel engine [125]. A small DCMD pilot unit with capacity of 1.3 – 3.5 L/h and membrane area of 0.67 m^2 was tested by using waste heat (< 40°C) from gas fired power station [84]. The memsys VMD desalination plant installed in Maldives (described earlier) is also powered by waste heat (at temperature of about 80°C) from a diesel generator [129].

Kullab and Martin [16] investigated air gap MD for flue gas condensate treatment via pilot plant trials at a biomass-fired CHP unit in Sweden. It was the first study to examine coupling of MD technology with district heating, although the integration was considered within the boundaries of the CHP facility and not within the DH network. This study will be discussed subsequently in more detail (in section 3.2) in relation to the

present investigation. Additional background information on district heating now follows.

3.1 District heating – background and focus on Sweden

A DH network is a centralized facility used for heating and distributing water to consumers by using a network of pipelines. When the heated water reaches the consumer (for example a residential building), the heat is distributed through heat exchangers in substations to supply domestic hot water and space heating via radiators or forced air heaters. The centralized heat production within district heating systems can be placed in one or several heat production units such as hot water boilers, heat pumps, and CHP. Generating and distributing heat from a central facility can have economic and environmental advantages as compared to decentralized options such as small-scale boilers or heating systems. Moreover, different heat sources can be used, including biomass, municipal solid waste, and industrial waste heat [133]. Integration with CHP is one of the efficient ways of incorporating with DH networks. Such systems have high distribution in Europe [130], and in Sweden most district heating is produced in biomass-fired CHP facilities [131].

The Swedish heating market amounted to 100 TWh and 100 billion SEK turnover for 2013–2014 [132]. District heating stood for more than half of the total heating demand (Figure 3.1 (a)) and regarding total annual turnover, district heating represents 40% of the total heating whereas electric heating and heat pumps contributed to 45% (Figure 3.1 (b)). District heating was found to be the largest heating category in multi-family houses and premises, whereas electricity based heating was largest in single-family houses [132]. The CHP contributions for the Swedish DH system in 2014 and 2015 were 22 TWh and 23 TWh respectively [133], which showed an increase from 43% in 2014 to 45% in 2015 of the total district heating produced.

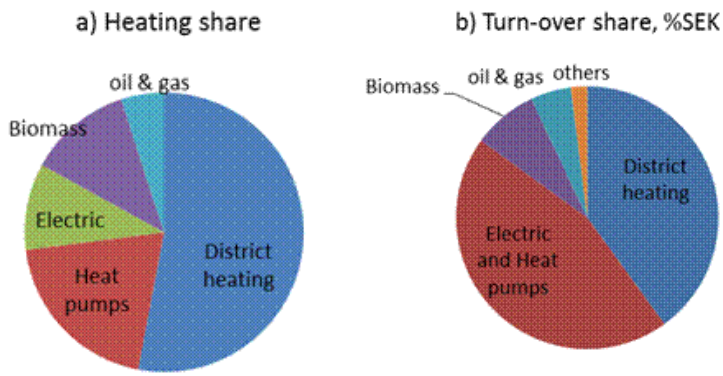

Figure 3.1. Different heating sources share in terms of annual heating (a) and total turnover (b) in the Swedish heating market for years 2012-2014 [132].

Even though district heating has a large share of heating among the energy sources, the annual heating demand is forecasted to be reduced by nearly 10% in 2025 when compared with the estimated demand for 2007 as shown in Figure 3.2. The main contributor to this decrease is the improvements in energy efficiency of multi-family houses and premises. This is most evident for building heating, where the specific heat demand per square meter has been reduced by the magnitude of one percent per year for the period of 1995 – 2012 [132]. Climate change, specifically global warming, could have a significant contribution as well. Yet there remain opportunities for the district heating market in Sweden. As it is mostly derived from biomass, district heating is considered environmentally friendly and contributes to the renewable share of the Swedish energy supply. The increase in CO_2 taxes on fossil fuels, the green certificate system and subsidies to biomass cogeneration plants should keep the district heating market attractive in the future. As most of the district heating is produced in combined heat and power plants, the development and increase in the supply of heat through district heating technology will also lead to an increase in electricity production as a result.

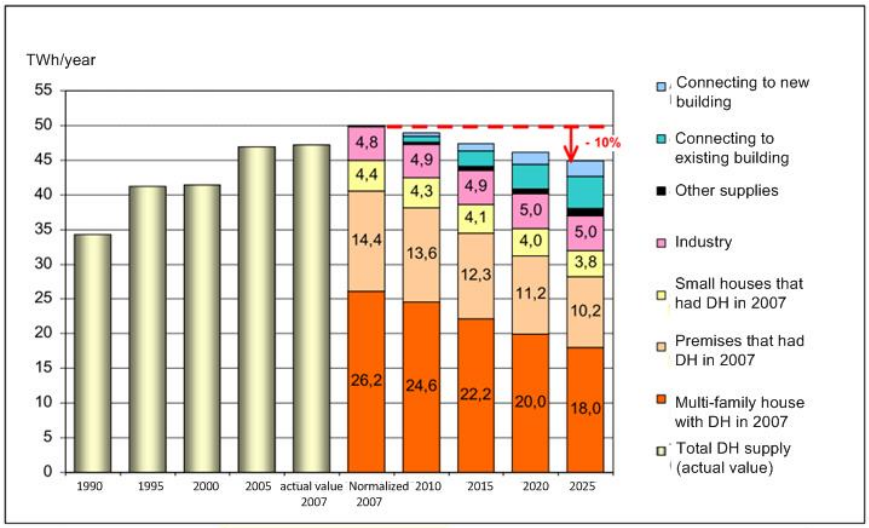

Figure 3.2.The Swedish district heating supply development according to calculations carried out in a project "District heating in the future: the need (edited from [134]).

Furthermore, industrial DH demand is expected to increase slightly from 4.8 to 5.0% in the next ten years (see Figure 3.2), which indicates that industrial application of DH will contribute to the expansion of DH network in the future. District heating can be used in a range of industrial processes, e.g. for replacing more costly steam in food processing plants and chemical industries. There have been a few research projects in Sweden dedicated to identifying potential DH applications in industrial processes. According to Steen *et al*. [135], the largest DH user in 2012 was the electronics industry including those manufacturing computers, optical components, and other electrical equipment, amounting to an annual DH demand of 561 GWh. The forestry and wood products industry, vehicle manufacturing industry, steel and metal processing plants, food and drinks industries, chemical industries and pharmaceuticals, and pulp and paper industry are among the other industrial customers with measurable demand for 2012 [135]. Additional potential industries identified at a concept stage include the following: painting and coating, degreasing in workshops, concrete production in constructions, cleaning, drying, past-eurizing process in food industries, washing in textile and laundry industries; drying in wood workshops,

heat-driven absorption chillers in supermarkets, and sanitation and high-temperature pretreatment of substrates for biogas production [135 – 137].

The pricing of district heating in Sweden is unregulated and varies from one area to another. The respective district heating supplier sets prices according to standard business practices, with negotiation occurring with larger customers (housing associations, municipalities, or industry).

3.2 Thermal integration with district heating networks

As previously stated, MD has not been considered for integration with DH networks with the exception of Kullab and Martin [16], who investigated MD integration inside a CHP plant where heat is supplied from the line where heat is supplied to DH. The main objective of this study was to experimentally evaluate the long-term performance of the AGMD system, including membrane fouling. Even though MD-DH integration was assumed for full-scale simulation, the study did not address DH supply – MD demand heat balance and economic analyses of such integrations.

In examining DH networks more closely, temperature levels of supply and return lines are a primary factor in determining relevant MD integration approaches. Both supply and return temperatures depend upon the season, with higher temperature levels required as the outdoor temperature drops. (Temperature levels also vary between DH networks owing to embedded features, such as age of heat exchange equipment, length of DH supply and return lines, etc.) Supply temperatures can vary from 100°C in the winter to 70°C in the summer, while return temperatures correspondingly vary from 65 to 35°C [138]; mean annual supply temperatures of 86°C and 47°C, respectively, are representative values for a range of networks [139]. Both supply and return lines in a DH network can be used as heat sources to drive the MD process, and the return line can also serve as heat sink. The choice of connecting an MD process from one or both of these lines could be based on the system capacity, possibility of heat recovery at the location of the application, or a trade-off between capital costs and operating and maintenance costs. When considering MD-DH integration, it is important to keep the

industrial process in focus as well. Thus three systems need to be considered (Figure 3.3–3.5): MD system, DH network, and industrial process served by the MD system. Three generic MD-DH integration cases are possible, as explained below.

Case 1: MD driven by DH return line

In this case, shown in Figure 3.3, the feed to the MD system is heated by the DH return line, whose temperature can vary from 65°C–35°C depending upon the season, loads, and location along the line (i.e. return temperatures are lowest at the end of the DH network). An external heat sink such as a water body or cooling tower is the most likely scenario given the low temperatures involved, although thermal integration with the industrial process is possible. This type of MD integration delivers a relatively low temperature to the MD feed which leads to a lower production rate, but can be favorable if the heat price is low.

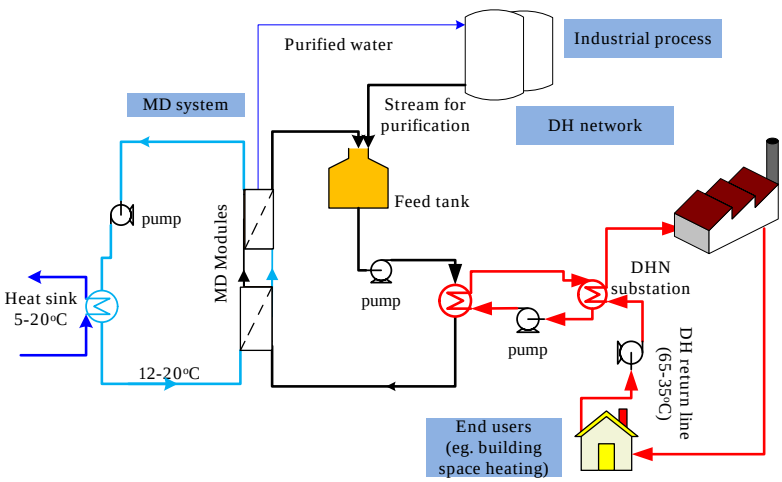

Figure 3.3. Case 1 configuration where feed to the MD system heated by a DH return line

Case 2: MD driven by DH supply line

In the second case of MD-DH integration (Figure 3.4), a DH supply line (100–70°C) can be considered a heat source for the MD system. The feed temperature can vary from about 90°C to 70°C, depending on DH supply line temperature. Use of the industrial process or other local heating needs can serve as a heat sink in addition to other cooling sources.

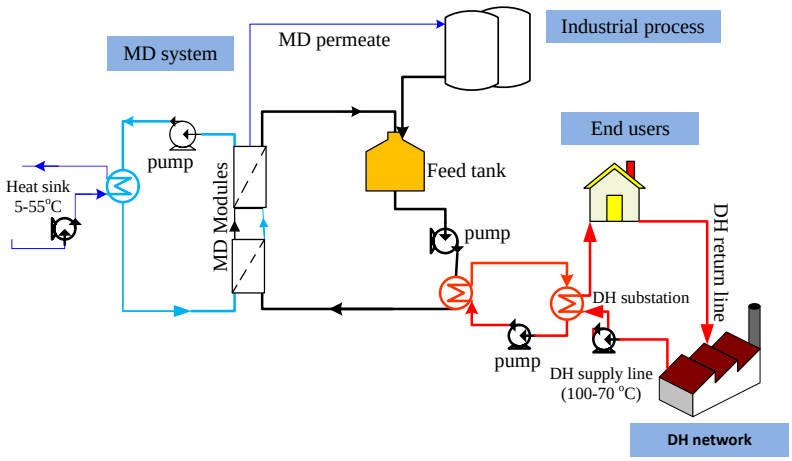

Figure 3.4 Case 2 MD-DH configuration where MD system is connected to a DH supply line

Case 3: DH supply line as heat source and return line as heat sink respectively

In the third case, shown in Figure 3.5, the MD system is considered to be integrated between a high temperature (100–70°C) DH supply line for heating the feed and a low temperature (35–50°C) DH return line used as cooling water. No other external cooling water source is assumed to be used here.

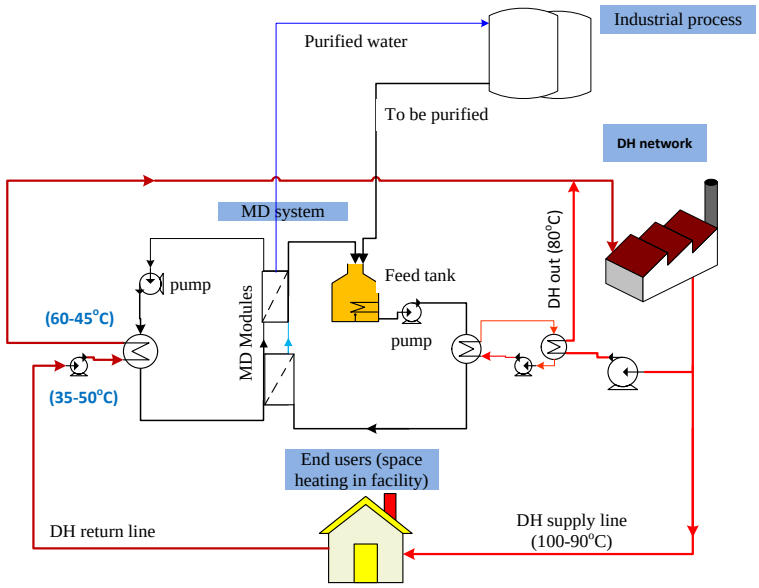

Figure 3.5. Case 3 configuration with the MD system placed between DH supply and return lines

3.3 Industrial case studies considered for the DH driven MD systems

In many industries different types of separation processes are required including water purification, recovery of valuable products from aqueous streams, and treatment of liquid waste or wastewater. Water purification is an important part of these separation processes in industrial production. Even though process water quality and complexity of wastewater compositions vary between industries, the trend of increased reuse or recycling of process streams together with stricter emission regulations lead to additional needs for water purification in the future.

Various possible application areas for MD were identified in this study with DH networks in focus, including treatment of flue gas condensate,

supplying ultrapure water, separation processes in the food industry, wastewater purification, reconcentration of valuable products, desalination, and others. Some of the processes that came to attention during identification of potential applications but not taken as case studies are discussed in following sections.

Treatment of flue gas condensate has been investigated previously from a pilot trial of MD [16]. The study showed that MD has very high efficiency (up to 99.9%) removal of heavy metals and ions present in the condensate, except for ammonia and carbon dioxide which passed through the membrane as volatiles. Later on, another study aimed at reducing the pH of the feed so that the ammonia gas in the condensate would be dissolved and leaking through the membrane would be prevented [140]. Even though the removal efficiency of MD for heavy metals and other ions was confirmed, addition of acids to the MD feed did not show complete dissolving of ammonia gas. The addition of acids to the feed for a longer time also risks the life of membranes and hence this application was not considered as a potential industrial application for this study.

Ultrapure water supply for processes such as semiconductor manufacturing [105], and pharmaceutical production, along with water purification in the food and beverage industry were other applications that were considered. While there is a significant amount of interest in employing MD technology in semiconductor manufacturing [141] the industry is no longer present in the Nordic countries. Ultrapure water standards for pharmaceuticals (pharmacopoeia) require the use of RO as a water treatment step, so the viability of MD as a replacement technology is judged to be low. Few studies showed that membrane distillation could be used for concentrating juice products [47, 115] and for the treatment of wastes from the production plants. However, none of these applications are judged to be of significant interest for the Swedish or Nordic industrial sector in this study. Desalination is also not a priority water supply technology in the Nordic countries, so this application has not been considered.

Cutting fluid wastewater purification was identified as a potential application. For example, Volvo Trucks in Skövde employs ultrafiltration (UF) and RO to treat cutting fluid effluent. Even though these used wastewater treatment procedures are fairly advanced, none were fully capable of removing all organics. A sample of UF-treated cutting fluid wastewater was sent to KTH for testing in a bench-scale MD unit. Preliminary unpublished results showed a low separation efficiency, which was linked to undesired wetting (i.e. penetration of liquid phase across the membrane). Therefore this application was judged to be not viable.

Skåne University Hospital in Lund has been in contact with Kraftringen Energi AB to explore the possibility of treating small amounts of wastewater associated with cancer treatment. Although promising, this application has some complexities in terms of hygiene and toxicity; hence it is suggested that it be considered for future work. Tekniska Verken AB in Linköping suggested MD as a water treatment technique for use in municipal swimming pools. The suggestion came at the latter part of the project period, hence it could not be considered. Water purification and reconcentrating at Arla Foods, Kalmar facility was done as a prestudy [142], and the poor thermal integration yields a high district heating demand for MD in this particular application. Hence this case study was omitted.

The three industrial case studies selected as potential DH driven MD applications that are believed to be promising for near future applications are the following:

- Drug residue removal from municipal wastewater treatment plant (WWTP) effluent: Municipal WWTPs employ quite complex sequences of purification and generally release safe effluents to the environment. However trace pollutants such as drug residues cannot be removed completely. A study on performance of MD systems for removal of pharmaceutical residues and economic assessments for anticipated large scale applications is discussed in Chapter 5.

- Wastewater treatment at AstraZeneca in Södertälje: It is theoretically possible to place MD between the district heating network and end users in order to achieve advanced treatment for a smaller wastewater line replacing the activated carbon treatment method. A technoconomic analysis of this process is presented in Chapter 6.
- Reconcentrating of ethanol from carbon dioxide-scrubber water at Agroetanol bioethanol production plant in Norrköping: The concept involves off-loading of the distillation column via the introduction of MD technology. The detailed analysis and discussion on this case study is presented in Chapter 7.

These proposed applications and designed systems will help add new applications of district heating in addition to improvements in the performance and economy of industrial processes. The use of DH for such industrial processes would promote its generation and use, which in turn will contribute increasing the fraction of renewables in the global energy mix. It is this notion that supplying heat for membrane distillation via district heating integration for industrial applications will play an important role in the expansion of renewable heat and electricity. In addition to the environmental benefits, the economic benefit of utilizing MD in bioethanol plant is, of course, the primary aim of this type of integration.

4 Experimental Methods and Systems Analyses

For experimental investigations analyzing the performance of membrane distillation systems, three types of AGMD module prototypes – Xzero, HVR and Elixir – were employed. The membrane material used for all the MD modules is PTFE with PP support. The membrane characteristics are 0.2 mm thickness, 0.2 µm average pore size, and 80% porosity. The Xzero module is part of a pilot-scale system, while HVR and Elixir modules were laboratory based. Xzero and Elixir modules are semi-commercial, i.e. the majority of key design features (membrane size, materials of construction, etc.) are more or less identical to the expected final product.

4.1 The AGMD pilot plant

The AGMD pilot plant was built in a joint project between KTH Royal Institute of Technology, IVL Swedish Environmental Institute, and Xzero AB. An illustration and photograph of the pilot plant is shown in Figure 4.1. The plant consists of ten AGMD modules arranged in five cascades, each containing two modules connected in series (denoted a and b in Figure 4.1).

The MD modules are assembled and supplied by Xzero AB and installed at Hammarby Sjöstadsverk, Stockholm, Sweden. The active membrane area for each module is 2.3 m^2 (with a total membrane area of 2.6 m^2) and they are constructed from a stack of ten cassettes, each containing two membranes. The size of one module is 63 cm wide and 73 cm high with a stack thickness of 17.5 cm. During the experiments, data was logged for parameters connected to the control system. Type-T thermocouples installed close to the MD modules inlet and outlet streams (see Figure 4.2) were used to measure temperatures, which were recorded

by the monitoring system. System control and data (temperature, pressure, and flow rates of feed and cooling water) were registered on a personal computer with Citect Runtime SCADA software installed. A YOKOGAWA DC402G dual cell conductivity analyzer (ranges of detection 1µS/cm – 25 mS/cm and accuracy of ±0.5%) was introduced to measure the conductivity of the product water. A Pt100 temperature sensor with an accuracy of ±0.4^{o}C was used for the measurement of the permeate temperature. Rotameters (±5% accuracy) were used to measure feed and cooling water flow rates.

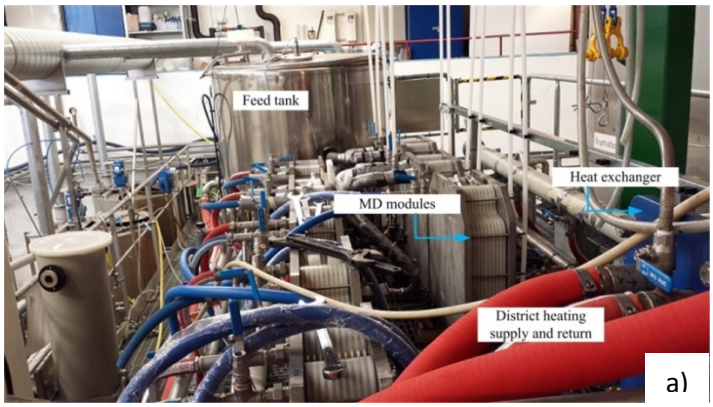

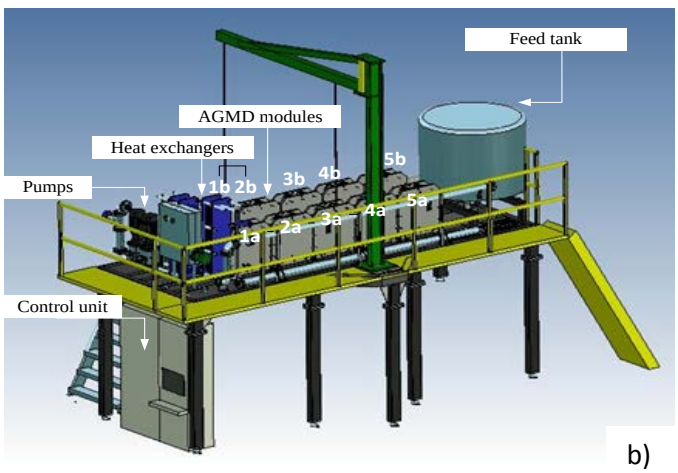

Figure 4.1. A Photograph (a) and 3D illustration (b) of the pilot membrane distillation system at Hammarby Sjöstadsverk.

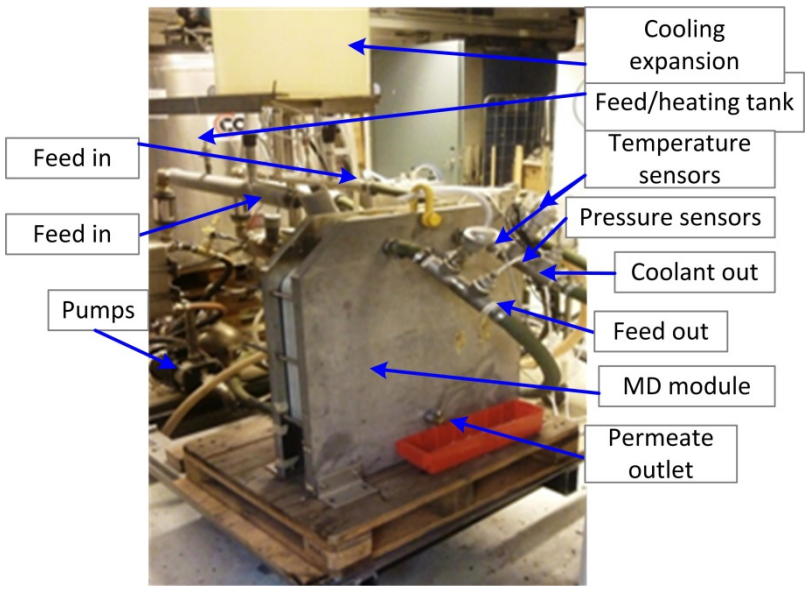

Figure 4.2. Features of the Xzero's 10-cassettes AGMD module

4.1.1 Experimental procedures

For the first test of pharmaceuticals removal by AGMD, effluent water from the municipal wastewater treatment plant at Henriksdal, Stockholm was filled into the feed tank of the MD system. Samples were taken every time the tank was filled, and conductivity and temperature were measured using the integrated sensors. During the tests for the effects of temperature and flow rates, permeate water (product water) was returned to the tank to keep the concentration constant. During the second stage test of concentrating the feed water, initial and final volumes at the points of sampling were measured and recorded.

Throughout the trial, feed and cooling water flow rates were kept a maximum flow rate of 1200 L/h based on a maximum pressure drop

across modules of 0.2 bar in serially connected modules, as recommended by the module supplier. (This arrangement allows for the temperature drop across each side to be as low as possible, thus enhancing yield.) The pharmaceutical removal test was run for three trials from October 2012 to June 2013, where each trial lasted for about a week. A concentrating test followed immediately after the third test and continued for more than three weeks with shutdowns during evenings. The concentrating test was carried out in three stages by refilling the tank with the feed, when minimum level is reached. At each stage feed and permeate water samples were taken and stored in a refrigerator for analysis of the concentration of the pharmaceutical residues.

4.1.2 Trials for removal of pharmaceuticals from wastewater

The MD tests, hereafter called trials 1 to 4, were performed to evaluate the removal of pharmaceuticals from municipal wastewater after standard biological treatment including sedimentation and sand filtration. Before it was supplied to the feed tank of the MD system, the feed water was pre-filtered with cartridge filter (10 μm). The first two trials compared the removal of pharmaceutical residues by two pairs of MD modules, the first pair (modules 1a and 1b) and last pair (modules 5a and 5b) as shown in Figure 4.1. During trials 1 and 2, the water was concentrated in the feed tank (1 run) by circulation without the addition of new feed water. For trial 1, feed temperatures were 53°C and 73°C whereas 57°C and 74°C were taken for trial 2. The experimental procedure for this case was done using a pair of electric heaters (12 kW each) to reach higher feed temperatures. These temperatures simulate the temperatures in return and supply lines in DH network. In trial 3, samples from both feed and permeate were taken during initial, half way and final stages of concentration in order to determine the degree of concentration of the pharmaceuticals. During trial 4, the feed tank was refilled with wastewater when the minimum volume in the tank was reached. Feed water was added 5 times to the same level as there was from the start to achieve a higher total concentration ratio. Similar temperatures were chosen for the third and fourth trials as in for Cases 1 and 2 while the temperature of the cooling water was kept at about 15°C for all four trials.

4.1.3 Method for analysis of pharmaceuticals

Water samples collected from the MD experiments (100 ml from the feed tank and 500 ml from permeate) were analyzed following the U.S. Environmental Protection Agency (EPA) method 1694 for determination of pharmaceuticals and personal care products (PPCPs) in multi-media environmental samples by high-performance liquid chromatography combined with tandem mass spectrometry (HPLC/MS/MS). The samples collected were spiked with surrogate standard Ibuprofen-d3 and Carbamazepine-13C15N. The sample was shaken for half an hour with a small addition of ethylenediaminetetraacetic acid (EDTA) before purification on a solid-phase extraction (SPE) column (200 mg Oasis HLB, Waters). The SPE column was preconditioned with methanol followed by milli-Q-purified water. Afterward, the sample was added to the column at a flow rate of two droplets per minute. The analytes were eluted from the column using methanol followed by acetone. The sample extract was evaporated to dryness under a stream of nitrogen at 40°C. The sample was reconstituted in methanol:water (1:1) and centrifuged before it was transferred to a vial.

The final determination of the concentration of pharmaceuticals in the samples was performed on a binary ultra-fast liquid chromatography (UFLC) system with auto-injection (Shimadzu, Japan). The chromatographic separation was performed on a C18 reversed phase column (dimensions 50 x 3 mm, particle size 2.5 µm; XBridge, Waters) at a temperature of 35°C and a flow rate of 0.3 ml/min. The mobile phase consisted of 10 mM acetic acid in water (A) and methanol (B). The UFLC system was coupled to an API 4000 triple stage quadrupole (MS/MS) (Applied Biosystems) with an electrospray ionization interface (ESI) applied in both positive and negative mode.

The accuracy of the chemical analysis for pharmaceuticals varies between the different substances analyzed. In this study, standard deviation ranged from 6 to 21%, with an average of 13%. This is based on investigations with four spiked samples prior to the real sample analysis. Percentage removal calculations were performed taking the method

detection limits as the possible highest concentrations of not detected pharmaceuticals.

4.1.4 Permeate flux analysis

Permeate flux (J) for a given MD unit can be defined as the total volume of product water obtained per unit area per unit time at a specified conditions (i.e. feed flow rate and temperature, cooling flow rate and temperature, membrane area, etc). The permeate flux (L/m^2h) was calculated using the volume of permeate collected within a given sampling time from the module's effective membrane area as follows:

$$\dot{m}_p = \frac{v}{t} \tag{4.1}$$

$$J = \frac{\dot{m}_p}{A} \tag{4.2}$$

where t and A refer time in h and membrane area in m^2 respectively. Data for the permeate yield was obtained from manual measurements by collecting a liter of permeate and recording the time required to fill the vessel. Permeate rate was calculated for cascades that each consisted of two modules connected in series as a and b (4.6 m^2 active membrane area) as shown in Figure 4.1.

Permeate yield is mainly affected by the feed temperature and flow rate for constant feed sample composition, cooling water, and membrane properties. In this study, feed flow rate, feed temperature, and cooling temperature were considered while keeping the other parameters (membrane, feed, and cooling flow rate) fixed at a time. Permeate flux is also used to compare different modules' performances.

4.2 Laboratory scale experimental setup and procedure

Two AGMD module types denoted HVR (photograph shown Figure 4.3 (a)) and Elixir (Figure 4.3. (b)), were tested at KTH to supplement results

obtained from the pilot facility and to characterize performance with water/ethanol feedstocks. Both modules have identical cassette-membrane inserts and differ only in condensation surfaces: the HVR module utilizes a heavy aluminum plate, while the Elixir module employs a thin-plate stainless steel condensation surface, with design features taken from commonly used plate-and-frame heat exchangers. Figure 4.3 shows a schematic of the experimental setups.

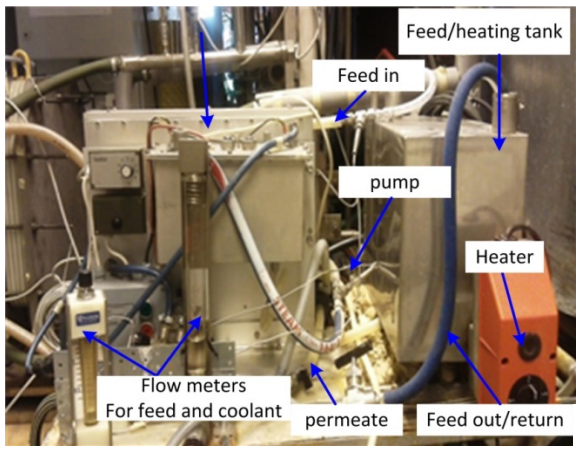

a)

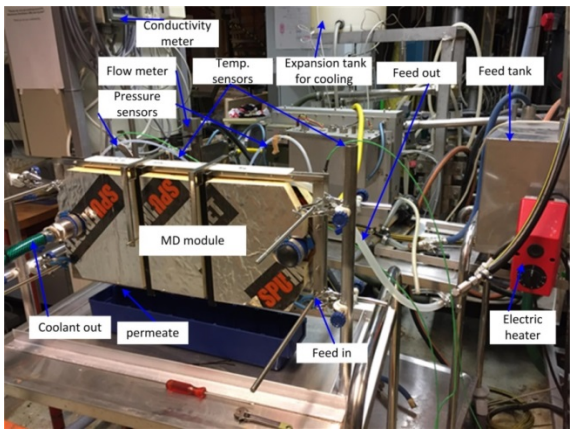

b)

Figure 4.3. Membrane distillation test units at KTH Energy Department, a) HVR module, b) Elixir module.

Two immersion heaters (combined rate of 4.5 kW) provide temperature control to feed water contained in a 24-liter tank (Figure 4.4 (a)). A small circulation pump and bypass valve allow the hot-side flow rate to be controlled, and a rotameter is employed to measure flow rate. Once-through tap water was used as a heat sink, which can be heat exchanged with a fan to obtain the lowest cooling temperature possible. Here a second rotameter with built-in control valve measures cold water flow rate in the cooling channel. Product ethanol is measured with a graduated cylinder and stopwatch, typically during a 30– minute period of steady operation. The obtained permeate was returned to the feed tank. In this case, the feed concentration was constant over the entire course of the AGMD investigations. For temperature measurement, thermocouples were installed at the inlets and outlets of the module and were connected to a data logger (Keithley 2701 DMM with a 7706 card). Experimental errors are as follows: temperature, ±1.50^{o}C; flow rate, ± 0.1 L/min; yield, ± 0.02 L/h.

The AGMD-HVR module consists of a 2.4 cm separation between two vertical condensation plates, behind which are located serpentine cooling channels. The experimental setup is almost similar to the case of AGMD-Elixir module but the condensate plate design is different (plate surface shape and thickness), and it consists of 2.1 cm separation between two stainless steel thin plates. A PP cassette with membranes attached to either side is placed between the condensation surfaces (cassette dimensions 42 cm wide by 24 cm high, total membrane area 0.19 m^2) for both MD modules. This arrangement provides for an initial gap of 9 mm on each side, although the actual gap size is reduced by bulging of the membranes during operation. The feedstock is introduced at the bottom of the cassette and flows out from the top, as seen in Figure 4. 4. (b).

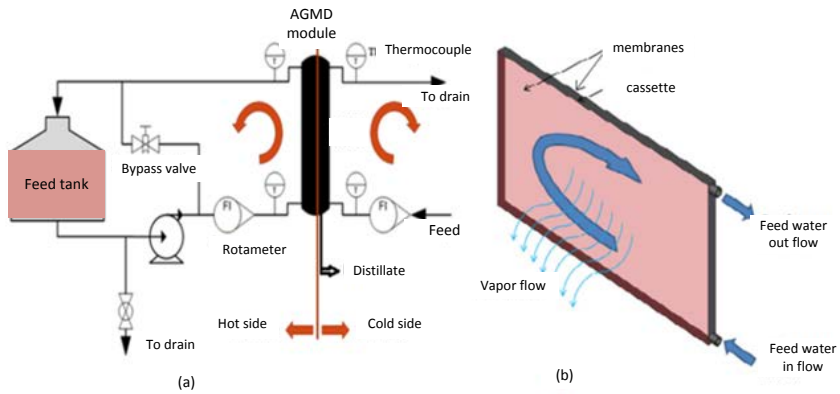

Figure 4.4. (a) MD bench scale unit setup at KTH lab (b) Membrane Cassette (MD) [35]

For the HVR AGMD experiments, the procedure consists of analyzing the performance of the system under different operating conditions, namely, various feed temperature and flow rate levels. The summary of test parameters for both modules is given in Table 4.1.

Table 4.1. Experimental conditions for the ethanol-water separation

Parameters	Value for HVR module	Value for Elixir module
Effective membrane area, m^2	0.38	0.38
Feed flow, L/min	2	4
Cooling flow, L/min	4, 10	2.3
Feed Ethanol % (wt./wt.)	4, 65	5
Feed temp. (^oC)	40, 45, 50	33
Cooling temp. (^oC)	13.5	15

4.3 Energy demand calculations

Removal performance of the MD process is the main parameter in evaluating MD's suitability for the desired water treatment applications; however, the other important issue for the feasibility of the technology for large scale applications is the energy demand. In addition to the amount of energy, which is mostly heat required for evaporating the feed water,

the type of energy and its cost are also crucial components in the technoeconomic study of the technology. During MD processes, a substantial amount of heat is transferred through the membranes, mainly as latent heat but partially also from conductive heat transfer.

4.3.1 Heat demand analysis

The energy demand analysis for Xzero MD unit was carried out on data collected during the pharmaceutical residue removal test from a period of more than 300 h or about 40 days of intermittent operation in total, during which the MD system was always shut down overnight. A number of tests were carried out focusing on independent variables like feed and cooling temperatures and flow rates. The energy analysis was conducted by considering a pair of modules connected in series as shown in Figure 4.1, which enables the system to have internal heat recovery. For the bench scale MD units, performance data was obtained from tests carried out using tap water and prepared ethanol-water solution as feeds.

Regarding post-processing, acquired data were analyzed to identify stable feed and cooling temperature values at particular operational conditions. The readings over a specified period were then averaged and used for the heat demand calculations. Moreover, a statistic test (Q-test at 0.05 CL) was used to decide if a suspicious value in a set of data is an outlier and so should be rejected. Errors or uncertainties on the reported values were calculated considering both the instrumental accuracy and standard deviations during measurements.

A feed-to-coolant temperature difference ΔT is defined for reference purposes as:

$$\Delta T = T_{f,i} - T_{c,i} \tag{4.3}$$

where $T_{f,i}$ and $T_{c,i}$ are the inlet temperatures of the hot feed and coolant, respectively.

The calculation of heat demand in the MD process focused on evaluating the change in heat transfer rate (heat input) on the feed water side in relation to possible sensible heat recovery on the cold side.

$$\dot{Q}_i = \dot{m}_i * c_p * \Delta T \tag{4.4}$$

The specific heat required to drive the MD process has been estimated in two ways: total specific heat input and the net specific heat demand for the production of a unit volume of permeate.
Specific heat input from the hot side,

$$\dot{Q}_{sp} = \left[\dot{m}_f * c_f * \left(T_{f,i} - T_{f,o}\right)\right]/\dot{v}_p \tag{4.5}$$

Net specific enthalpy change across the MD module[*],

$$\dot{Q}_{net} = \left[\dot{m}_f c_f \left(T_{f,i} - T_{f,o}\right) - \varphi \dot{m}_c c_c \left(T_{c,o} - T_{c,i}\right)\right]/\dot{v}_p \tag{4.6}$$

where $\dot{m}$ and $\dot{v}$ stand for mass and volume flow rates respectively, c denotes specific heat capacity of water, subscripts c and f stand for cold and feed, p for permeate, i and o represent inlet and outlet, respectively. The variable φ refers to the possibility of heat recovery on the cold side, and assumes a value of 1 if heat is recovered or 0 otherwise. The permeate heat loss can be determined from the temperature of permeate and its flow rate as follows in Eq. (4.7) with reference to the surrounding temperature:

$$\dot{Q}_p = \dot{m}_p * c_p * (T_p - T_o) \tag{4.7}$$

where T_p is the permeate's measured temperature and T_o is the reference temperature. There is also a small amount of electrical energy required for running the two low-pressure pumps which were also calculated from the flow rates of water and pressure drop across the modules as follows in Eq. (4.8).

[*] In (4.5) and (4.6) mass flow rate is assumed to be constant during single pass across feed side, i.e. $\dot{m}_f \gg \dot{m}_p$, and concentrations of contaminants in the aqueous feed are low.

$$\dot{Q}_p = (\Delta P * v)/\mu \tag{4.8}$$

where ΔP is the pressure drop, v is the volume flow rate in m^3/h, and μ is the pump efficiency. When specific and total input heat are known for a large scale MD system, the permeate production rate can be calculated using the relation in Eq. (4.9).

$$M_p = \frac{Q_{sp}}{Q_i} \tag{4.9}$$

4.3.2 MD module heat loss calculations

AGMD generally has lower latent heat loss than DCMD due to the air gap barrier introduced between the hot feed and coolant sides. While the majority of heat from the feed is recovered on the cooling side, a significant amount of heat can flow to the surrounding from permeate, or from the module surfaces through natural convection. Hence, it is important to determine heat losses by those mechanisms and evaluate net heat demand so that module improvement design considers minimizing the heat losses. Balancing the heat contents of all streams around the module can give an account of lost heat. In other words the heat delivered by the hot feed balances the heat gains in coolant stream, permeate and the convective heat transfer through the surrounding air. The difference between these supply and gains is the real loss that is difficult to minimize. The different heat flows around the modules and the rate of net heat loss are described in Eq. (4.10).

$$\dot{Q}_l = \dot{Q}_{net} - (\dot{Q}_{cv} + \dot{Q}_p) \tag{4.10}$$

where, $\dot{Q}_{net}$ the rate of net heat transferred from feed, $\dot{Q}_{cv}$ the heat transfer rate due to convectional process, and $\dot{Q}_p$ is the heat transfer rate from the permeate.

External frames of the Xzero AGMD modules considered in this study are made of steel plates attached next to rubber insulators separating the

cooling plate from the outer cover. During the experiments, the steel covers were warmer than the room temperature causing heat loss to the surroundings. Free convection heat loss from the MD module surfaces was considered in addition to heat loss through the permeate. Free convection was considered as the main cause of heat loss to the surroundings. This is because there was no ventilation near the module that would affect the movement of air around the MD modules. Radiative losses along with conductive losses through the base and attached piping are assumed to be negligible.

The heat loss calculation was done using Engineering Equation Solver (EES) first by calculating the coefficient of heat transfer and then determining the heat transfer rate from the hot plates to the atmosphere very far from the module using Eq.(4.11).

$$\dot{Q}_{cv} = h * A * (T_p - T_\infty) \tag{4.11}$$

here, $\dot{Q}_{cv}$ is the heat transfer rate by convection, h is the heat transfer coefficient, A is the area of the module surface and T_p and T_∞ are temperatures of the module surface and the atmospheric air far from the module respectively. The dimensions of the Xzero AGMD modules used to determine A in Eq. (4.11) are shown in Figure 4.5.

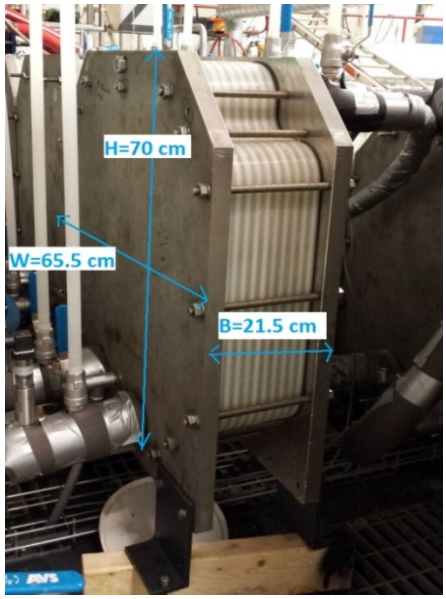

Figure 4.5.The Xzero AGMD module and its dimensions used for free convection heat loss calculations

Thermal efficiency was determined to analyze the effect of different feed temperatures on the efficiency of the MD process.It was calculated from the ratio of the latent heat of vaporization (ΔH_{vap}) of the feed mixture to the specific heat input (Q_{sp}) from equation (2) as:

$$\eta = 100 * \left(\frac{\Delta H_{vap}}{\dot{Q}_{sp}}\right) * \frac{\rho}{3600} \tag{4.12}$$

where the ratio $3600/\rho$ is a unit conversion factor for Q_{sp} from kWh/m^3 obtained from equation (3.2) into units of kJ/kg and ρ takes the value for the density of permeate.

4.4 Exergy analyses

The exergy rates of each stream throughout the MD system and the exergy efficiencies of the MD modules are analyzed by taking the basic exergy definitions [143] and relationships for MD models as reported in the literature [144–146]. The intensive parameters governing the MD

process are temperature and composition, and exergies related to kinetic and potential are not considered. Hence the exergy rate is the sum of the physical and chemical exergies of streams as given by equation (4.13).

$$Ex = Ex_{ph} + Ex_{ch} \tag{4.13}$$

Ex_{ph} represents the thermomechanical exergy based on the temperature of the stream and Ex_{ch} refers to the chemical exergy from the chemical potentials of the solute components in the stream. The physical exergy can be expressed in terms of heat enthalpies and entropies at the specified condition (h, s) and reference condition (h_o, s_o) by equation (4.14).

$$Ex_{ph} = (h - h_o) - T_o(s - s_o) \tag{4.14}$$

The individual exergies due to pressure and temperature are calculated independently and sum up to give physical exergy. Even though the working pressure in MD is generally very low, its effect could be detected in exergy destruction calculations due to pressure changes especially in series configured modules. These pressure and temperature related exergies are given as follows, in equations (4.15) and (4.16) [144, 147].

$$Ex_p = \dot{m} * (p - p_o)/\rho \tag{4.15}$$

$$Ex_T = \dot{m} * c * [(h - h_o) - T_o * (s - s_o)] \tag{4.16}$$

Chemical exergy based on the chemical potentials or concentrations of the components in the stream is calculated as in equation (4.17).

$$Ex_{ch} = -\dot{m} * N_s * R * T_o * lnx_s \tag{4.17}$$

$$\text{where } N_s = (1000 - \sum C_j/\rho)/MW_s \tag{4.18}$$

$$\text{and } x_s = {}^{N_s}\Big/\left[N_s + \sum(\beta_j * C_j/\rho * MW_s)\right] \tag{4.19}$$

The exergy change across the MD module or any other component of the MD system is calculated from the differences in inlet and outlet exergies as:

$$\Delta Ex = \sum Ex_i - \sum Ex_o \tag{4.20}$$

The second law efficiency of the MD system is the ratio of the minimum exergy input required (which is equivalent to the minimum work of separation) to the total actual exergy input:

$$\varepsilon = (W_{min}/Ex_i) * 100 \tag{4.21}$$

The minimum work input required for the MD process is the difference between outgoing and incoming total exergies of the hot stream:

$$W_{min} = Ex_p + E_{f,o} - Ex_{f,i} \tag{4.22}$$

The exergy destruction due to irreversibility in the process is calculated by subtracting exergy difference from the sum of electrical and thermal exergies [147] according to the Gouy–Stodola formula,

$$Ex_{dest} = S_{gen}T_0 \tag{4.23}$$

where T_o is the reference temperature, and S_{gen} is the entropy generated due to irreversibility in the process and given as:

$$S_{gen} = \Delta S_{total} = \Delta S_{source} + \Delta S_{sink} = \frac{Q_{source}}{T_{source}} + \frac{Q_{sink}}{T_{sink}} \tag{4.24}$$

where the Q_{source} and Q_{sink} represent for the heat lost and gained from the heat source and sink respectively.

The electrical exergy input for the pumps is:

$$Ex_{el} = \frac{m * \Delta P}{(1000 * \eta_p} \tag{4.25}$$

where ΔP is the pressure head in Pa and η_p is for pump efficiency. Electrical energy consumed for driving the pumps is taken as pure exergy. For simplicity the exergy destroyed can be expressed a percentage as related to the exergy input:

$$\varphi = 100 * \frac{Ex_{dest}}{Ex_i} \tag{4.26}$$

Ex_{dest} of a component is then calculated the fraction of exergy destruction by the particular component in comparison to the total destroyed exergy,

$$\mathrm{Ex_{dest}} = 100 * \frac{\mathrm{Ex_{dest,i}}}{\mathrm{Ex_{dest,total}}} \tag{4.27}$$

where $Ex_{dest,i}$ is the exergy destroyed in component i, and $Ex_{dest,total}$ is the total exergy destroyed in the MD system.

For the distillation columns the exergetic inputs are from the feed (f) and the heat added in the reboiler (r) whereas the exergetic outputs are from the products i.e. distillate (d) and bottom (b), and also the heat removed in the condenser (cd) defined as [148]:

$$Ex_{loss} = T_0 * S_{gen} = Ex_f - Ex_d - Ex_b + Q_r * \left(1 - \frac{T_o}{T_r}\right) - Q_{cd} * \left(1 - \frac{T_o}{T_{cd}}\right) - Q_{col} * \left(1 - \frac{T_o}{T_{col}}\right) \tag{4.28}$$

$$\varepsilon = 100 * \frac{W_{min}}{(W_{min} + Ex_{loss})} \tag{4.29}$$

$$\text{where, } W_{min} = Ex_b + Ex_d - Ex_f \tag{4.30}$$

Similarly for the MD process the minimum required work (W_{min}) is calculated from,

$$W_{min} = Ex_p + Ex_{f,i} - Ex_{f,o} \tag{4.31}$$

where, the subscripts *p*, *f,i* and *f,o* refer permeate, feed into out of the MD modules respectively.

4.5 Capacity requirement and heat demand calculations for large-scale MD systems

The experimental investigations on the performance of the tested AGMD module for the desired separation application serve as one parameter for the engineer's assessment if it can be applied for large-scale production. The capacity requirement and heat demand of a large-scale MD plant can be simulated by scaling up of experimental test results. The full-scale simulation includes calculation of membrane area required, heat demand for the MD plant, and the portion of heat that could be recovered for space and wastewater supply heating. Two MD module designs were considered for the simulation of large-scale applications: Xzero and Elixir. The separation efficiency exhibited by each module for a given feedstock is assumed to be interchangeable; tests with arsenic-contaminated water [35] demonstrate this validity. Each MD system considers parallel arrays of two series-connected modules for enhancing internal heat recovery. The total membrane area (A_m) for the desired total purification rate (M_p) can be calculated from the pair of series-connected module's membrane area (a_m) and measured permeate flux for the particular module:

$$A_m = a_m * \frac{\dot{M}_p}{\dot{m}_p} \tag{4.32}$$

4.6 Economic assessment

For a complete evaluation of the feasibility of membrane distillation technology at industrial scale, both the technological and economic aspects should be taken into consideration. As the MD technology is not yet fully commercial, it is difficult to obtain accurate data for economic evaluations. However, large scale costs can be estimated using a capacity method, which is based on assuming a reduction in specific costs with increasing capacity [123]. The cost C_I for a given anticipated capacity K_I, can be derived from a reference capacity K_{ref}, its reference cost C_{ref} and degression coefficient m according to Eq. (4.33).

$$\mathrm{C_I} = C_{ref} * (\frac{\mathrm{K_I}}{\mathrm{K_{ref}}})^{\mathrm{m}} \tag{4.33}$$

Degression coefficient, m is usually in the range of 0.5 to 1, for pumps and heat exchangers is taken to have 0.8, due to cost reductions in increasing power and heat transfer area respectively. The cost reductions for tanks and pumps are proposed with a degression coefficient of 0.6 and 0.85 was taken for MD modules [123].

The major parameters during economic evaluations of membrane distillation are: capital expenditure (CAPEX), operational and maintenance expenditures (OPMEX), and the unit cost of purified water using the technology. The capital cost includes costs of MD modules, heat exchangers, pumps, pre-treatment and post-treatment units, sensors and control units, civil works and infrastructure like district heating line connection. These capital costs were then distributed over the amortization time n of the MD plant assuming a fixed interest rate of z and capital expenditures CAPEX to obtain the annual CAPEX (C_a) by using Eq. (4.34).

$$C_a = \frac{z * (1+z)^n}{(1+z)^n - 1} C_I \tag{4.34}$$

OPMEX for the MD plant include costs of service and maintenance, insurance, membrane replacement, personnel, analyses, thermal energy, electricity, chemicals and disposal (Eq. 4.35). Annual service and maint-

enance (SM) cost for MD system is assumed here to be 2.5% of the capital expenditure, insurance (In) costs is taken to be 0.5% of CAPEX. Annual labor cost a_L is calculated from the unit labor cost C_L of 0.03 $\$/m^3$ [149]. Chemicals are mainly required for cleaning the membranes and also during analyses, and the annual cost for chemical and disposal C_{CD} is calculated from chemical related expenses of 0.018 $\$/m^3$ of purified water [149]. The total annual operational and maintenance cost $OPMEX_a$ is the sum of all those annual costs listed above:

$$OPMEX_a = C_{In} + C_M + C_L + C_{th} + C_{el} + C_{CD} \tag{4.35}$$

Annual permeate production rate is calculated from permeate flow rate m_p and the number of hours in a year as:

$$M_p = 8760 * m_p \tag{4.36}$$

Annual costs for heat C_{th} and electricity C_{el} are also derived from annual heat Q_a and electricity El_a demands and specific heat Q_{sp} and electricity El_{sp} costs.

The membrane replacement costs are derived from the assumption that the lifetime of membranes in modules is five years which corresponds to three replacements in the whole lifetime of the MD plant. Annual membrane costs a_M are estimated from Eq. (4.34) assuming amortization time n of five years and replacing CAPEX for membrane costs.

Finally, the unit cost of purified water, C_w is calculated from the sum of all the annual costs and divided by the sum to the annual permeate production using Eq. (4.37).

$$C_w = \frac{(C_a + C_M + C_{th} + C_{el} + C_I + C_{SM} + C_L + C_{CD})}{M_p} \tag{4.37}$$

5 Integration of Membrane Distillation in Wastewater Treatment Plants

Municipal wastewater treatment plants involve combinations of filtration, biological or chemical degradation, adsorption, sedimentation, and disinfection. Modern WWTP's release pathogen-free treated water with satisfactory levels of chemical oxygen demand (COD), biological oxygen demand (BOD), and other parameters. However, trace substances such as pharmaceutical residues are starting to become a concern. The exact impact that such very low concentrations may have on ecosystems is uncertain, although research has shown a possible link between pharmaceutical residues and altered fish behavior [150], thus implying that even small pharmaceutical pollutant levels affect aquatic habitats. It was reported [151] that treated municipal wastewater contains a variety of drug residues, and the elimination of such substances is difficult even with modern water treatment methods [152–154]. A study carried out on effluents from four WWTPs in Sweden [155] showed that 85 out of the 101 pharmaceuticals considered in the survey were detected in at least one of the effluents of the WWTPs with diclofenac having the highest concentration at 3.9 µg/L. Some levels of pharmaceuticals were also detected in surface water, biota and in drinking water samples [155].

In order to achieve near-complete removal of pharmaceutical residues, at least one or more advanced techniques in addition to currently adopted methods are required. Concerning membrane processes, it was reported that nanofiltration and reverse osmosis are efficient for removal of pharmaceuticals due to their lower pore sizes than the micro and ultrafiltration membrane processes [156, 157]. The limitations of such high-pressure driven membrane techniques are the high electric power demand, the high risk of membrane fouling by the natural organic matter, and discharge of concentrates [158, 159]. The performance of a biological

reactor using activated sludge was evaluated for removal of ibuprofen, naproxen, and sulfamethoxazole in a Spanish WWTP [160]. Percentage removals of 70% for ibuprofen, 40–55% for naproxen and around 67% for sulfamethoxazole were obtained [160]. M. Clara et. al. [161] studied the removal efficiency of a membrane bioreactor (MBR) and made comparisons with activated sludge plants in Austria. The results from their study showed that high removal percentages (97–99%) could be attained for ibuprofen by both MBR and conventional WWTPs. The MBR process was found to remove a maximum of 65% of sulfamethoxazole and up to 32% of it by the conventional WWTP. The studied methods did not show the removal of carbamazepine [161]. In other investigations [160–164] ultrafiltration (UF) and nanofiltration (NF) were tested for retaining pharmaceuticals. Even though average retention by NF for some pharmaceuticals like naproxen was as low as less than 10%, it was found to be a higher percentage of retention (30–90%) than by UF which had typical retention percentages of less than 30%. In another study [152], nanofiltration showed retention of 90% for hydrochlorothiazide and100% for diclofenac, even though higher retentions were obtained from reverse osmosis. Researchers from China [165] experimented with degradation of pharmaceuticals by photolysis and oxidation in the presence of hydrogen peroxide which resulted in the destruction of pharmaceuticals in the range of 25–95%, but here the decomposition reaction produced smaller organic compounds whose effect should be considered. Treatment by activated carbon and ozone were studied as a polishing step after MBR treatment to remove remaining pharmaceutical residues [166]. Membrane distillation was tested as an on-line method for estimating pharmaceutical residue levels via reconcentrating pharmaceuticals [98]. To date there are no complete studies that consider MD systems for the removal of pharmaceutical residuals.

In this chapter, MD powered by DH networks is explored for possible applications in municipal WWTP's. Handling such large flows of municipal WWTP effluents by MD requires very large membrane area and hence is costly. The interest here is to examine if a fraction of the effluent could be treated as a complement to the WWTP, or as a means to provide ultrapure water or other process water stream.

5.1 Removal of pharmaceuticals from WWTP effluent

Prior to testing feed from WWTP effluent was analyzed for the concentrations of pharmaceutical compounds. Among the 37 different compounds analyzed in the treated wastewater, 21 were detected in the first and second trials, while 22 and 20 substances were detected in trials 3 and 4, respectively. (See section 4.1.2 for a detailed description of the experimental procedure.) Results of the WWTP effluent analyses from the four different trials are summarized in Figure 5.1. These results show that the treated wastewater effluent still has some amounts of pharmaceuticals left even though the concentrations are very low with a maximum of 1 µg/l.

The MD permeate analyses from trials one and two yielded values under method detection limits for all pharmaceutical compounds except for Sertraline (see exact detection limits at each analysis in Tables A.1 to A. 7 in Appendix). In trial three, samples from initial, halfway and final stages of concentration of a single feed batch were analyzed. Among the 37 analyzed pharmaceuticals, Metoprolol and Citalopram were detected in the MD permeate. The pH of the concentrate during this trial changed through the concentration step from 7.0 to 8.5 while the pH of the permeate was between 6.5 and 6.9 (except for one measurement of 7.4 at half tank). This pH change could be caused by the build-up of responsible ions during the concentration process.

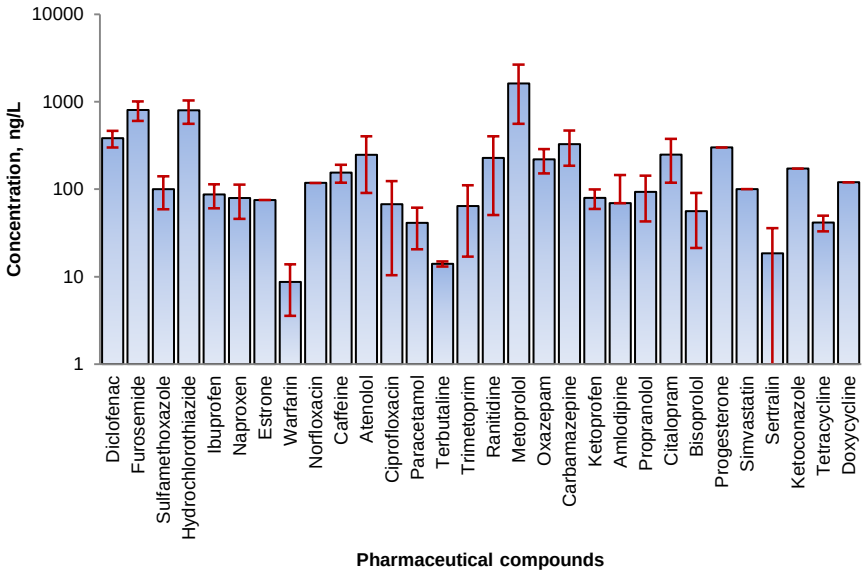

Figure 5.1. The concentrations of pharmaceutical residues in WWTP effluent water during trials 1-4.

All ten MD modules gave similar removal performance for all the pharmaceutical compounds tested. Only Metoprolol and Citalopram analyses showed very small differences in their concentrations between modules 4a and 5a during trial three. It is during this trial that these compounds were detected in permeate samples, although the percent removals were greater than 99.5% in both cases.

During the concentrating test from trial four, the concentrations of pharmaceuticals were generally found to increase with a decrease in volume of the MD feed in the tank. The concentrating stage followed three steps in which a total of about 2000 liters of the feed was concentrated to about 300 liters; that means 85% recovery. The result of analyses of the pharmaceutical residues from the MD feed during these concentration steps is summarized in Figure 5.2.

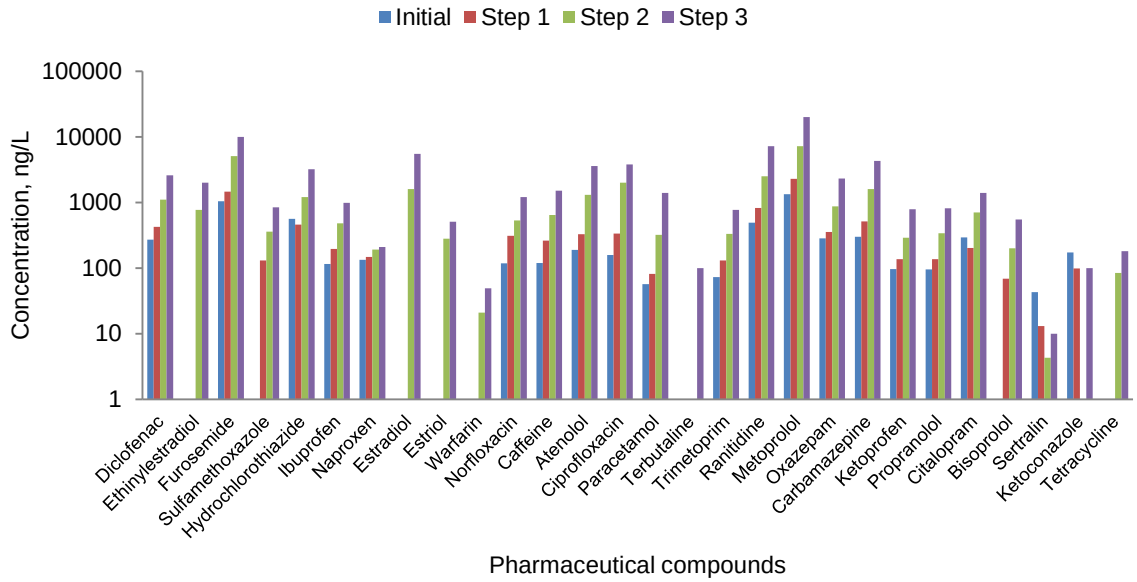

Figure 5.2. Levels of the pharmaceutical compounds analyzed in the MD feed during concentrating trial 4.

Permeates analyses from the concentrating steps (trial 4) showed that only Caffeine (51.5%–100% removal) at first stage of concentration and Sertraline (-70%–100% removal) in all the three stages were detected. Sertraline followed a slightly different trend both in permeate and feed during the concentrating process as shown in Figure 5.3. This unique trend could be attributed to high log K_{ow} value (5.76) which makes its adsorption and permeation potential through the organic membranes higher. The adsorbed Sertraline onto membrane and hose surfaces could later be desorbed and create the type of ups and downs in the concentrations of the feed and permeate as seen in Figure 5.3.

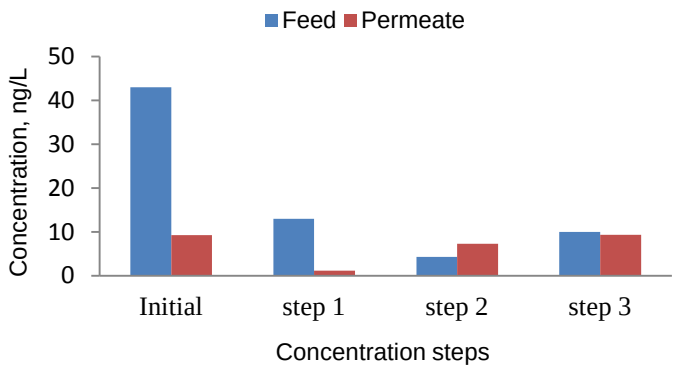

Figure 5.3. Levels of Sertraline in feed and permeate at each step of concentration during trial four.

When the performance of the AGMD tested is compared with related membrane-based technologies from literature, in most cases, NF and RO were found to have comparable removal performances. The summary of comparison in removal percentage between AGMD and eight other processes is given in Table 5.1. The removal efficiency of AGMD in most cases is greater than the other competing technologies. It is evident that RO has an efficiency of removal close to AGMD. However the performance of RO is highly affected by feed concentrations while the removal efficiency of MD shows little deterioration for such cases.

Table 5.1. Summary of the percentage removal by different processes from literature and comparison with results from present study

		Activated Sludge	*MBR*	*MBR+(Fs)*[*]	*NF+UF*	*NF*	*RO*	*UV Ox*[†].	*FO*	*MD*
	References	[47[*], 50]	[48[*], 50]	[164]	[167]	[152]	[152]	[165]	[168]	Present study
1	Atenolol	0–97	65–77							100
2	Carbamazepine	-122–58	0* -22–23		0–80	98–99	99–100		95–100	100[‡]
3	Ciprofloxacin			90						100
4	Diclofenac	-143–80	-8–87	-105	0–70	100	100		90–100	100
5	Estradiol			47	0–77					100
6	Estriol				0–80					100
7	Estrone			78	0–90					100
8	Ethinylestradiol				0–90					100
9	Hydrochlorothiazide	0–76	0–66.3			85–95	90–100			100
10	Ibuprofen	70*, 52–99	90*89–99.8	99	15–80			0–45	82–97	100
11	Ketoprofen	9–91	43.9–97			90–105	50–115			100
12	Metoprolol	-1–77	29–58			90–105	50–110			99.9–100
13	Naproxen	40–55*,-2–98	71–99	94	0–20				63–95	100
14	Norfloxacin			70						100
15	Propranolol	59	65–77							100
16	Ranitidine	24–42	29–95							100
17	Sulfamethoxazole	67*,-138–99	57–90		0–60	90–105	100			100
18	Trimetoprim	-40–40	47–66		0–80					100

[*] Flocculation followed by sedimentation

[†] Oxidation with UV

‡ 100% removal means the substance is found to be below detection limit

The MD application studied here requires evaporation of a large amount of water, which might seem disadvantageous with other chemical methods such as adsorption by activated carbon. However, activated carbon requires costly disposal of used adsorbent, and it does not guarantee zero liquid discharge scenario in industries.

Concentration levels of the analyzed pharmaceuticals showed a generally increasing during reconcentration experiments. For example during trial three the feed was concentrated in two steps, first to half feed-volume and in the second step further to a quarter of the initial volume. The change in concentrations of some of the pharmaceuticals did not show a proportional inverse relationship as shown in Table 5.2. There can be many reasons as for why some of the pharmaceuticals increase in their concentration as high as eight times the initial level though volume is reduced only to about a quarter of the initial volume. One reason could be the contamination of the feed from the surfaces of recirculating tank, hoses, and membranes as the MD system had been used previously for similar tests. Others like Terbutaline, Sertraline, and Tetracycline were detected in the feed but not in the concentrate. This also could be because of adsorption of these compounds on the surfaces of tubes, the tank and membranes during the MD process which led to decrease in their concentration in the concentrates.

Table 5.2. Concentrations (ng/L) of the detected pharmaceuticals during concentrating steps in trial 3

Substance:	*Feed*	*1/2 feed*	*1/4 feed*
Atenolol	515	740	2540
Bisoprolol	114	152	405
Caffeine	190	424	1413
Carbamazepine	562	702	1644
Ciprofloxacin	73	121	633
Citalopram	439	513	692
Diclofenac	481	496	795
Furosemide	966	780	1683
Hydrochlorothiazide	612	124	115
Ibuprofen	112	130	52
Ketoprofen	68	29	136
Metoprolol	3403	4861	13787
Naproxen	66	50	82
Oxazepam	124	56	75
Paracetamol	66	77	218
Propranolol	174	198	374
Ranitidine	286	260	1405
Sulfamethoxazole	164	185	284
Trimetoprim	137	201	648

5.2 Permeate flux

An overview of permeate flux as a function of feed temperature is presented in Figure 5.4. Permeate yield increases with increasing difference in temperature between module feed and coolant. As this temperature difference is reduced, the vapor pressure difference across the membrane decreases which in turn reduces the permeate flux (equation 2.2). Permeate yield was found to be lower in the second module (roughly 40–65% of the first module) owing to the lower feed inlet temperature.

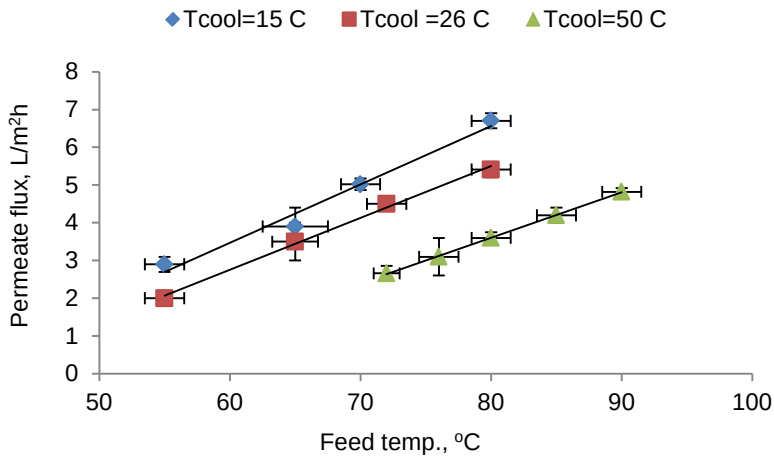

Figure 5.4. Permeate fluxes from different feed and cooling water temperatures at 1200 l/h module feed and cooling flow rates.

Another important parameter is the module feed flow rate, which also has a positive relationship with permeate flow rate. The permeate yield for different flow rates of module feed and coolant is shown in Figure 5.5. An increase in those flow rates increases the permeate yield with a linear trend, in line with results obtained by other researchers [51, 169]. Even though increasing the feed flow rate results in increasing the permeate production, pressure drop and hence pumping power also increase which will have an effect on the operation economy. In addition there is a maximum pressure drop that should not be exceeded to maintain the integrity of the membrane.

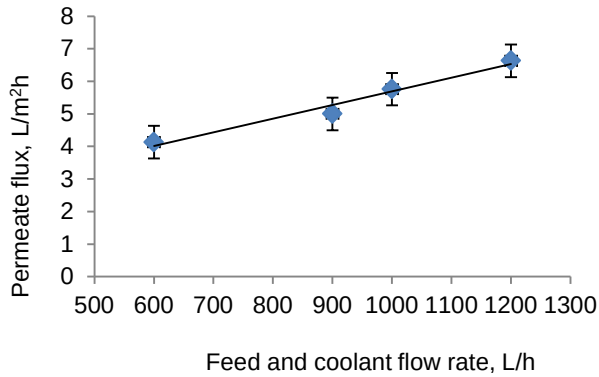

Figure 5.5. Permeate yield at different module feed and cooling water flow rates (600 –1200 L/h) at constant module feed temperature of 80°C and coolant temperature of 15°C.

Knowing the effect of feed flow rate on permeate yield helps designers choose the right pumping unit. For the ranges of feed flows tested, the specific electricity demand was 0.35 kWh/m^3, indicating that such conditions have a low electricity demand unlike the high-pressure membrane based technologies like RO.

As discussed in the introduction part, membrane fouling is a challenge in any MD process and particularly when the feed contains organic matter such as in wastewater treatment cases. The experimental study performed previously on these MD modules using treated municipal wastewater as feed did not include membrane fouling examinations. However, the signs of severe membrane fouling such as a decline in the permeate flux or quality of permeate were not observed during the 300 h test period.

5.3 Heat demand analysis

5.3.1 Specific heat demand

The results of the specific heat demand analyses at different feed and coolant temperatures are summarized in Figure 5.6. One reason for the rise in heat demand with increasing feed temperature can be due to improved heat transfer to the coolant at higher temperature difference across the membrane or higher temperature difference between feed in

and feed out streams as in Eq. 3.2. Even though the permeate flux is also higher for hotter feeds, the greater heat losses to the module covers and the surrounding air play a significant role, especially at higher coolant temperatures. The role of heat loss in raising the specific heat demand can be seen more significantly for coolant temperature of 50°C in Figure 5.6. The net heat demand at a coolant temperature of 50°C, on the other hand, is declining with increasing feed temperature, which is due to the greater heat recovery at higher feed temperature.

For MD-DH integration Cases 1 and 2 (Figures 3.4 and 3.5), the specific heat demand at 15°C coolant is lower than at 26°C coolant due to the larger permeate flux at lower coolant temperature. For calculations of annual heat demand for an anticipated plant capacity 15°C coolant temperature was considered. Case 1 integration enables the CHP plant operators to receive lower temperatures of district heating return which will help them to increase electricity production and hence enhance their competitiveness in the market through green certificates. The higher temperature difference across the membrane in Case 2 leads to a higher permeate yield than in Case 1. The specific heat demand at 80°C feed temperature is found to decrease as cooling temperature decreases from 50 to 15°C. Two factors play a role for this trend, the first is the increasing permeate flux and the second is reduced heat loss at lower cooling temperature.

As summarized in Figure 5.6, Case 3 integration considers both the feed and cooling temperatures at relatively high values, and exhibits a higher heat demand than the previous two cases. However in this case heat can be recovered from the cooling side, which makes the net specific heat demand the parameter of interest when discussing this case. The reduction in net specific heat demand with increasing feed temperature in Case 3 is due to the increased heat transfer to the cooling water, which is recovered. This approach of MD integration has advantages of recovering heat from the relatively high-temperature return line of DHN and from the cooling outlet in addition to the favorable heat gain from the DH supply line.

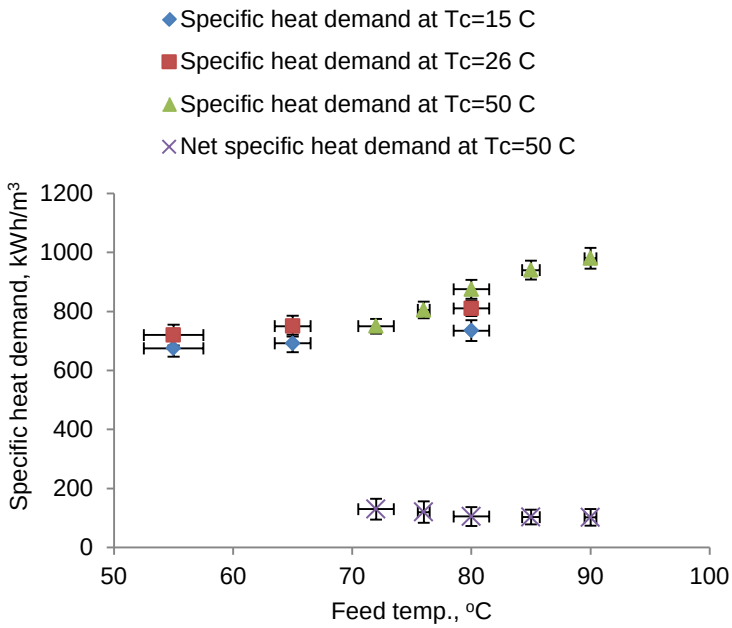

Figure 5.6 Specific heat demand and net heat demand at 1200 l/h module feed and cooling water flow for different module feed and cooling temperatures.

5.3.2 Heat losses from the MD modules

The heat transfer rate from the module surface to the surroundings due to natural convection was determined using Eq. (3.7). The calculated values of the heat transfer coefficient (h) for free convection lies in the range of 1 to 10 W/m^{2}K, which is in the lower range of heat transfer coefficient values for natural convective cooling by air. The result of heat loss calculation is summarized in Table 5.3. The total heat loss Q_l increased at higher feed and coolant temperatures which indicate more heat transfer from module surfaces and permeate. In theory, one can avoid heat losses due to convection from module surfaces and sensible heat loss from permeate is carried out by using the most advantageous condensation surface, insulation and heat recovery mechanism. The calculated heat demands using Eq. 4.8 could be lowered significantly achieving specific heat demands in the range of 655 kWh/m^3 (Case-1) to 882 kWh/m^3

(Case-3). For Case-3, with possible heat recovery from coolant side will have net specific heat demand of 4–80 kWh/m^3. The heat loss calculations show that how much the efficiency of the tested modules are affected and showed the need for better module developments to minimize heat losses from the MD modules.

Table 5.3. Heat loss through the permeate (Qp) and free convection (Qcv.) given as kWh/m^3 of produced permeate at different module feed and cooling temperatures

Cooling temp. °C	Feed temp. °C	Spec. Q_p, kWh/m^3	Spec. Q_{cv}. kWh/m^3	Total heat loss, kWh/m^3
15	55	17	15	32
15	65	23	15	38
15	80	32	9	41
26	80	38	11	49
50	80	52	21	73
50	90	62	36	98

5.3.3 Economic evaluation of anticipated large scale water purification

A large-scale MD plant of 10 m^3/h is considered to estimate the heat demand and economy of large scale MD water purification. Table 5.4 gives the key data for the three cases investigated, with heat demands taken from experimental values presented in the previous section. The number of modules required is highest for Case 3 and lowest for Case 2. Case 2 is the most favorable from a yield perspective. Comparing Cases 2 and 3, the former requires a lower number (half) of modules but demands the highest heat energy, while the latter saves more heat at the expense of a larger number of modules. The choice of integration case is therefore based on a compromise between the number of modules and the heat demand.

Table 5.4 Summary of thermal energy demand and number of modules required for an MD plant capacity of 10 m^3/h

	Specific heat demand, kWh/m^3			No. of MD modules
Case	$\dot{Q}_{sp}$	Recovered $\dot{Q}_{sp}$	$\dot{Q}_{net}$	
1	692	0	692	1176
2	735	0	735	644
3	875	770	105	1212

The system capital cost calculation is based on data presented by Kullab and Martin [170] and includes skid, MD modules, pumps, heat exchangers, tank, electrical equipment, piping, and other items. The capital cost of purified water production was estimated based on five years' lifetime for membranes and a twenty-year operational span of other MD equipment in the system. The capital expenditure for the MD pilot plant is given in Figure. 5.7. As can be seen from the CAPEX analysis result, MD modules and assembly takes the highest share, followed by other costs. However, due to the economy of scale, a degression coefficient is used in capital expenditure calculations for large-scale systems, hence higher capacity MD plants will have lower specific CAPEX.

The cost for commercial productions could potentially be reduced by careful review of components and suppliers, as well as by optimization of the assembly procedures. The results of specific CAPEX for the three cases at different plant capacities are given in Figure 5.8. Case 2 has the lowest specific CAPEX due to the higher permeate flux and so fewer numbers of modules are required. Cases 1 and 3 have nearly overlapping specific CAPEX values due to the very close permeate flux, and so closer number of MD modules is required for a particular production capacity. Hence, Case 2 specific CAPEX showed a reduction from \$50000 to \$20000 per (m^3/h) when the plant capacity increases from 10 to 100 in m^3/h. For an anticipated plant capacity of 8000 m^3/h, which is the average effluent production from the Stockholm WWTP at Henriksdal, specific CAPEX will be as low as \$9800 and \$16000 per (m^3/h) for Cases 2 and 1 respectively. In this case the annual district heating demand to drive the corresponding MD system would be in the range of 50 to 68

TWh. However the annual district heating production in Stockholm was 13 TWh in 2015 [171, 172], therefore such a large MD system is unrealistic Considering an upper limit of 10% of Stockholm's annual district heating for the MD system, the capacity of purification will be limited to 215, 200 and 150 m^3/h for Cases 1, 2, and 3 respectively (as shown by the red line in Figure 5.8).

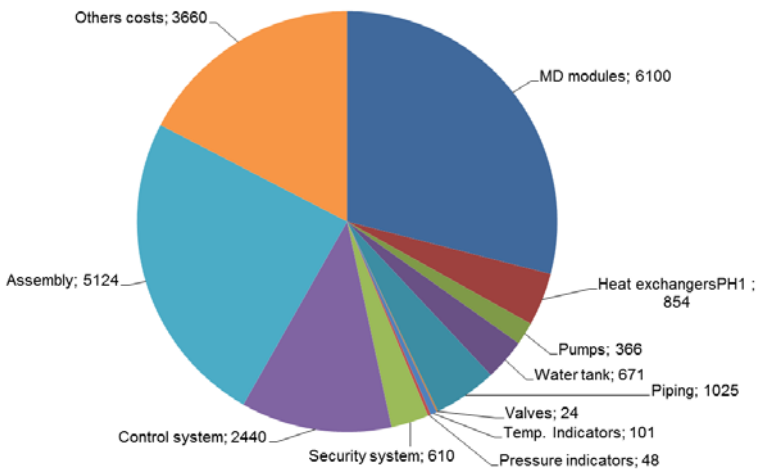

Figure 5.7 CAPEX contributions ($) of different components for the reference MD pilot plant

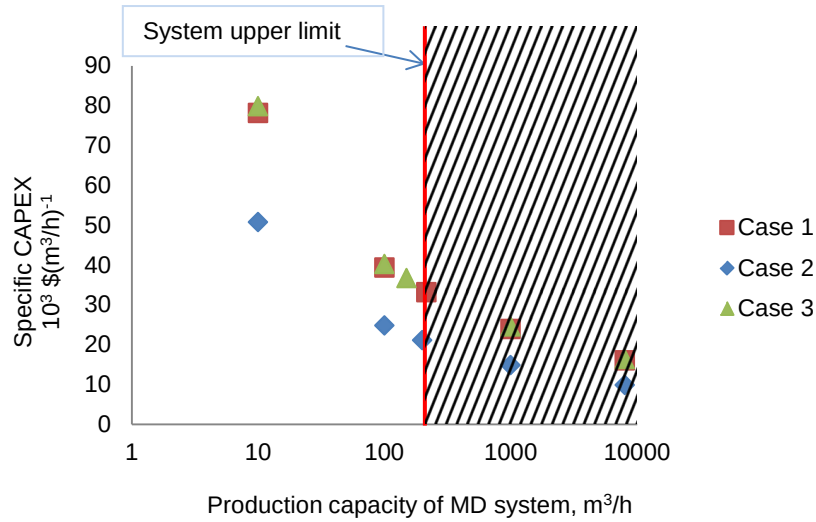

Figure 5.8 Specific CAPEX of MD system for the three cases at different plant capacities.

The overall annual operational and maintenance expenditure (OPMEX) for a plant capacity of 10 m^3/h is summarized in Figure 5.9. From the calculation of OPMEX, it was found that heat cost has the highest contribution of about 94% from the other OPMEX shares followed by initial CAPEX (3.4%), service and maintenance (1.2%) and costs of membranes (0.7%). The annual cost of heat is found to be highest for Case 2 followed by Cases 1 and 3 which is due to the larger heat demand for Case 2 than the other cases.

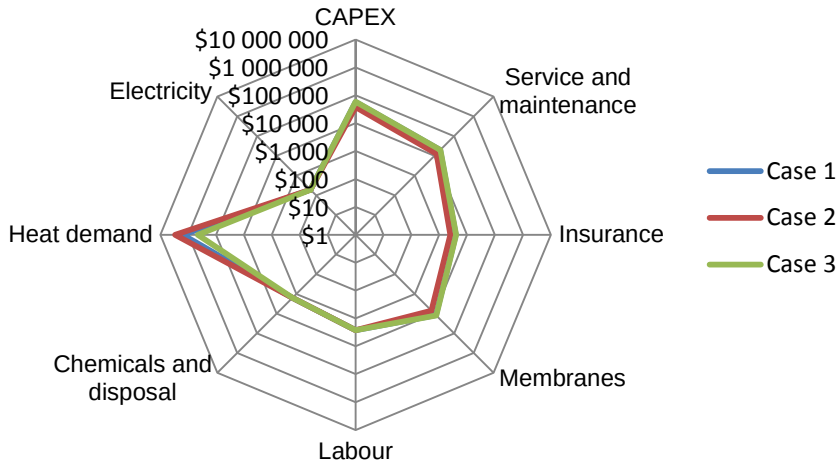

Figure 5.9 Annual costs in USD of each type of expense for the MD plant capacity of 10 m^3/h.

The summary of unit costs for different MD plant capacities in each of the three cases is given in Table 5.5. The unit cost differences across the four plant capacities for a specific case are due to the effect of the economy of scale reflected from CAPEX. For a particular plant capacity, the unit costs of water purification among the three cases are significantly different due to variations in heat demands.

Table 5.5. Unit cost of water, C_w in [$/m^3$] for the three cases at different MD plant capacities in m^3/h

Case	10	100	1000	8000
1	19.13	18.55	17.29	17.17
2	34.56	34.17	36.13	36.08
3	6.35	5.75	5.53	5.44

Estimated cost of purification are at least an order of magnitude higher than what was found by Kullab and Martin [170], which can be explained

by the assumed specific thermal demand. Similar values are achieved with Case 3 with the assumption that heat losses are avoided and permeate heat exchange is employed. The result of this analysis is given in Figure 5.10, which shows the unit cost of $\$1.4/m^3$ at a feed temperature of 90^oC, taking the calculated net specific heat demand of $4kWh/m^3$.

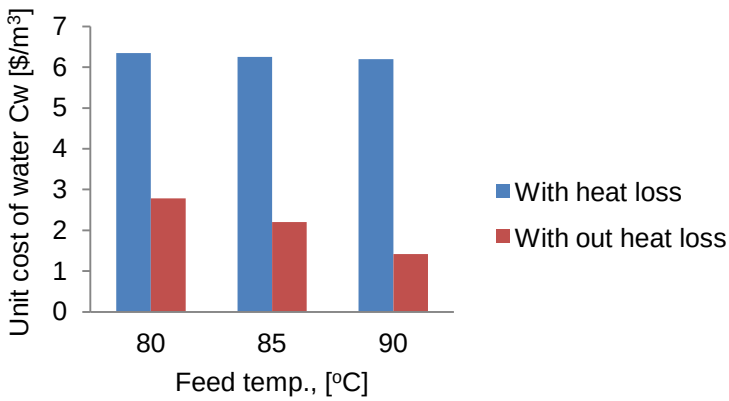

Figure 5.10 Unit cost of purified water in the theoretical case of minimizing heat losses due to natural convection and through permeate. The analysis is for Case 3 integration considering $10m^3/h$ plant capacity.

As stated earlier, from the investigated MD-DH integrations Case 2 has the minimum system requirement in terms of the number of modules which translates into the lowest capital investment. However, Case 2 has the maximum heat demand and so the highest specific cost of purification. In summary, Case 2 is found to have the highest cost of purification with $\$34.5/m^3$ per cubic meter of permeate. Even though the capital investment is very much higher than Case 2 and slightly greater than Case 1, Case 3 could be the preferred solution for its minimum overall specific cost of purification at less than $\$5.44/m^3$. The advantages and disadvantages of each case of MD-DH integration are summarized in Table 5.6. The parameter that remains unchanged is the removal efficiency, which is dependent on the membrane characteristics and feed nature in which these were kept the same for all tests of the three cases.

Table 5.6. Summary of advantages and disadvantages of each of the three cases MD-DH integration regarding some major parameters

Case	Advantage	Disadvantage
1	Lowest heat demand	No heat recovery, lowest permeate flux, so the largest number of modules required
2	Highest permeate flux per module Lowest number of modules required and so smallest CAPEX	No heat recovery Highest unit cost of water purification
3	Heat recovery possible Lowest unit cost of water purification	Lowest permeate flux, so requires large membrane area (investment)

When cost comparison is made between the competing technologies RO and MD, costs will obviously be higher for the MD due to the higher specific energy (heat) demand. Unit cost water purification by RO is reported from $\$0.28/m^3$ for treating effluent from conventional activated sludge [25] to $\$0.83/m^3$ for PV powered RO for desalination [26], whereas \$5.4 to $36/m^3$ were calculated for the DH powered MD analyzed in this study.

5.4 Concluding remarks

The study on removal efficiency of pharmaceutical residues by AGMD modules and related technoeconomic analyses were covered in this chapter. The highly effective drug residue removal by the AGMD module suggests that the process is feasible for the considered application. The economic analyses also showed that majority of the cost related to the water purification process comes from the cost of thermal energy. However, the heat demand could be optimized with proper MD-DH integration which can lead to a lower specific heat and eventually reduce the unit cost of such water purification. In addition to proper MD-DH integration, module design improvement should be given due consideration in future MD studies in order to minimize heat losses. A

treatment concept will also have to take into account the handling of concentrate. From the experimental and simulation results it can be concluded that membrane distillation, with its high removal performance and the possibility of running with low-grade heat, is a potential alternative for purifying water with pharmaceutical residues and similar contaminants, especially in cases where waste heat is available. The pharmaceutical removal test results showed that the tested MD modules offered high efficiency which remains same even for highly concentrated feeds.

6 District Heating-driven MD for Wastewater Purification in Pharmaceutical Industries

Wastewater from pharmaceutical plants usually contains very complex mixtures of contaminants including antibiotics, steroids, antidepressants, anti-inflammatories, beta-blockers, lipid-lowering drugs, and stimulants [173, 174]. These are classified as hazardous wastes, as they pose a potential long-term risk to aquatic and terrestrial organisms [175, 176]. As a result both oxidation and adsorption steps are required in addtion to standard methods (filtration, flocculation, etc.) for handling such a wastewater stream. The degradation of pharmaceuticals by oxidation includes such techniques as ozonation as pretreatment or post treatment for membrane filtration technologies [177, 178] and Fenton oxidation [179]. Adsorption techniques are also widely used for removal of pharmaceutical residues from effluents of WWTPs. Activated carbon is the most commonly utilized and efficient adsorbent as reported by many researchers [180, 181]. Although effective such measures have limitations, either in separation efficiency or cost.

In this chapter, district heating-driven membrane distillation is considered as a novel technology for wastewater treatment in the pharmaceutical industry. The AstraZeneca production facility at Gärtuna is chosen as a case study. Previously reported experimental data from two semi-commercial module prototypes (Xzero and Elixir) are incorporated into a thermo-economic analysis.

6.1 AstraZeneca pharmaceutical WWTP case study

The WWTP at Astra Zeneca, Gärtuna receives 850–900 m^3/day effluent from several product lines. Generally speaking, this facility includes features seen in other modern pharmaceutical WWTP's, namely

bioreactors and activated sludge treatment. However, as these processes are not efficient enough to fully remove the residues, additional treatment steps such as activated carbon treatment, chemical precipitation, and floatation are included. There are two separate wastewater supply streams, as shown in Figure 6.1. Wastewater Stream 1 is collected from the main parts of the production lines and has an average flow rate of 33 m^3/h. This stream follows a cleaning procedure starting from biological treatment with fungi and bacteria, followed by activated carbon adsorption and finally sand filtration and polishing. Stream 2, with an average flow rate of 3 m^3/h, originates from tablet production lines and consists of substances that would be decomposed at low pH and destroy the fungi used in the biological treatment step. Therefore, this stream has to be pretreated separately before joining the main WWTP. The pretreatment inlet stream has pH in the ranges of 12–14, mostly due to the high levels of sodium hydroxide upstream, with total organic carbon (TOC) concentrations from 250–400 mg/L and total nitrogen (TN) from 15 – 25 mg/L. The main wastewater stream has a TOC of in the range 300 –700 mg/L, 10 –40 mg/L of TN and TP 1–8 mg/L [182].

Figure 6.1 illustrates a schematic of the WWTP showing the main flows and treatment components. Generally speaking, the Gärtuna facility includes features seen in other modern pharmaceutical WWTP's, namely bioreactors and activated sludge treatment. However, as these processes are not efficient enough to fully remove the residues, additional treatment steps such as activated carbon treatment, chemical precipitation, and floatation are included.

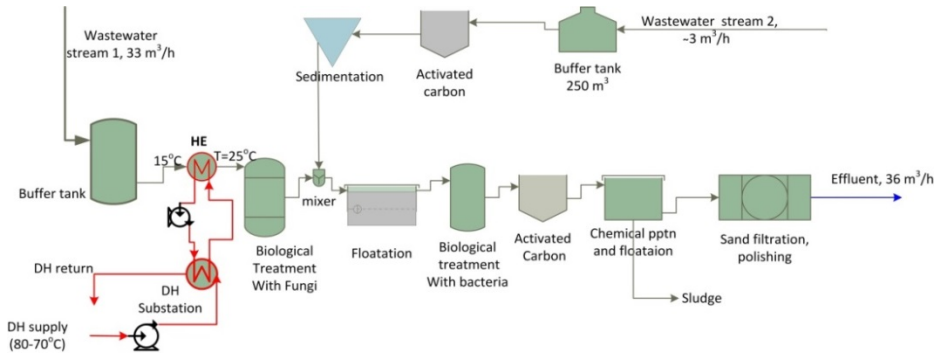

Figure 6.1. The major streams and processes in the WWTP facility at AstraZeneca

After the buffering tank, the main wastewater stream is heated from about 10–20°C to up to 25–30°C before entering the bioreactor. The WWTP is connected to district heating network as part of its thermal needs. The treatment procedure for Stream 2 involves activated carbon treatment followed by sedimentation, where the compounds that would decompose and destroy the bio-agents are removed. Effluent is discharged into a mixer, where it combines with Stream 1 to proceed with similar purification process.

The methods applied in this case study involve system analyses and optimization including mass and energy balance calculations with input obtained from pharmaceutical industry, coupled with results MD experiments on the removal of pharmaceutical residues. This study is based on the previous investigations [140, 142] on pilot scale experiments on both removal efficiency of MD for pharmaceutical residues and energy demand. Even though the feed used was effluent from municipal WWTP, concentrating procedures of the feed to a very high concentration (up to 8 times initial concentration) were followed to simulate a real pharmaceutical wastewater.

The process in this case study considers the integration of three different processes, as shown in Figure 3.3: Industrial process (pharmaceutical production), membrane distillation system, and district heating network. The MD system is fed with the wastewater stream to be treated from the pharmaceutical plant. Heat is provided from the DH supply line, while

MD module cooling water supplies low-grade process heat and space heating.

6.1.1 Options for membrane distillation integrations at AstraZeneca WWTP

Wastewater Stream 2 was chosen as a viable candidate for introducing MD technology. This stream can be separated from the current WWTP process and fed directly to the MD unit for purification, replacing the activated carbon and sedimentation steps. The schematic diagram for the integration of MD in the WWTP is shown in Figure 6.3. This approach disregards the need to dispose of used up carbon or sedimentation residues. Instead, a highly concentrated liquid wastewater is produced, and the product water is contaminant free and could conceivably be reused, for example for cleaning. MD can thus lead to a zero liquid discharge treatment system provided that the concentrate is disposed of properly (i.e. incinerated).

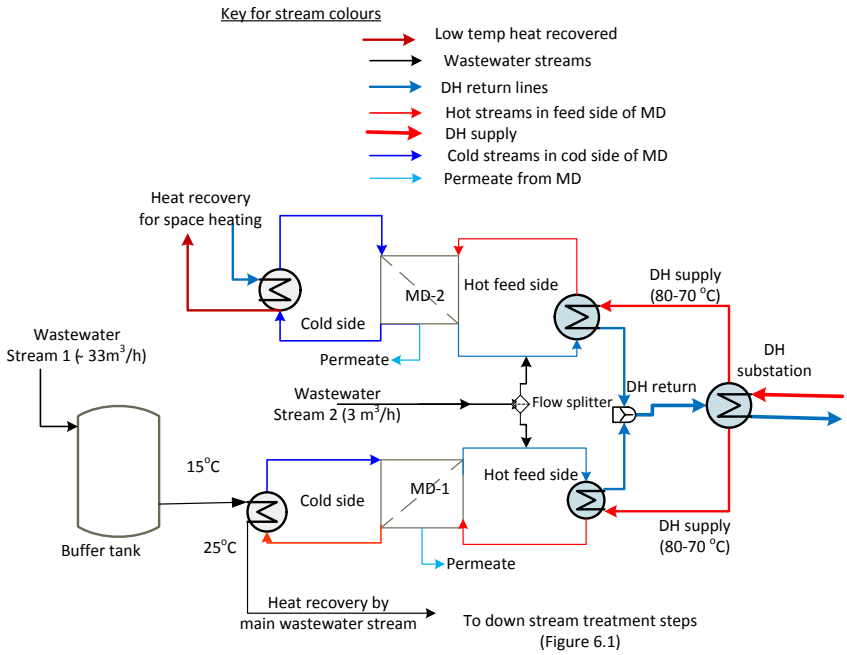

Figure 6.2. The integrated WWTP-MD system for treatment of Stream 2.

The DH network supplies heat at about 80°C for the MD system. Two MD subsystems are employed: MD-1 utilizes wastewater Stream 1 as a coolant, and its size is determined by the heat duty of Stream 1 in the base case; and MD-2 is integrated with space heating and is sized to handle the remaining flow of wastewater from Stream 2 (Figure 6.2). Both MD-1 and MD-2 utilize two series-connected modules connected in parallel to adjacent trains. The rate of heat transfer while maintaining the main wastewater stream for raising its temperature from 15 to 25°C, is calculated from the flow rate and rise in temperature of 10°C (using Eq. 4.4).

For MD-1 modules, the total permeate rate that could be obtained is estimated from the specific heat recovered (Eq.4.5) and the total heat recovered by the wastewater coolant at the large-scale plant Q_I as follows:

The required permeate flow rate from MD-2 is found from the difference between the total purification and purification rate from MD-1. After the purification rates are known for each set of modules (MD-1 and MD-2), the membrane area required for each set of MD is derived from the permeate fluxes of the reference bench scale and large-scale MD systems and membrane area for the reference bench scale MD system using Eq. (4.32).

Following this, the heat demand for both MD-1 and MD-2, and amount of heat recovered from MD-2 is computed from the corresponding purification rates, specific heat demand, and heat recovered in the small-scale reference modules respectively. Total heat demand of the MD units is calculated from the sum of heat demands of MD-1 and MD-2 modules. Annual heat demands and heat recoveries have been calculated from specific heat demands and annual purification of 26280 m^3 wastewater by assuming 8760 hours of operation per year. In the base case (i.e. current WWTP without MD), the total purchased district heating energy was 20205 MWh for 2014 [182]. Seasonal variations have been neglected in this analysis.

6.2 Performance of the AGMD modules

Table 6.1 shows a comparison of performances of the tested Xzero module with Elixir prototype modules. Elixir MD module has better permeate flux and lower net specific heat demand. The permeate flux difference is due to the increased heat transfer across the cooling plate that facilitates condensation (i.e. plastic vs. metal surfaces). Due to its high permeate flux and comparably lower net specific heat demand, the Elixir module can be the preferred module among the two modules when heat recovery is possible. When heat recovery is deployed, the Elixir MD module is highly energy efficient. The better heat transfer and higher condensation rates of the product water in the Elixir MD module are due to the thinner cooling plate thickness, and the improved geometry of cooling plate surfaces as described in section 4.2.

At feed temperature of 80°C, the Xzero's pair of MD modules requires specific heat input of 735 and 875 kWh/m^3 at cooling temperatures of

15°C and 50°C respectively. The heat demand at higher a cooling temperature (50°C) is higher due to both smaller permeate flux and higher heat loss at 50°C than at 15°C. For MD-1 modules, the net heat demand is 82 kWh/m^3 as the majority of the heat input is recovered by the wastewater Stream 1. Similarly for MD-2 modules, due to the higher heat loss and lower permeate flux, the net specific heat demand is greater (105 kWh/m^3) than for MD-1 arrays. With Elixir MD module's performance considered as MD-1 set of modules, the permeate flux is nearly three times greater as compared to Xzero with much smaller net specific heat demand of 7.4 kWh/m^3 as opposed to Xzero's net specific heat demand of 105 kWh/m^3. For MD-2 set of Elixir, lower specific heat input and slightly higher net heat demands are observed as compared to MD-1 set. This is because heat recovery is limited at higher cooling temperature due to the lower temperature difference across the membrane.

Table 6.1. Base case performances of the two modules used in the large-scale simulation regarding permeate flux and specific heat demands, at a feed temperature of 80°C and coolant temperatures of 15°C and 50°C.

Module	Cooling temperature, °C	Membrane area (m_a), m^2	Permeate flux, L/m^{2}h	Specific heat input, kWh/m^3	Net specific heat, kWh/m^3
Xzero	15	4.6	6.7	735	82
	50		3.5	875	105
Elixir	15	0.38	18	827	7.4
	50		12	672	11.5

6.3 Heat demand analysis for full-scale case

The conditions and performance of both AGMD types for the entire array of large-scale WWTP system are summarized in Table 6.2.

Table 6.2. Summary of the performance and heat demand calculation results for the full array MD system at the WWTP

MD type		Feed temp. ,^{o}C	Coolant temp.,^{o} C	Membrane area required, m^2	Permeate yield, m^3/h	Annual heat input demand, MWh	Annual heat recovered, MWh
Xzero	MD-1	80	15	87	0.58	3780	3360
	MD-2	80	50	691	2.42	18500	16300
Elixir	MD-1	80	15	25.5	0.47	3390	3360
	MD-2	80	50	210	2.53	14900	14700

The total annual heat demand to drive an all Xzero MD system is 22300 MWh from which 16300 MWh of heat is theoretically available for space heating from MD-2. However, this heat is not enough to supply the heating demand for the buildings in the facility; this is because the annual demand for space heating, calculated from purchased district heating in 2014 is 16800 MWh [182]. Hence, an additional heat of 570 MWh is required to meet the space heating demand. Hence, the total DH demand of the WWTP with integrated Xzero MD system becomes 22800 MWh.

Similarly, for Elixir MD modules, heat demand calculations were carried out for the 3 m^3/h capacity wastewater stream. For the full-scale MD system, annual heat demand of 18300 MW is required to run the MD unit. From this heat input to the MD system, 3360 MWh is recovered by the wastewater Stream 1 and the remaining 14600 MWh is available for space heating. However, when compared with 16800 MWh space heating requirement, an additional heat of 2200 MWh needs to be supplied. Therefore, the total DH demand for the Elixir AGMD integrated WWPT becomes 20500 MWh (see Figure 6.3).

The capacity requirement regarding membrane area and share of permeate production for the industrial scale MD system by each type of MD module are also calculated as given in Table 6.3. Accordingly, MD-2 arrays take a larger share of permeate production and so the membrane area requirement is high for both Xzero and Elixir modules. This is because of the number of MD-1 modules is limited by the amount of heat that could be recovered using wastewater Stream 1. The number of modules in MD-2 were limited by the space heating demand, which was

found to exceed the MD cooling requirement for both module types. The comparison between the Xzero and Elixir modules regarding membrane area requirement shows that the total membrane area required by the Elixir was smaller than the membrane area required for Xzero system which is in proportion to the permeate flux ratio of Elixir to Xzero modules.

Figure 6.3 presents a summary of the annual heat demand for the full-scale MD system when Xzero or Elixir modules were considered for purification of wastewater Stream 2 in the WWTP case study. As the total heat that could be recovered from the MD for space heating is higher when Xzero modules are used than from Elixir, lower extra heat is required for the purpose of space heating in this. However, more heat input is required to drive the Xzero modules than Elixir modules. When compared with the annual district heating purchased by the facility, the increase in overall heat demand due to integrating MD is about 13% for Xzero and only 1.4% for Elixir.

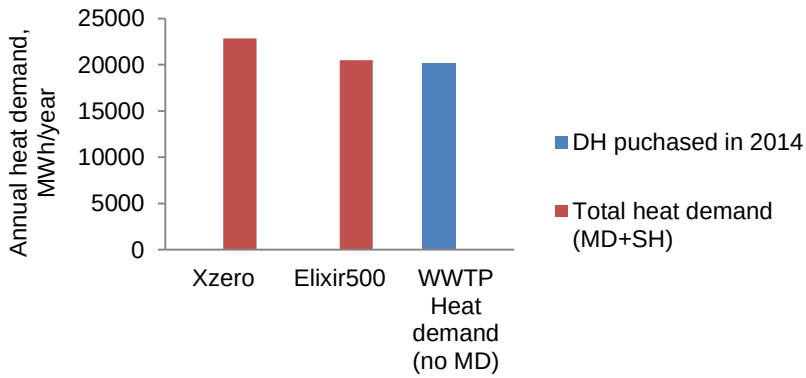

Figure 6.3. Summary of the annual heat demands before and after MD integration and the extra heat demand for the MD integrated WWTP at AstraZeneca pharmaceutical

6.4 Economic analysis of the full-scale MD system

The capital investment for the full-scale 3 m^3/h MD system is calculated from the reference small-scale MD pilot plant. The CAPEX for full-scale integration of Xzero MD system is more than twice of the CAPEX for

Elixir modules, as summarized in Table 6.3. For Xzero MD system, the MD modules represent the highest cost (40% of total CAPEX) followed by the cost of assembly and engineering works (28%) and control systems (7.5%). The cost distribution for Elixir modules is 33% for MD modules, 32% for assembly (design and installation engineering work) and other expenses 11%. The percentage of MD modules' expense is reduced for Elixir as a lower number of membrane area is required.

Operational and maintenance expenses of the MD system are mainly derived from the cost of the heat supply. The annual operational cost analysis as summarized in Table 6.3 shows that the annual cost for the heat stands the highest for both module types. For Xzero modules, the annual heat cost is about 77% of the total annual cost including distributed CAPEX. However, for Elixir modules, the percentage of annual heat cost is only 45% of the total annual expenses. When heat losses are minimized, the annual heating cost for Xzero modules could be reduced to about $45600 (52%).

Table 6.3. Economic analysis results for the two MD module types integrated into the WWTP

	Cost type	Elixir	Xzero	Xzero (heat loss minimized)
CAPEX (USD)	MD modules	46800	127000	
	Heat exchangers	6000	15200	
	Pumps	1800	3600	
	Water tank	3200	6570	
	Piping	5000	10000	
	Valves, temp. and pressure indicators	1100	1700	
	Security and control system	14700	30000	
	Assembly	45400	92000	
	Others costs	17700	36000	
	Total	141000	322000	
	Annual CAPEX	10400	23700	23600
Annual OPMEX (USD/year)	Service and maintenance	3500	8000	8000
	Insurance	700	1600	1600
	Membranes	1900	6200	6200
	Labour	800	800	800
	Chemicals and disposal	500	500	500
	Heat demand	15700	145000	45600
	Electricity	1600	1600	1600
Unit cost (USD/m^3)	W_{unit}	1.3	7	3.3

Comparison of the unit cost of water purification between the two modules gives \$7/m^3 for Xzero and \$1.3/m^3 for Elixir modules. The unit cost from the Xzero modules could be lowered to \$3.3/m^3 (decrease of 47%) through simple measures for reducing heat losses, e.g. added insulation. The current annual overall cost for the pretreatment of the same sub-stream at Astra Zeneca Pharmaceutical Wastewater Treatment Plant (AZ-WWTP), using activated carbon and sedimentation, is about \$87200. The unit cost of pretreatment currently is, therefore, about

$3.3/m^3$. Compared with the currently AC treatment expenses, the scenario employing MD treatment with Elixir modules yields a cost savings of about $2/m^3$. Moreover, the AC pretreatment in its current form is unable to yield a zero liquid discharge scenario.

6.5 Concluding remarks

In this chapter district heating integrated MD has been investigated for application in pharmaceutical WWTP. Economic assessment for replacing activated carbon treatment process using two types of AGMD modules is evaluated. The full-scale MD simulation results from the analysis highlighted the technoeconomic feasibility of MD system for the new application in pharmaceutical WWTP. Differences in the heat recovery and permeate flux between the the two MD modules reflected in the variation of investment and overall unit cost of purification. For such a smaller purification capacity explored in this case study, installing MD modules and supplying the necessary heat from DH is practical and also economical. MD is promising to be commercialized and installed in such full-scale systems however seasonal variations in the DH need to be considered for complete of understanding of such integrations.

The next chapter presents a case study highlighting the potential for MD technology to complement existing processes in bioethanol production.

7 District heating Integrated Membrane Distillation for Ethanol and Water Recovery in Bioethanol Plant

In November 2016, the European Commission issued a revised Renewable Energy Directive targeting a minimum of 27% renewables in the total EU energy demand by 2030 [183], which replaces the 2012 RE Directive [184]. Bioethanol is a promising fuel supply to help increase RE mixes in the future, especially for transportation. It can be derived from sugar cane, sugar beet and other starch-containing plants such as wheat, corn, straw, and wood [187]. The annual global bioethanol production has almost doubled from 45 000 000 m^3 in 2007 from 87 000 000 m^3 in 2014 [185]. The two countries, USA and Brazil produced about 85% of the global share in 2015 as shown in Figure 7.1. The environmental and economic benefits (including subsidies) are the main reasons for the increasing supply of bioethanol, leading to a reduction in petroleum demand [186]. The majority of the large scale production of bioethanol currently employs yeast fermentation of sugars extracted from crop-based feedstock, followed by separation of the bioethanol from the fermented broth by distillation [188]. Large scale bioethanol production processes often require significant amounts of energy, especially heat in the form of steam for the heaters, evaporators, and distillation [189]. The costs related to this heat supply have a direct impact on the economic feasibility. To produce economically competitive ethanol, lowering the energy demand and hence the associated costs must be taken into consideration.

Research and developments in Sweden and the wider Nordic region are pushing for construction of advanced bioethanol production plants. A demonstration pilot plant of ethanol production from hemicellulose in Örnsköldsvik, Sweden has been in production since 2004. The plant has a

capacity of 2 tons of dry raw material per day and SEKAB Group purifies the ethanol in a single distillation column which can concentrate ethanol up to 90% [190] and output of 18 million liters per year [191]. In 2015, St1 Nordic Oy built a bioethanol plant in Gothenburg from biowaste. The bioethanol plant is the fifth in addition to the four similar plants in Finland and it has annual production capacity of 5 million liters 100% wt. ethanol from 18 thousand tons of bakery waste [192]. St1's Norwegian subsidiary has also planned to invest in a 50 million liters per year bioethanol production plant in Norway to be operational by 2021. The raw materials for this plant are considered to be sawdust and wood chips. The developments in similar and advanced bioethanol productions are expected to continue as ways of achieving energy security and encouraging renewable energy.

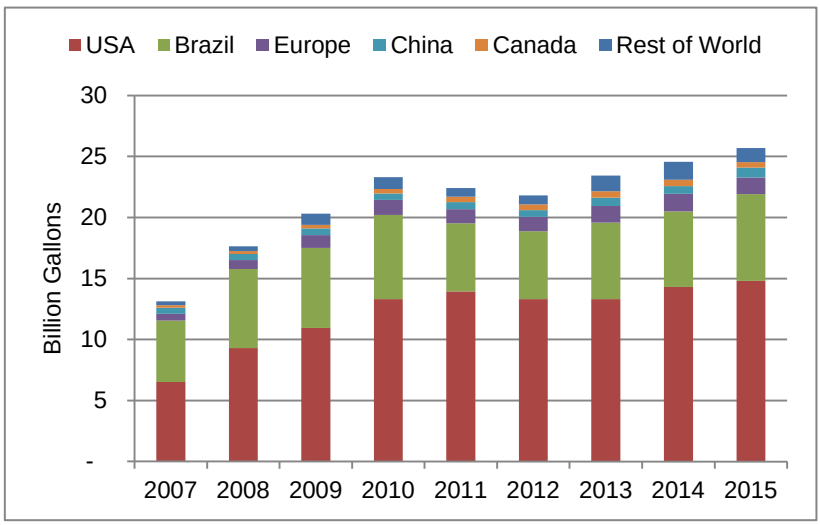

Figure 7.1. Global Ethanol Production by Country/Region and Year [185]

As mentioned in Chapter 2, membrane distillation has been examined in a variety of industrial applications, and bioethanol production is no exception. Previous studies on separation of ethanol-water mixtures by MD reported promising results mainly regarding separation efficiencies. A study of AGMD for reclaiming fermentation products including acetone, n-butanol, and ethanol (ABE) from aqueous solutions was

investigated by Banat and Al-Shannag [193]. They found out that the most effectively removed compound was n-butanol, and temperature, air gap width, and alcohol concentration all affect the flux and selectivity of compounds recovery. Garcia-Payo *et al.* [34] used different membrane materials and operation parameters including feed temperatures, flow rates, and different ethanol concentrations to evaluate AGMD separation efficiency. The authors reported increases in permeate fluxes with an increase in temperature and rate of the feed solution and decrease in air gap thickness. Banat and Simandl [33] studied AGMD for ethanol–water separation process by using PVDF membranes. Here it was reported that from a maximum feed concentration 10 wt% ethanol and feed temperature ranges of 40–70°C, and ethanol selectivity 2–3.5 was achieved [33]. Membrane distillation integration with fermentation process in ethanol production has been investigated as well. Gryta *et al.* [118, 194] have studied the fermentation of sugar using a tubular bioreactor integrated with an MD system. The removal of fermentation broth by-products by MD was found to increase the efficiency and the rate of sugar conversion to ethanol. Moreover, MD integration with fermentation enabled to achieve a higher content of ethanol in the broth due to continuous removal of ethanol and other products which otherwise would inhibit the fermentation [194]. Similarly, another research group [117] reported the effect of MD integrated continuous ethanol recovery on the effect of fermentation degree of sugars in the broth and total ethanol production in the comparison between batch fermentation and MD-integrated processes. They concluded that the fermentation bioreactor coupled with MD increases the total output of ethanol, hence minimizing the economy of ethanol production plants. Finally, DCMD and VMD have been investigated by several researchers for extracting ethanol from various feeds [33]. Shi *et al.* [46] conducted experiments on 5 wt.% ethanol–water mixture by VMD and found that both ethanol and water fluxes increased with increase in temperature or vacuum degree, though the separation factor decreased [46].

The above literature review revealed that studies on the efficiency of MD systems in terms of achieving high ethanol percentages in permeates, along with a technoeconomic analysis for large-scale systems, have not been considered. Moreover, district heating powered membrane

distillation is an interesting novel concept. As energy efficiency is one important parameter in optimizing the economy of bioethanol production, this study aims at minimizing the energy demand through the integration of MD technology for the specific application of recovering ethanol from low ethanol percentage scrubber water. This investigation is based on a particular bioethanol plant – Lantmännen Agroetanol, Norrköping, Sweden – as a case study. Specifically, the analysis considers replacing the high-temperature steam-driven distillation process used for ethanol-water separation with a low-grade heat source (district heating) to drive the MD system. An experimental investigation with a laboratory scale MD unit is employed in an overall comparison between conventional distillation and MD technology, including system analysis based on mass and energy balance calculations. We also discuss the evaluation of a new and improved MD module performance and economic feasibility of its integration with district heating network for the proposed application.

7.1 The bioethanol plant and MD system integration

The bioethanol production plant considered in this study is the only large-scale manufacturer and supplier of grain-based fuel ethanol in Sweden. It uses wheat, rye and barley as raw material cereals. Around 660,000 tons of grain is processed to produce 230,000 m^3 of ethanol annually. The four major processes in the ethanol production plant are: i) mash preparation (which includes milling and liquefaction); ii) fermentation, where yeast is added to the liquefied mash solution, converting sugars to ethanol and carbon dioxide; iii) distillation and dehydration, where ethanol is distilled from the mash with remaining water separated by molecular sieve to achieve a product of 99.7% ethanol; and iv) evaporation and drying, where the alcohol-free mash is dried and pelleted for animal feed. The schematic diagram in Figure 7.2 shows the major steps from milling to producing final ethanol product.

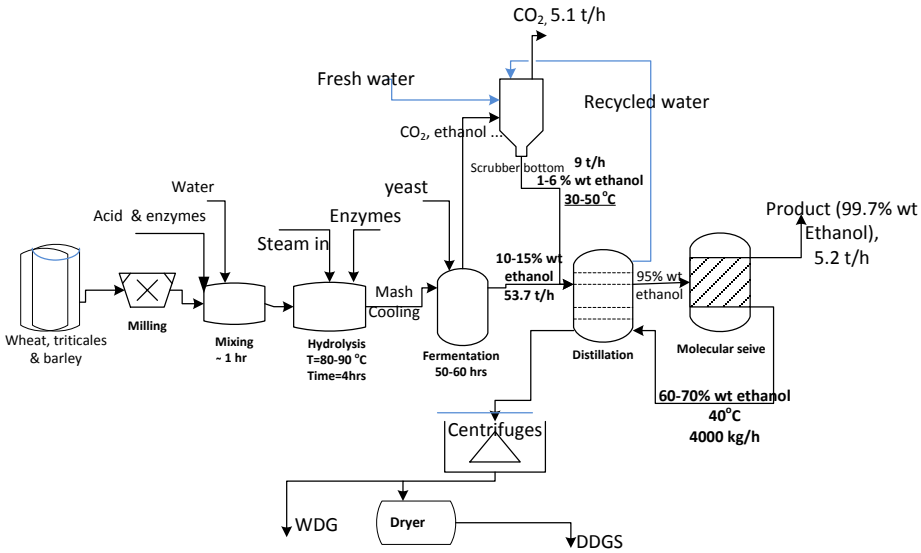

Figure 7.2. Schematic layout representing the major processes and components in the bioethanol production plant at Lantmännen Agroetanol.

Most of the energy demand in the bioethanol plant can be attributed to evaporation and milling processes. The total energy supplied for evaporation and distillation is in the form of steam (about 85% of the total energy input) and electricity (12-13% of total energy input). This is because distillation and drying take place at high temperatures, 120°C and 140°C respectively. The parameters for the steam into and out of the bioethanol plant are summarized in Table 7.1. From the total steam supplied, 95% of it is used for distillation and drying processes. The steam is supplied at 16 bar from the nearby cogeneration facility, Händelöverket in Norrköping. A steam injector converts the steam to 2–5 bar so that the correct temperature is maintained for the distillation and drying process. Condensate from the ethanol plant has a temperature of about 110°C which is returned to the steam supplier.

Table 7.1. Steam and mass flow data for the different parts of steam from the boiler to condensate [195].

	Steam at Boiler	Steam to the bioethanol plant	Condensate
Pressure, bar	110	16	2
Temperature, ^{o}C	540	204	110
Enthalpy, kJ/kg	3464	2795	461
Output, MW	21.5	22.3	3.3
Mass flow, kg/s	6.2	8	7.2

The MD application and the resulting integration in this study focus on recovering ethanol and water from scrubber water. The scrubber water is derived from the plant's CO_2 capture process, which first dissolves the CO_2 gas released above the fermentation tank into water. After the CO_2 is captured, the remaining water exiting the scrubber contains 1% to 6% ethanol by weight. In many bioethanol industries, the scrubber water is recycled back to the plant as part of cook-water makeup. Recirculating this scrubber water before removing the ethanol will have two main disadvantages. One is the wastage of the ethanol without being recovered as the ethanol-eating bacteria within the cook water tank consumes it. The other challenge of recycling the scrubber water before separating the ethanol is the stress ethanol creates on the yeast in the fermentation tank that hinders the fermentation processes [118].

However in the process considered in this study, and as shown in the schematic diagram in Figure 7.2, scrubber water is mixed with the mash after the fermentation tank. This process will eliminate the above problems of ethanol presence in the fermentation tank or losing ethanol being eaten by bacteria. However, as distillation is a thermally intensive process, and the resulting cost related to heat increases as ethanol concentration in the mash decreases. Hence, adding the scrubber water to the mash will further dilute it, resulting in decreasing the efficiency of the distillation column by increasing heat demand and also reducing the effective space inside the columns.

From a general system perspective, the proposed layout integrates three different subsystems: the bioethanol plant, MD system and district

heating network. The integration of MD into DH system could be either from low-temperature return side of the DH as shown in Figure 3.4 or could be connected with the high-temperature supply line of DH as in Figure 3.5. The second connection is required when the MD system requires higher feed temperature of more than 60^{o}C. The integration of membrane distillation to a district heating return line was considered in Chapters 4 and 5.

The MD system will be supplied by a stream of ethanol-water mixture feed from the bioethanol plant to recover the ethanol and water for reuse. The heat is provided to the MD system by the DH network through plate heat exchangers by connecting either from the high-temperature supply line of the district heating or from the low-temperature side return line of the DH network, depending on the MD system production requirements. The MD system can provide low-grade heat for subsequent processes by adjusting the cooling loop temperature level. (Use of the DH supply line as a heat source and DH return line as a heat sink is theoretically possible but has not been considered owing to practical limitations.) This arrangement allows for feed reconcentration by making use of the circulation tank, and there is a continuous supply of the permeate product which can be reconnected to the plant for further process or reuse.

The proposed MD system integration bypasses the distillation column and introduces MD for the recovery of ethanol and pure water from the scrubber water as shown in Figure 7.3. Reconcentrating the reject stream from the molecular sieve is another option for MD integration; however, the relatively high ethanol concentration is expected to be too demanding for this technology at such large-scale and would be better dealt with by the distillation columns hence this option is not considered here.

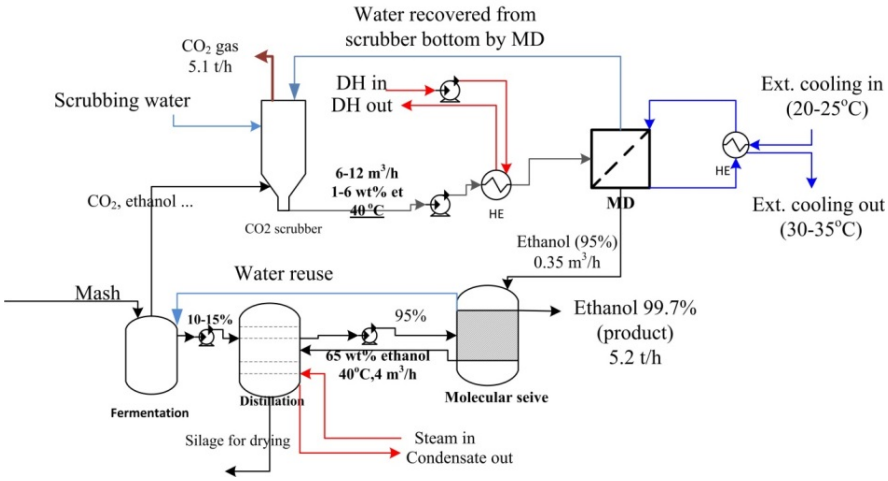

Figure 7.3. The bioethanol production plant layout with the integration of MD for separating water-ethanol mixture from scrubber bottom.

The scrubber water feed to the MD is at a fairly high temperature (40°C), and the additional few degrees temperature rise can be readily obtained from district heating. Even though the considered plant is not currently connected to the DH network, the adjacent cogeneration facility is located in close proximity and presumably could be connected. Heat is rejected from the MD system at a low temperature, and it is assumed that this heat cannot be recovered for other purposes. This system integration enables recovery of all the water for reuse and also the ethanol for further dehydration without affecting the efficiency of the distillation column.

7.2 Ethanol-water separation experimental results

MD tests utilized a simulated scrubber bottom mixture (ethanol-water) of 4-5% and 65% ethanol by weight feed as described in section 4.2. This synthetic water-ethanol feed may not represent the real feed composition, as in the latter case there could be small amounts of other substances like acetone and butanol. Such a case is beyond the scope of the present study. The temperatures of feed and cooling water were also simulating the real condition in the bioethanol plant case considered. The flow rate of the

cooling water was also investigated in preference to the flow rate of the feed as the former had the possibility of variations without costing much energy. The performance parameters sought were permeate flux, ethanol percentage of the permeate, thermal energy dissipated in the process in terms of specific heat demand and thermal efficiency of the process.

The ethanol recovery test results obtained from the HVR modules are shown in plots from Figure 7.4 to Figure 7.7. The results for permeate flux at different feed temperatures from the various percentage of ethanol in the feed and coolant flow rate are summarized in Figure 7.4. The permeate flux (in liters of permeate per hour per square meter of the effective membrane are used) shows a trend of increase for all the four cases tested with increasing feed temperature. The flux also improves slightly for higher coolant flow rates and greater ethanol percentage in the feed. The minimum flux obtained was from the lowest feed temperature and smallest coolant flow rates at 4% ethanol feed, whereas the maximum permeate flux was obtained from the highest feed temperature and higher coolant flow rate tested at 65% ethanol feed. The increased permeate flux is due to the higher relative rise of ethanol's partial pressure as compared to water, owing to its lower boiling temperature .

Ethanol percentage in the permeate is dependent on all the feed temperature, feed ethanol content and also slightly on the coolant flow rate as shown in the results summarized in Figure 7.5. Similar to the permeate flux, ethanol content showed improvements with rising of these variable parameters, and are again linked to ethanol's relatively higher vapor pressure. The permeate's ethanol percentage from both 4% and 65% scrubber water feeds show closer values at the same temperature and coolant flow rates, which can explain its minimum dependency on feed ethanol concentration.

The specific heat demand, which relates the heat required to produce a cubic meter of ethanol permeate (95% equivalent), also showed an increase with feed temperature. The specific heat input saw a maximum value in Case 2, where both the feed ethanol content and coolant flow rates are lower. This is due to the limited partial vapor pressure of ethanol

in the feed which requires more heat to vaporize and also the higher coolant flow rate facilitates heat uptake from hot to cold side of MD module.

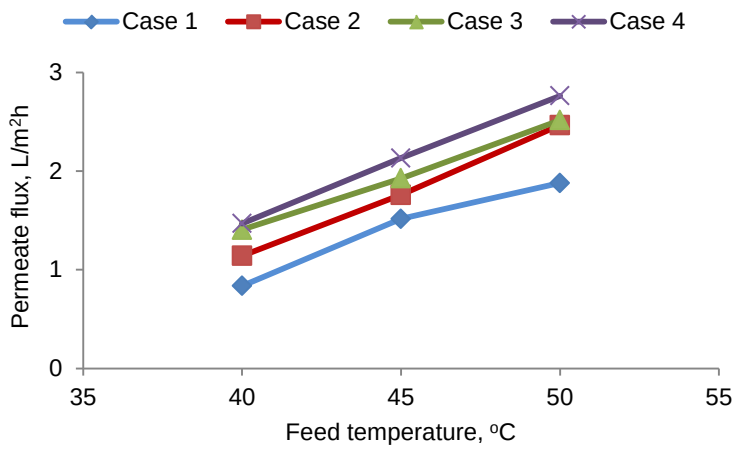

Figure 7.4. Permeate flux for the four cases investigated as a function of the change in temperature across the modules.

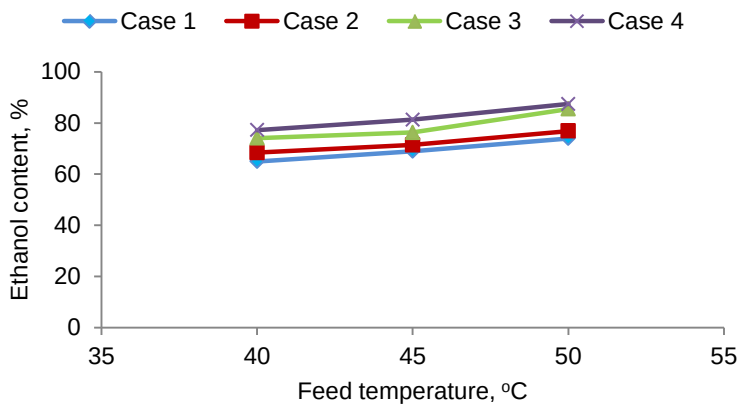

Figure 7.5. Ethanol percentage in the permeates from the four cases investigated.

Even though the trend for the 4% ethanol feed is similar to the trend for the 65% ethanol feed (Figure 7.6); the rate of increase for the 65% ethanol feed is slightly lower than for the 4% feed, which can be due to approaching to being saturated as the ethanol content is high and temperature is closer to the boiling point of the ethanol than for the water.

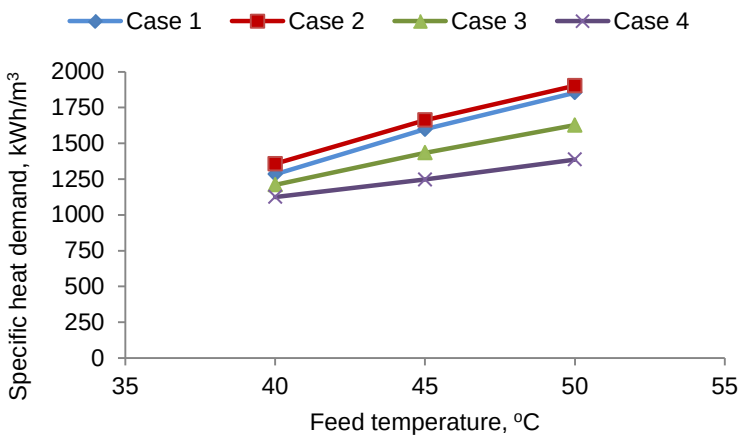

Figure 7.6. Specific heat demand of the MD process for the four cases investigated.

The thermal efficiency (η) of the MD processes at different feed temperatures lies between 20 and 40% as summarized in Figure 7.7. The thermal efficiencies of the four cases at a feed temperature of 40°C are relatively closer to each other than at the higher feed temperatures, suggesting here the feed temperature has a more pronounced effect on the thermal efficiency than the other two factors. Thermal efficiency as calculated from equation 3.8, depends on the latent heat and specific heat input at a given feed temperature. Since higher feed temperatures cause larger specific heat demands, thermal efficiencies also showed lower values due to higher heat loss. This is confirmed from the least thermal efficiency of Case 2, where coolant rate is higher causing larger losses. Case 4, with significantly higher ethanol in feed showed the highest thermal efficiency. Even though coolant flow rate is higher in Case 4 than Case 3, but in case 4 the high coolant rate contributed to a larger permeate flux than from Case 3 (as shown in Figure 7.4), so the efficiency of this case is higher.

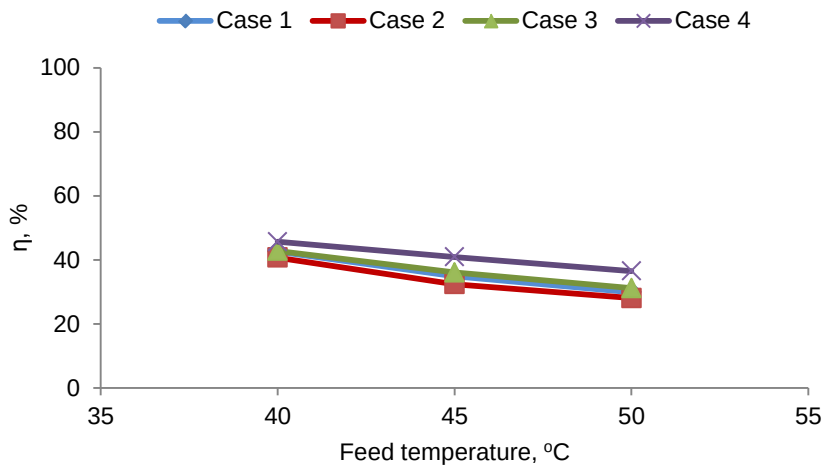

Figure 7.7. The thermal efficiency of the tested MD process for the four cases investigated.

The results of performance from the Elixir MD module are summarized in Table 7.2. The results are obtained from specific operation conditions similar to those in the CO_2 scrubber water stream. For feed and coolant flow rates of 4 and 2.3 mL/min respectively, the permeate flux from Elixir module at 33°C feed temperature is comparable with the flux from HVR at 40°C (1.9 L/m²h) at same flow rates of feed and coolant, due to the improved efficiency from the introduced stainless steel cooling plates. The specific heat demand for the Elixir modules is slightly higher than the corresponding HVR modules at 40°C. However this heat is better utilized for the production of higher concentration ethanol permeate, which is about 10% compared to the ethanol in Case 1 of HVR module. Hence, the Elixir module showed higher thermal efficiency than the corresponding HVR module.

Table 7.2. Summary of performances of the Elixir MD module for ethanol-water separation

Parameters	Value
permeate flux, L/m^2h	1.89
spec. heat input (kWh/m^3)	1633
permeate ethanol fraction, %	77
net specific heat demand, kWh/m^3	37.3
thermal efficiency	63,7

7.3 Heat demand and exergy efficiency comparisons between MD and distillation systems

When evaluating the suitability of the proposed integration, comparisons were made between the distillation columns and MD in terms of the heat demand as both methods require thermal energy. The parameters of interest are the specific thermal energy consumed to produce a cubic meter of 95% ethanol product, the annual heat demand, and exergy efficiency of the two processes. For the distillation column, a specific heat demand of 815 kWh per cubic meter of ethanol produced is required when 10–12% ethanol feed is concentrated to 95% ethanol product. From this, the annual heat demand for recovering ethanol (95%) from the scrubber water (4%) would be about 3200 MWh. Similarly, for the MD module heat demand, specific heat demand of Elixir modules were taken as basis. Calculations were done for annual heat demand of the large industrial scale proposed. As the obtained specific heat demand is for a product of 77% ethanol, appropriate calculations were done to estimate the heat demand for obtaining 95% ethanol product from the MD unit. Similar approaches can be used to estimate the specific heat demand of HVR MD modules for the targeted 95% ethanol production from the 65% ethanol production data. Practically the 95% ethanol production can be achieved by increasing the feed flow rate and reconcentrating the permeate. However, for the large-scale ethanol production case considered and subsequent comparison, only Elixir MD modules were considered. The choice is based on the fact that the HVR modules are only assembled for lab-scale tests and hence are not scalable for larger productions.

A summary of heat demands of MD and distillation column processes for recovering ethanol from scrubber water is given in Figure 7.8. It is evident from the results that in both the specific and annual heat demands, the MD has higher values than the distillation column. This is expected as there are series of heat recoveries in case of distillation columns but not in MD system. Moreover, the distillation column utilizes a higher grade of heat (steam) as compared to the MD system (district heating), so the system economics will play a major role in MD system integration which leads to a slight decrease in distillation column loading with a concomitant increase in productivity.

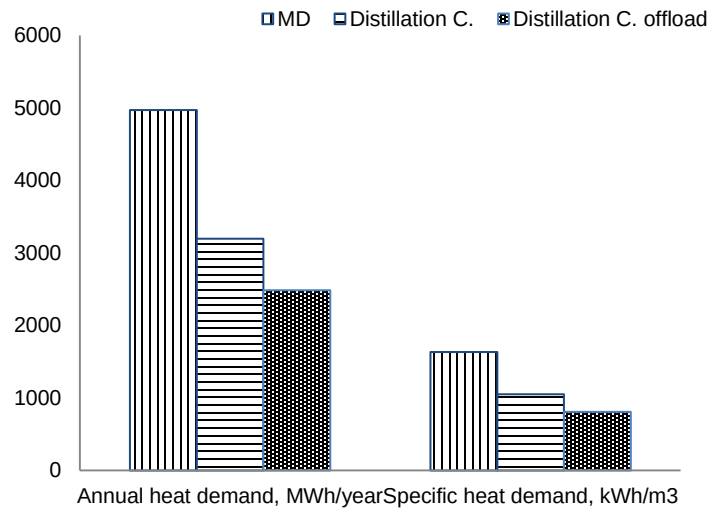

Figure 7.8. Annual and specific heat demands of the MD (Elixir) and distillation columns for concentrating scrubber water-ethanol to 95% ethanol product.

Exergy analysis is also performed to compare the efficiency of the MD and distillation processes which involve heat of different qualities, low-grade heat from DH and high-grade heat from steam respectively, and hence a reasonable comparison is made regarding exergy efficiency and exergy loss from entropy generations. The exergy loss for the distillation column is much higher due to the entropy generated in process mainly from the condenser. The distillation columns have integrated internal heat recoveries from the rectifier to first stage columns which are reflected in

the relatively higher exergy efficiency as shown in Table 7.3. The exergy efficiency of the MD process is higher, as the low-grade heat does not generate as much entropy as that of the steam from distillation to the condenser or surroundings in general.

Table 7.3. Exergy and second law efficiencies of MD and Distillation processes for the ethanol-water separation application investigated

Process	Ex_{loss}, kW	η, %
MD	20	21.5
Distillation column	415	15.5

7.4 Economic assessment

The economic assessment of this MD integration considers all costs related to the capital investment along with annual operation and maintenance costs. The capital investment is based on the required membrane area for the large scale production along with auxiliary equipment such as pumps, piping, valves, storage tanks, and control system. Capital costs for the distillation columns can vary from one plant to another depending on the type of material used stainless steel or carbon steel. Useful data about capital and operational expenditures (CAPEX and OPMEX) of distillation columns were obtained from the particular industry taken as a case study and for the MD system, data from a previous study [170] were considered. CAPEX for the MD in this study includes the cost of DHN expansion to the ethanol plant. Taking an average price of 36 $/MWh and 62 $/MWh for district heating and steam, respectively [196], and assuming an exchange rate of 0.12 $/SEK, the subsequent economies of the two systems is summarized in Table 7.4. The MD system has lower capital expenditures and also operating and maintaining costs than the distillation column systems. Hence, the distillation columns' very high capital expenditure and running cost made the total annual cost more than twice the MD's annual cost. Through this type of MD and DH integration in the ethanol plant, nearly 0.87 M$ annual cost saving is achieved with MD technology.

Table 7.4. Summary of the annual costs (US dollars) of the MD and Distillation systems for ethanol recovery from scrubber water

Economic parameters	MD	Distillation C.
CAPEX, M$	0.51	1.10
annual OPMEX, M$	0.06	0.32
Annual heat cost, M$	0.18	0.20
Total annual cost, K$	0.75	1.62
Investment payback time, years	1–2	2–4

A literature survey for investigations on energy demand analysis and economic assessment of similar large-scale distillation processes revealed that very few have been reported. Some studies reported performance of different ethanol production subsystems based on simulations with Aspen plus or HYSYS. For example, a 40 million gallon per year ethanol production plant in Minnesota was reported to have a thermal demand of 990 kWh/m^3, with up to 40 percent of the heat demand attributed to distillation [28]. Another similar analysis considered the replacement of the distillation column with pervaporation for continuous fermentation [197]. The results showed that the energy saving pervaporation process has same ethanol percentage output as from first stage distillation column (40% wt.), though a higher capital cost than distillation was reported due to membrane replacement costs.

7.5 Concluding remarks

This chapter presented the technoeconomy of district heating driven MD for an industrial-scale recovery of ethanol and process water. Results from laboratory experiments with two air gap MD prototypes showed that a product of up to 75 wt.% ethanol permeate could be obtained from a 4% ethanol feed. The thermal energy demand 1630 kWh/m^3 for 77% wt. from Elixir module was taken for the scale-up simulation study. Cost comparisons between MD and to be replaced distillation process showed that annual saving of about 0.87 M$ could be achieved. Exergy analyses of the two processes also showed that less available work is lost due to entropy in MD than the steam-driven distillation columns.

In addition to the economic and technological advantages of this integration over the current distillation system, the novel arrangement allows the bioethanol plant to significantly reduce fresh water supply to the scrubber, which will improve the water balance in the plant. Increasing the efficiency of the distillation column by freeing available space for the feed from the fermentation broth, and promoting the production and distribution of district heating as a way of supporting renewable heat sources are some other gains of this MD integration in the bioethanol industry.

Tests with real samples are suggested to see how frequently membranes should be replaced and so the cost. This is because the real sample from scrubber bottom may contain other substances and may affect the performance of membranes. Further investigations are also recommended to address issues of the system's sensitivity to district heating cost and fluctuations in the ethanol fuel market. A study on the possibility of waste heat recoveries in the bioethanol plant should also be considered as it affects the energy balance and cost of such integrations.

8 Exergy analysis of AGMD Systems for Water Purification Applications

In addition to the performance parameters evaluated in the case studies presented in Chapters 5–7 – i.e. permeate flux, specific heat demand and thermal efficiency – a more detailed examination of the considered MD system components is instructive for pinpointing significant losses within an exergetic perspective. Unlike energy, exergy is destroyed and can only be conserved when all processes occurring in a system and its surrounding environment are reversible [143]. This thermodynamic irreversibility in a system can be quantified and referred to as exergy destruction. Therefore, the exergy efficiency of processes is a measure of their approach to ideality or reversibility [198]. The exergy rates in streams of processes associated with heat transfer like MD depends mainly on the temperature at which the process occurs in relation to the temperature of the environment. The exergy efficiencies of such processes are dependent on heat recovered and heat losses through module surfaces to the surrounding atmosphere. Hence, exergy analysis provides unique insights into the types, locations, and causes of losses and aids in identifying improved thermal integration. In addition, contrasts can be drawn to competing membrane-based technologies (for example RO) that are mechanically driven and not thermal. In reviewing the literature on this topic, Banat and Jwaied [199] conducted exergy destruction analyses for compact and large-scale solar-powered MD systems. They reported that most of the exergy destruction was in the MD modules with 98.8% and 55.14% for compact and large scale systems respectively. Exergy efficiency of a 24,000 m^3/day DCMD desalination plant operated with and without heat recovery system was reported as 28.3% and 25.6% for the desalination plant with and without heat recovery, respectively [9]. They also reported energy demands of 39.7 kWh/m^3 and 45 kWh/m^3 for the same plant with and without heat recovery, respectively.

Another study [144] on energetic and exergetic analysis of RO/MD and NF/RO/MD hybrid systems for production capacities of 904 and 836 m^3/h respectively reported specific thermal energy demand ranging from 2.25 to 15 kWh/m^3. The exergy destruction due to entropy production for each hybrid system was reported in the range of 7300 to 15100 MJ/h. Macedonio and Drioli [145] carried out an energetic, exergetic and economic evaluation of seawater desalination. The integrated system consisted of microfiltration, nanofiltration, membrane crystallization (MCr), RO and MD, where MCr was applied on NF retentate, and MD was applied on RO retentate. Without energy recovery, the specific energy demand (SED) was found to be 28 kWh/m^3. When a pressure exchanger is included as an energy recovery device, a slightly lower SED (27.5 kWh/m^3) was obtained. The reported exergetic efficiencies ranged from 15.8% without energy recovery to 21.9% when including the pressure exchanger and internal heat recovery.

It is clear that MD modules are responsible for the majority of the exergy destruction in water purification or desalination systems employing this technology. The challenge remains to develop MD modules with improved exergy performance regarding the temperature and pressure losses across the membrane. Indeed temperature dependency on exergetic efficiency and exergy destruction is a key parameter, since MD technology offers freedom in selecting heat source and heat sink temperatures when integrated with other processes. Such aspects have not been covered in sufficient detail in previous studies. Also, to the authors knowledge, air gap membrane distillation has not been considered previously in this context.

8.1 Description of the AGMD modules investigated

The present analysis is based on two types of semi-commercial AGMD modules for a new application of water treatment where contaminants in the feed are at relatively low concentrations. The study covers calculations of the exergy destruction contributions of the components of each MD system considered. Also, the effects of various feed to coolant temperature differences are analyzed, and comparisons were made with previous results on similar systems. The experimental setup and

procedure are as described in sections 3.1 and 3.2 for the Xzero and Elixir AGMD modules respectively. Streams considered in the exergy analyses of each module are as shown in Figure 8.1 and 8.2.

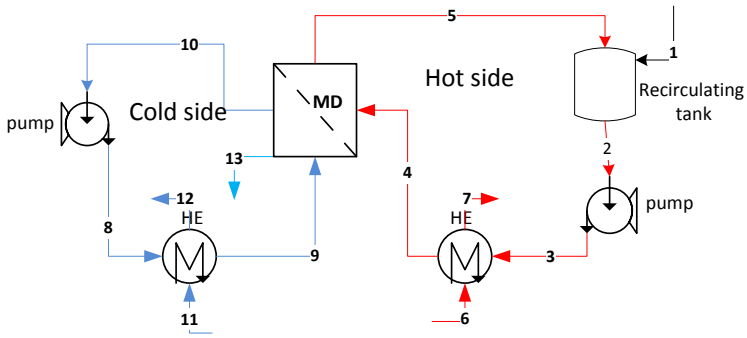

Figure 8.1. The Xzero AGMD unit used and the different streams considered

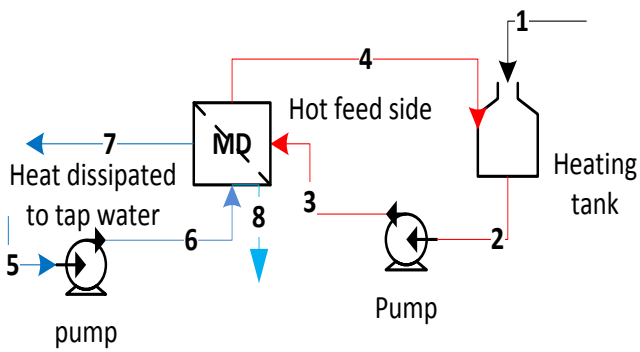

Figure 8.2. Water and heat streams considered in the Elixir AGMD lab unit

The reference state and experimental conditions are given in Table 8.1. Data for the exergy analysis is taken for one cascade of MD modules containing two modules connected in series. The pressure drop across the MD modules is very low, less than 0.019 MPa. The concentration of total dissolved solutes in the feed water is also relatively low in comparison to seawater desalination applications (two orders of magnitude or less). As the three different cases have different feed and

cooling temperatures, the exergy rates will be mainly affected by these temperature differences.

8.2 Exergy efficiency of the AGMD modules

Results from the permeate production rates for the two types of AGMD units are summarized in Figure 8.3 in terms of kilograms per square meter of membrane per second (kg/m^2s) calculated from equation 2.1. The flux decreases as the temperature difference decreases across the MD module, which is due to the decline in the rate of condensation and a concomitant drop in transmembrane transport of vapor across the membrane as the temperature difference decreases. Higher specific heat demands accompany this increase in permeate flux with increasing ΔT. The lower feed temperature condition generally shows a lower permeate flux, as observed for Xzero module's performance at 65°C and 80°C. When fluxes from the two MD modules are compared, the flux from Elixir MD unit is nearly three times higher than that of the Xzero MD unit at the same feed temperature and ΔT (65°C).

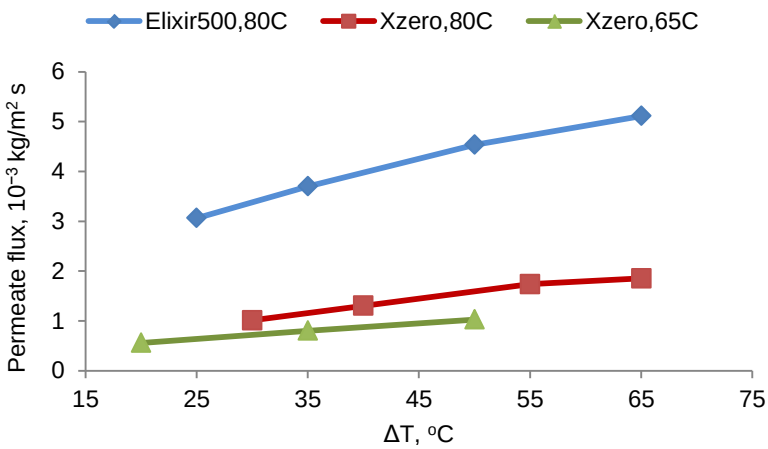

Figure 8.3. Permeate flux of Xzero and Elixir AGMD systems at different temperature differences for feed temperatures of 80°C and 65°C.

The other thermodynamic performance parameters — exergy efficiency, exergy destruction, and specific heat input — are summarized for both modules in Figures 8.4 and 8.5. For both modules types, exergy efficiency improves when the feed–coolant temperature difference goes up. With the Xzero unit at a feed temperature of 80°C, exergy efficiency more than doubled as ΔT increased from 30°C to 65°C. This increase is linked to the improved heat recovery at the heat sink for a higher ΔT, also reflected in the decrease in exergy destruction at a higher values ΔT compared to lower levels (Figure 8.4). The trend is similar for both feed temperatures of 80°C and 65°C. However, the lower feed temperature condition generally shows lower exergy efficiency and higher exergy destruction when compared to the corresponding performance at higher feed temperatures. For this MD unit, it can be said that a higher feed temperature and ΔT favor higher flux and exergy efficiency and lower exergy destruction at the expense of additional specific heat demand.

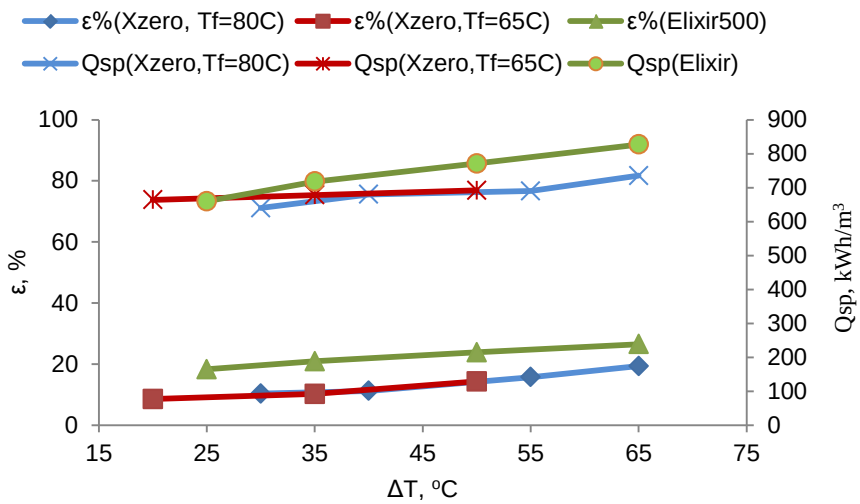

Figure 8.4. The performance of Xzero and Elixir AGMD systems regarding exergy efficiency and specific heat demand at different feed–coolant temperature differences for fixed feed temperatures of 80°C (for both modules) and 65°C (only for Xzero).

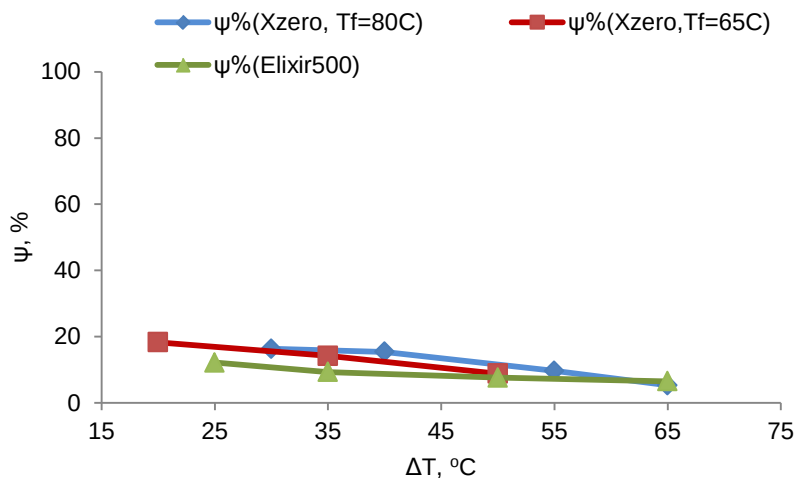

Figure 8.5. Exergy destructions and specific heat demand at different feed–coolant temperature differences for fixed feed temperatures of 80°C (for both modules) and 65°C (only for Xzero).

Similarly, for the bench scale AGMD unit, the general trend in the performances with a change in ΔT is the same as that of the results from the pilot-scale AGMD system. The effect of improved condensation in the Elixir module is reflected in the higher specific heat input owing to the higher heat transfer across the module. Hence, higher exergy efficiency and lower exergy destruction are achieved for the Elixir unit as compared to the Xzero module. The lower specific heat demand for the Xzero module results from the reduced heat transfer across the condensation plate in comparison to the other module, though the Xzero showed severe heat losses from the frames and cover to the surrounding atmosphere by free convection as in covered in section 5.3.2. For both types of MD systems, it is evident that a lower temperature difference across the module reduces performance, including the permeate flux and exergy efficiency.

As the pressure drop across the AGMD modules is low (0.01 to 0.02 MPa) and mass balance is achieved across the MD unit, exergy losses from pressure are not significant. Chemical exergy effects are negligible owing

to the low concentrations of contaminants in the feed. Hence, the major contributor to the exergy destruction is the heat loss from the modules to the surroundings and the latent heat transferred with the permeate. The heat transfer rates across the module can be assisted by employing condensation plates with good heat conduction, minimizing heat losses to the module frames and covers, and using membranes of lower heat conduction properties.

8.3 Exergy destruction share of components

Considering each component of the MD as an open system, the exergy destruction contributions can be pinpointed. Doing so will enable system designers to optimize the performance of the components. The result from calculations of exergetic destruction contributions of each component from both MD systems is summarized in Figure 8.6. The maximum fraction of exergy destruction in both MD types comes from the MD modules. However, the percentage is higher for the Xzero module (58%) than for the Elixir (43%). The pumps are in both cases the lowest contributors of exergy destruction. The re-concentrating tank contributed 34% of the exergy destruction to the Elixir unit, which was caused by the heat losses through the steel wall and evaporation occurred through openings in the cover as a source of heat was electric heaters. Even though in both types of MD modules it is found that the MD modules contribute the highest exergy destruction, the Elixir modules showed a lower percentage than those of the Xzero modules. The lower percentage of exergy destruction for the Elixir MD module is mainly due to the improved heat transfer capability of the condensation plates used and hence the higher degree of heat recovery from the cooling side of the module.

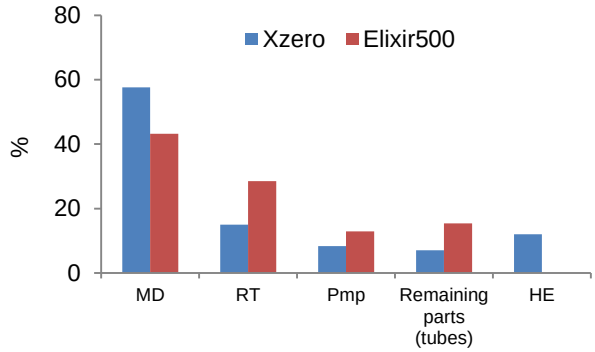

Figure 8.6. Percentage contribution of exergy destruction from the different components of each AGMD system: RT-Reconcentrating Tank, HE-.Heat Exchange, Pmp-pumps; MD-MD modules

A literature search for exergy efficiency analyses for related water purification processes, such as RO, revealed wide discrepancies in the values. Table 8.1 summarizes exergy efficiency for some of the standalone and integrated processes. In contrast to MD, the majority of the exergy rates in RO are derived from the high pressures involved, i.e., 15–25 bar for brackish water and 60–80 bar for seawater, hence the related pressure drop as reflected in improved efficiencies when a pressure exchanger is considered [200]. The very low exergy efficiency of MD reported [199] was from the one powered by solar thermal energy, and the high exergy losses were due to the MD and heat exchanger units. The MD units' exergy efficiency values are relatively closer to each other than with RO. If we make comparisons between systems of similar processes and capacities, we see, for example, that the MD with a capacity of 0.3 m^3/day [199] and Elixir from the present study have comparable exergy efficiency.

Table 8.1. Summary of exergy efficiencies for different MD configurations and RO from the literature.

Process	Capacity, m^3/day	Exergy Efficiency, %	Reference
RO	7250	4.3	[201]
RO	2850	0.72	[202]
SWRO	7586	5.82	[203]
MF-NF-RO	12,408	30.9	[204]
MD on RO retentate	22,344	19.1–21.9	[204]
MD	0.31	0.3	[199]
DCMD with HR	24,000	28.3	[9]
DCMD without HR	24,000	25.6	[9]
AGMD (Xzero)	0.22–0.73	8.54–19.32	[This study]
AGMD (Elixir)	0.1–0.17	18.3–26.5	[This study]

8.4 Concluding remarks

This chapter presented exergy analysis of MD systems using thermodynamic data from a set of experiments on two types of AGMD modules. The assessed MD units showed different exergy efficiencies mainly due to the differences in module size and the type of condensation plates used. The exergy efficiencies were also affected to different degrees by the feed–coolant temperature differences in both types of modules. For the Xzero MD module, the exergy efficiency was not significantly affected by the difference in temperature across the module, whereas, for Elixir, a higher temperature difference across the module yielded higher exergy efficiencies and lower exergy destruction. The exergy efficiency results showed that the materials selection of the condensation plate plays a role in optimizing the performance of MD systems. This is clearly an important part of the MD system design and optimization, as the MD module contributes to the majority of the exergy destruction. Materials that could be considered for optimum heat transfer across modules and hence less exergy destruction from MD modules include stainless steel and high-density polyethylene, which have better thermal conductivities than polypropylene. The selection of membrane and support material should also be considered when designing MD modules, as membrane and support materials, unlike condensation plates, should have less thermal conductivity for better thermal efficiency of modules overall.

9 Conclusions and Recommendations

Membrane distillation has been shown to be a promising separation technology not only for water purification applications in process water production for industries, but also for recovering valuable by-products and removing pollutants from wastewater effluents.

This dissertation presented some potential applications of MD systems integrated with DH networks that could be preferred over current practices in the industries. District heating networks are well-established systems of producing and distributing heat in a centralized unit. Even though DH demands in houses and buildings may decrease in the future owing to increased energy efficiency, industries have the potential to expand their reliance on such systems. Identifying DH networks as a reliable heat source for large-scale MD systems is promising regarding its continued viability.

A short summary of the three case studies now follows. The first application considered drug residue removal from municipal WWTP effluent. The analyses of samples from its effluent proved that 30 pharmaceutical substances were quantified in levels from 10 ng/L to about 1 mg/L, which shows that conventional WWTP is not capable of completely removing these active substances. The release of such small quantities of pharmaceutical residues may not have an immediate effect on aquatic life, but the continuous release and longer time bioaccumulation in ecosystems is potentially detrimental. Pilot-scale AGMD was tested for removing those same detected drug residues, and the technology was found to completely remove all substances except Sertraline, which was detected in the concentration of less than 15 ng/L. Trials on concentrating the feed have also shown that similar removal efficiencies were achieved by AGMD. Permeate flux and specific heat demand varied depending on temperature difference across the module.

Thermal efficiency analysis also showed this trend which suggests less efficient process at higher feed temperatures. The economic assessment of full-scale MD system at various capacities showed that thermal energy cost contributed for more than 75% of the annual cost. This means any system design improvements targeting to minimize heat demand will also reduce the economy of such applications.

The second application also focused on pharmaceuticals, but as a novel wastewater treatment method in industrial production. This study considered a wastewater stream of 3 m^3/h capacity with energy demand and overall economic analysis compared to conventional technology (activated carbon). A favorable DH network integration was identified such that heat purchased at 2014 levels could be employed to drive the MD system while simultaneously providing necessary process heat. It was found that in addition to economic gains, a zero liquid discharge purification scenario could be achieved with MD technology.

Recovery of valuable product and possibility of recycling process water in bioethanol production is the third process investigated. The separation performance of two types of AGMD modules for ethanol-water mixtures was tested at laboratory scale, and scaled-up simulations carried out to assess the economy of such large-scale integrations. Even though the specific heat demand of the MD was found to be higher than for conventional distillation, the overall annual cost becomes lower which makes MD economical. The proposed approach showed that it is technically feasible to partially offload the steam-driven distillation columns with DH-driven membrane distillation.

Finally, exergy efficiency assessment was applied to help identify components of an MD system for their exergy losses. The exergy analysis revealed that the MD modules contribute to the maximum exergy destruction of the system. The exergy efficiency was found to be affected by the temperature across the module which increases with increasing temperature difference. This study showed that selection of materials used to build components contributes to exergetic losses in addition to the temperature variations.

Membrane distillation is a promising technology for the applications investigated in this dissertation. The separation efficiency of the AGMD systems was found to be on par or superior than other technologies for the case studies under consideration. Thermal energy demand was assessed to drive the MD systems effectively. MD modules were applied as the same purpose as heat exchangers to make use of district heating more efficiently. District heating networks are judged to be a sustainable source of heat for future MD systems in industrial applications. DH expansions and increased use in industries is an encouraging scenario for MD modules developers and suppliers. The trend that more and more DH is coming from biomass based cogeneration plants is another positive factor for using DH to drive MD systems. These types of MD-DH integrations would contribute for the market expansion and use of DH over other heat sources. If DH is supplied biomass based CHP, it could increase production of electricity and therefore play a significant role in increasing the share of renewable energy sources (RES), which in turn will reduce primary energy demand.

MD has the technical, economic and environmental benefits for the promising applications discussed in this study. However, there are still challenges for it to be commercially viable. Future studies should focus on developing large-size MD modules suitable for large-scale industrial applications. The design improvement could also be in their design so that heating demand would be optimum. Pilot tests are also recommended for the ethanol recovery and pharmaceutical wastewater purification cases. This is because the real stream from these processes is a mixture of many more components than water and ethanol or pharmaceutical substances whose presence potentially affects the performance of membranes. Hence, fouling of membranes due to other organic components in the feed affects the frequency at which they should be cleaned or replaced which affects the cost of purification. Furthermore, possibilities to recover waste heat could be explored especially in the bioethanol plant where heat released from mash cooling could potentially be used to drive MD systems.

References

[1] UN Water Cooperation and UN Water Cooperation 2013, “2013 - United Nations International Year of Water Cooperation: Facts and Figure,” *Www.Unwater.Org*, 2013. [Online]. Available: http://www.unwater.org/water-cooperation-2013/water-cooperation/facts-and-figures/en/. [Accessed: 10-Nov-2016].

[2] UNEP, “Freshwater use by sector at the beginning of the 2000s,” 2010. [Online]. Available: http://www.unep.org/dewa/vitalwater/article48.html. [Accessed: 08-Nov-2016].

[3] Al Fry, “FACTS AND TRENDS,” *World Bussiness Council for Sustainable Development, WBCSD*. pp. 5–6, May-2005.

[4] J. Forster, “Water use in industry - Statistics Explained,” *Eurostatistics*, 2014. [Online]. Available: http://ec.europa.eu/eurostat/statistics-explained/index.php/Water_use_in_industry. [Accessed: 14-Dec-2016].

[5] (The European Parliament and the Council of the European Union) EPCEU, “Directive 2010/75/EU of the European Parliament and of the Council of 24 November 2010 on industrial emissions (integrated pollution prevention and control),” *Off. J. Eur. Union*, no. 1, pp. 1–103, 2010.

[6] M. Khayet and T. Matsuura, *Membrane Distillation: Principles and Applications*. Amsterdam: Elsevier, 2011.

[7] P. K. Weyl, “Recovery of demineralized water from saline waters,” U.S. Patent 3,340,186, 1967.

[8] M. E. Findley, “Vaporization through Porous Membranes,” *Ind. Eng. Chem. Process Des. Dev.*, vol. 6, no. 2, pp. 226–230, Apr. 1967.

[9] S. Al-Obaidani, E. Curcio, F. Macedonio, G. Di Profio, H. Al-Hinai, and E. Drioli, “Potential of membrane distillation in seawater desalination: Thermal efficiency, sensitivity study and cost estimation,” *J. Memb. Sci.*, vol. 323, no. 1, pp. 85–98, Oct. 2008.

[10] A. Alkhudhiri, N. Darwish, and N. Hilal, “Membrane distillation: A comprehensive review,” *Desalination*, vol. 287, no. 2012, pp. 2–18, Feb. 2012.

[11] G. Amy *et al.*, “Membrane-based seawater desalination: Present and future prospects,” *Desalination*, vol. 401, pp. 16–21, 2017.

[12] L. D. Tijing, J.-S. Choi, S. Lee, S.-H. Kim, and H. K. Shon, “Recent progress of membrane distillation using electrospun nanofibrous membrane,” *J. Memb. Sci.*, vol. 453, pp. 435–462, Mar. 2014.

[13] A. Hausmann, P. Sanciolo, T. Vasiljevic, M. Weeks, and M. Duke, “Integration of membrane distillation into heat paths of industrial processes,” *Chem. Eng. J.*, vol. 211–212, pp. 378–387, 2012.

[14] J.-P. Mericq, S. Laborie, and C. Cabassud, “Evaluation of systems coupling vacuum membrane distillation and solar energy for seawater desalination,” *Chem. Eng. J.*, vol. 166, no. 2, pp. 596–606, Jan. 2011.

[15] N. T. Uday Kumar, G. Mohan, and A. Martin, “Performance analysis of solar cogeneration system with different integration strategies for potable water and domestic hot water production,” *Appl. Energy*, vol. 170, pp. 466–475, May 2016.

[16] A. Kullab and A. Martin, “Membrane distillation and applications for water purification in thermal cogeneration plants,” *Sep. Purif. Technol.*, vol. 76, no. 3, pp. 231–237, Jan. 2011.

[17] P. Wang, M. M. Teoh, and T.-S. Chung, “Morphological architecture of dual-layer hollow fiber for membrane distillation with higher desalination performance,” *Water Res.*, vol. 45, no. 17, pp. 5489–5500, Nov. 2011.

[18] S. Yarlagadda, V. G. Gude, L. M. Camacho, S. Pinappu, and S. Deng, “Potable water recovery from As, U, and F contaminated ground waters by direct contact membrane distillation process,” *J. Hazard. Mater.*, vol. 192, no. 3, pp. 1388–1394, Sep. 2011.

[19] M. I. Ali, E. K. Summers, H. A. Arafat, and J. H. L. V, “Effects of membrane properties on water production cost in small scale membrane distillation systems,” *Desalination*, vol. 306, pp. 60–71, Nov. 2012.

[20] M. M. A. Shirazi, A. Kargari, and M. Tabatabaei, “Evaluation of commercial PTFE

membranes in desalination by direct contact membrane distillation," *Chem. Eng. Process. Process Intensif.*, vol. 76, pp. 16–25, Feb. 2014.

[21] E. K. Summers, H. A. Arafat, and J. H. Lienhard, "Energy efficiency comparison of single-stage membrane distillation (MD) desalination cycles in different configurations," *Desalination*, vol. 290, pp. 54–66, Mar. 2012.

[22] U. K. Kesieme and H. Aral, "Application of membrane distillation and solvent extraction for water and acid recovery from acidic mining waste and process solutions," *J. Environ. Chem. Eng.*, vol. 3, no. 3, pp. 2050–2056, Sep. 2015.

[23] D. Hou, G. Dai, J. Wang, H. Fan, Z. Luan, and C. Fu, "Boron removal and desalination from seawater by PVDF flat-sheet membrane through direct contact membrane distillation," *Desalination*, vol. 326, pp. 115–124, Oct. 2013.

[24] S. Gunko, S. Verbych, M. Bryk, and N. Hilal, "Concentration of apple juice using direct contact membrane distillation," *Desalination*, vol. 190, no. 1–3, pp. 117–124, Apr. 2006.

[25] A. El-Abbassi, A. Hafidi, M. Khayet, and M. C. García-Payo, "Integrated direct contact membrane distillation for olive mill wastewater treatment," *Desalination*, vol. 323, pp. 31–38, Aug. 2013.

[26] M. Khayet, "Treatment of radioactive wastewater solutions by direct contact membrane distillation using surface modified membranes," *Desalination*, vol. 321, pp. 60–66, Jul. 2013.

[27] L. Song, Z. Ma, X. Liao, P. B. Kosaraju, J. R. Irish, and K. K. Sirkar, "Pilot plant studies of novel membranes and devices for direct contact membrane distillation-based desalination," *J. Memb. Sci.*, vol. 323, no. 2, pp. 257–270, Oct. 2008.

[28] H. C. Duong *et al.*, "Treatment of RO brine from CSG produced water by spiral-wound air gap membrane distillation — A pilot study," *Desalination*, vol. 366, pp. 121–129, Jun. 2015.

[29] G. L. Liu, C. Zhu, C. S. Cheung, and C. W. Leung, "Theoretical and experimental studies on air gap membrane distillation," *Heat Mass Transf.*, vol. 34, no. 4, pp. 329–335, Nov. 1998.

[30] A. Cipollina, M. G. Di Sparti, A. Tamburini, and G. Micale, "Development of a

Membrane Distillation module for solar energy seawater desalination," *Chem. Eng. Res. Des.*, vol. 90, no. 12, pp. 2101–2121, Dec. 2012.

[31] H. C. Duong, P. Cooper, B. Nelemans, T. Y. Cath, and L. D. Nghiem, "Evaluating energy consumption of air gap membrane distillation for seawater desalination at pilot scale level," *Sep. Purif. Technol.*, vol. 166, pp. 55–62, 2016.

[32] H. Geng, H. Wu, P. Li, and Q. He, "Study on a new air-gap membrane distillation module for desalination," *Desalination*, vol. 334, no. 1, pp. 29–38, Feb. 2014.

[33] F. A. Banat and J. Simandl, "Membrane distillation for dilute ethanol," *J. Memb. Sci.*, vol. 163, no. 2, pp. 333–348, Nov. 1999.

[34] M. . García-Payo, M. . Izquierdo-Gil, and C. Fernández-Pineda, "Air gap membrane distillation of aqueous alcohol solutions," *J. Memb. Sci.*, vol. 169, no. 1, pp. 61–80, Apr. 2000.

[35] E. U. Khan and A. R. Martin, "Water purification of arsenic-contaminated drinking water via air gap membrane distillation (AGMD)," *Period. Polytech. Mech. Eng.*, vol. 58, no. 1, pp. 47–53, 2014.

[36] L. Gazagnes, S. Cerneaux, M. Persin, E. Prouzet, and A. Larbot, "Desalination of sodium chloride solutions and seawater with hydrophobic ceramic membranes," *Desalination*, vol. 217, no. 1–3, pp. 260–266, Nov. 2007.

[37] M. Khayet and C. Cojocaru, "Air gap membrane distillation: Desalination, modeling and optimization," *Desalination*, vol. 287, pp. 138–145, 2012.

[38] C. K. Chiam and R. Sarbatly, "Vacuum membrane distillation processes for aqueous solution treatment—A review," *Chem. Eng. Process. Process Intensif.*, vol. 74, pp. 27–54, Dec. 2013.

[39] K. W. Lawson and D. R. Lloyd, "Membrane distillation . I . Module design and performance evaluation using vacuum membrane distillation," *J. Memb. Sci.*, vol. 120, no. 1, pp. 111–121, 1996.

[40] C. Huayan, W. Chunrui, J. Yue, W. Xuan, and L. Xiaolong, "Comparison of three membrane distillation confi gurations and seawater desalination by vacuum membrane distillation," *Desalin. Water Treat.*, vol. 28, no. 1–3, pp. 321–327, Apr. 2011.

[41] G. A. Mannella, V. La Carrubba, and V. Brucato, “Evaluation of vapor mass transfer in various membrane distillation configurations: an experimental study,” *Heat Mass Transf.*, vol. 48, pp. 945–952, Jun. 2012.

[42] J. Zhang *et al.*, “Modelling of vacuum membrane distillation,” *J. Memb. Sci.*, vol. 434, pp. 1–9, May 2013.

[43] E. Drioli *et al.*, “Novel PVDF hollow fiber membranes for vacuum and direct contact membrane distillation applications,” *Sep. Purif. Technol.*, vol. 115, pp. 27–38, Aug. 2013.

[44] H. Fan and Y. Peng, “Application of PVDF membranes in desalination and comparison of the VMD and DCMD processes,” *Chem. Eng. Sci.*, vol. 79, pp. 94–102, Sep. 2012.

[45] R. Thomas, E. Guillen-Burrieza, and H. A. Arafat, “Pore structure control of PVDF membranes using a 2-stage coagulation bath phase inversion process for application in membrane distillation (MD),” *J. Memb. Sci.*, vol. 452, pp. 470–480, Feb. 2014.

[46] J.-Y. Shi, Z.-P. Zhao, and C.-Y. Zhu, “Studies on simulation and experiments of ethanol–water mixture separation by VMD using a PTFE flat membrane module,” *Sep. Purif. Technol.*, vol. 123, pp. 53–63, Feb. 2014.

[47] R. Bagger-Jørgensen, A. S. Meyer, M. Pinelo, C. Varming, and G. Jonsson, “Recovery of volatile fruit juice aroma compounds by membrane technology: Sweeping gas versus vacuum membrane distillation,” *Innov. Food Sci. Emerg. Technol.*, vol. 12, no. 3, pp. 388–397, Jul. 2011.

[48] B. Wu, X. Tan, K. Li, and W. K. Teo, “Removal of 1,1,1-trichloroethane from water using a polyvinylidene fluoride hollow fiber membrane module: Vacuum membrane distillation operation,” *Sep. Purif. Technol.*, vol. 52, no. 2, pp. 301–309, Dec. 2006.

[49] M. S. EL-Bourawi, M. Khayet, R. Ma, Z. Ding, Z. Li, and X. Zhang, “Application of vacuum membrane distillation for ammonia removal,” *J. Memb. Sci.*, vol. 301, no. 1–2, pp. 200–209, Sep. 2007.

[50] M. Khayet, P. Godino, and J. I. Mengual, “Theory and experiments on sweeping gas membrane distillation,” *J. Memb. Sci.*, vol. 165, no. 2, pp. 261–272, Feb. 2000.

[51] M. S. El-Bourawi, Z. Ding, R. Ma, and M. Khayet, “A framework for better understanding membrane distillation separation process,” *J. Memb. Sci.*, vol. 285, no. 1–2, pp. 4–29, Nov. 2006.

[52] Z. Xie, T. Duong, M. Hoang, C. Nguyen, and B. Bolto, “Ammonia removal by sweep gas membrane distillation,” *Water Res.*, vol. 43, no. 6, pp. 1693–1699, Apr. 2009.

[53] M. M. a. Shirazi, A. Kargari, and M. Tabatabaei, “Sweeping Gas Membrane Distillation (SGMD) as an Alternative for Integration of Bioethanol Processing: Study on a Commercial Membrane and Operating Parameters,” *Chem. Eng. Commun.*, vol. 202, no. 4, pp. 457–466, Apr. 2015.

[54] M. M. a. Shirazi, A. Kargari, D. Bastani, and L. Fatehi, “Production of drinking water from seawater using membrane distillation (MD) alternative: direct contact MD and sweeping gas MD approaches,” *Desalin. Water Treat.*, vol. 52, no. 13–15, pp. 2372–2381, Apr. 2014.

[55] M. Khayet, M. P. Godino, and J. I. Mengual, “Theoretical and experimental studies on desalination using the sweeping gas membrane distillation method,” *Desalination*, vol. 157, no. 1–3, pp. 297–305, Aug. 2003.

[56] L. Basini, G. D’Angelo, M. Gobbi, G. C. Sarti, and C. Gostoli, “A desalination process through sweeping gas membrane distillation,” *Desalination*, vol. 64, no. C, pp. 245–257, Jan. 1987.

[57] A. Sääsk, “Method for Making Purified Water and Electricity and A Device Therefor,” US 2011/0042314 A1, 2011.

[58] Aquaver, “Aquaver-case study,” 2014. [Online]. Available: http://www.aquaver.com/knowledge-center-articles/membrane-distillation-a-low-cost-breakthrough-technology-for-water-treatment/. [Accessed: 17-Nov-2015].

[59] P. Wang and T.-S. Chung, “Recent advances in membrane distillation processes: Membrane development, configuration design and application exploring,” *J. Memb. Sci.*, vol. 474, pp. 39–56, Jan. 2015.

[60] L. Francis, N. Ghaffour, A. A. Alsaadi, and G. L. Amy, “Material gap membrane distillation: A new design for water vapor flux enhancement,” *J. Memb. Sci.*, vol. 448, pp. 240–247, Dec. 2013.

[61] M. Gryta, “Osmotic MD and other membrane distillation variants,” *J. Memb. Sci.*, vol. 246, no. 2, pp. 145–156, Jan. 2005.

[62] W. Kujawski, A. Sobolewska, K. Jarzynka, C. Güell, M. Ferrando, and J. Warczok, “Application of osmotic membrane distillation process in red grape juice concentration,” *J. Food Eng.*, vol. 116, no. 4, pp. 801–808, Jun. 2013.

[63] J. Kujawa, E. Guillen-Burrieza, H. A. Arafat, M. Kurzawa, A. Wolan, and W. Kujawski, “Raw Juice Concentration by Osmotic Membrane Distillation Process with Hydrophobic Polymeric Membranes,” *Food Bioprocess Technol.*, vol. 8, no. 10, pp. 2146–2158, Oct. 2015.

[64] L. F. Sotoft, K. V. Christensen, R. Andrésen, and B. Norddahl, “Full scale plant with membrane based concentration of blackcurrant juice on the basis of laboratory and pilot scale tests,” *Chem. Eng. Process. Process Intensif.*, vol. 54, pp. 12–21, Apr. 2012.

[65] J. Warczok, M. Gierszewska, W. Kujawski, and C. Guell, “Application of osmotic membrane distillation for reconcentration of sugar solutions from osmotic dehydration,” *Sep. Purif. Technol.*, vol. 57, no. 3, pp. 425–429, Nov. 2007.

[66] D. Bessarabov and Z. Twardowski, “New opportunities for osmotic membrane distillation,” *Membr. Technol.*, vol. 2006, no. 7, pp. 7–11, Jul. 2006.

[67] F. He, J. Gilron, and K. K. Sirkar, “High water recovery in direct contact membrane distillation using a series of cascades,” *Desalination*, vol. 323, pp. 48–54, Aug. 2013.

[68] K. Zhao *et al.*, “Experimental study of the memsys vacuum-multi-effect-membrane-distillation (V-MEMD) module,” *Desalination*, vol. 323, pp. 150–160, Aug. 2013.

[69] L. M. Camacho *et al.*, “Advances in membrane distillation for water desalination and purification applications,” *Water*, vol. 5, no. 1, pp. 94–196, Jan. 2013.

[70] M. Khayet, “Membranes and theoretical modeling of membrane distillation: a review.,” *Adv. Colloid Interface Sci.*, vol. 164, no. 1–2, pp. 56–88, May 2011.

[71] L. Eykens, K. De Sitter, C. Dotremont, L. Pinoy, and B. Van der Bruggen, “Membrane synthesis for membrane distillation: A review,” *Sep. Purif. Technol.*, vol. 182, pp. 36–51, Jul. 2017.

[72] J. Zhang, J.-D. Li, and S. Gray, “Effect of applied pressure on performance of PTFE membrane in DCMD,” *J. Memb. Sci.*, vol. 369, no. 1–2, pp. 514–525, Mar. 2011.

[73] S. Adnan, M. Hoang, H. Wang, and Z. Xie, “Commercial PTFE membranes for membrane distillation application: Effect of microstructure and support material,” *Desalination*, vol. 284, no. null, pp. 297–308, Jan. 2012.

[74] A. Hausmann *et al.*, “Fouling of dairy components on hydrophobic polytetrafluoroethylene (PTFE) membranes for membrane distillation,” *J. Memb. Sci.*, vol. 442, pp. 149–159, Sep. 2013.

[75] A. Khalifa, D. Lawal, M. Antar, and M. Khayet, “Experimental and theoretical investigation on water desalination using air gap membrane distillation,” *Desalination*, vol. 376, pp. 94–108, Nov. 2015.

[76] F. Macedonio, A. Ali, T. Poerio, E. El-Sayed, E. Drioli, and M. Abdel-Jawad, “Direct contact membrane distillation for treatment of oilfield produced water,” *Sep. Purif. Technol.*, vol. 126, pp. 69–81, Apr. 2014.

[77] L. Francis, N. Ghaffour, A. S. Alsaadi, S. P. Nunes, and G. L. Amy, “Performance evaluation of the DCMD desalination process under bench scale and large scale module operating conditions,” *J. Memb. Sci.*, vol. 455, pp. 103–112, 2014.

[78] J. Xu, Y. B. Singh, G. L. Amy, and N. Ghaffour, “Effect of operating parameters and membrane characteristics on air gap membrane distillation performance for the treatment of highly saline water,” *J. Memb. Sci.*, vol. 512, pp. 73–82, 2016.

[79] D. Hou, G. Dai, J. Wang, H. Fan, L. Zhang, and Z. Luan, “Preparation and characterization of PVDF/nonwoven fabric flat-sheet composite membranes for desalination through direct contact membrane distillation,” *Sep. Purif. Technol.*, vol. 101, pp. 1–10, Nov. 2012.

[80] C. Feng, B. Shi, G. Li, and Y. Wu, “Preparation and properties of microporous membrane from poly(vinylidene fluoride-co-tetrafluoroethylene) (F2.4) for membrane distillation,” *J. Memb. Sci.*, vol. 237, no. 1–2, pp. 15–24, Jul. 2004.

[81] Y. Wu, Y. Kong, X. Lin, W. Liu, and J. Xu, “Surface-modified hydrophilic membranes in membrane distillation,” *J. Memb. Sci.*, vol. 72, pp. 189–196, 1992.

[82] H. Fang, J. F. Gao, H. T. Wang, and C. S. Chen, “Hydrophobic porous alumina hollow fiber for water desalination via membrane distillation process,” *J. Memb. Sci.*, vol. 403–404, pp. 41–46, Jun. 2012.

[83] J.-W. Wang, L. Li, J.-W. Zhang, X. Xu, and C.-S. Chen, “β-Sialon ceramic hollow fiber membranes with high strength and low thermal conductivity for membrane distillation,” *J. Eur. Ceram. Soc.*, vol. 36, no. 1, pp. 59–65, Jan. 2016.

[84] N. Dow *et al.*, “Pilot trial of membrane distillation driven by low grade waste heat: Membrane fouling and energy assessment,” *Desalination*, vol. 391, pp. 30–42, Aug. 2016.

[85] L. Li and K. K. Sirkar, “Influence of microporous membrane properties on the desalination performance in direct contact membrane distillation,” *J. Memb. Sci.*, vol. 513, pp. 280–293, Sep. 2016.

[86] M. Khayet, P. Godino, and J. I. Mengual, “Nature of flow on sweeping gas membrane distillation,” *J. Memb. Sci.*, vol. 170, no. 2, pp. 243–255, May 2000.

[87] A. S. Rattner, A. K. Nagavarapu, S. Garimella, and T. F. Fuller, “Modeling of a flat plate membrane-distillation system for liquid desiccant regeneration in air-conditioning applications,” *Int. J. Heat Mass Transf.*, vol. 54, no. 15–16, pp. 3650–3660, Jul. 2011.

[88] E. Drioli, A. Ali, and F. Macedonio, “Membrane distillation: Recent developments and perspectives,” *Desalination*, vol. 356, pp. 56–84, Jan. 2015.

[89] E. Guillén-Burrieza *et al.*, “Experimental analysis of an air gap membrane distillation solar desalination pilot system,” *J. Memb. Sci.*, vol. 379, no. 1–2, pp. 386–396, Sep. 2011.

[90] R. B. Saffarini, E. K. Summers, H. A. Arafat, and J. H. Lienhard V, “Technical evaluation of stand-alone solar powered membrane distillation systems,” *Desalination*, vol. 286, pp. 332–341, Feb. 2012.

[91] E. Guillén-Burrieza, G. Zaragoza, S. Miralles-Cuevas, and J. Blanco, “Experimental evaluation of two pilot-scale membrane distillation modules used for solar desalination,” *J. Memb. Sci.*, vol. 409–410, pp. 264–275, Aug. 2012.

[92] S. Adham, A. Hussain, J. M. Matar, R. Dores, and A. Janson, “Application of

Membrane Distillation for desalting brines from thermal desalination plants," *Desalination*, vol. 314, no. 2013, pp. 101–108, Apr. 2013.

[93] D. Singh and K. K. Sirkar, "Desalination of brine and produced water by direct contact membrane distillation at high temperatures and pressures," *J. Memb. Sci.*, vol. 389, pp. 380–388, Feb. 2012.

[94] H. Selcuk, "Decolorization and detoxification of textile wastewater by ozonation and coagulation processes," *Dye. Pigment.*, vol. 64, no. 3, pp. 217–222, Mar. 2005.

[95] C. Bellona, J. E. Drewes, P. Xu, and G. Amy, "Factors affecting the rejection of organic solutes during NF/RO treatment—a literature review," *Water Res.*, vol. 38, no. 12, pp. 2795–2809, Jul. 2004.

[96] J. E. Drewes, M. Reinhard, and P. Fox, "Comparing microfiltration-reverse osmosis and soil-aquifer treatment for indirect potable reuse of water," *Water Res.*, vol. 37, no. 15, pp. 3612–3621, Sep. 2003.

[97] K. Kimura, G. Amy, J. E. Drewes, T. Heberer, T.-U. Kim, and Y. Watanabe, "Rejection of organic micropollutants (disinfection by-products, endocrine disrupting compounds, and pharmaceutically active compounds) by NF/RO membranes," *J. Memb. Sci.*, vol. 227, no. 1–2, pp. 113–121, Dec. 2003.

[98] K. Gethard and S. Mitra, "Membrane distillation as an online concentration technique: application to the determination of pharmaceutical residues in natural waters," *Anal. Bioanal. Chem.*, vol. 400, no. 2, pp. 571–575, Apr. 2011.

[99] K. Gethard, O. Sae-Khow, and S. Mitra, "Carbon nanotube enhanced membrane distillation for simultaneous generation of pure water and concentrating pharmaceutical waste," *Sep. Purif. Technol.*, vol. 90, no. 2012, pp. 239–245, Apr. 2012.

[100] K. Gethard and S. Mitra, "Carbon nanotube enhanced membrane distillation for online preconcentration of trace pharmaceuticals in polar solvents.," *Analyst*, vol. 136, no. 12, pp. 2643–8, Jun. 2011.

[101] D. Hou, J. Wang, X. Sun, Z. Luan, C. Zhao, and X. Ren, "Boron removal from aqueous solution by direct contact membrane distillation," *J. Hazard. Mater.*, vol. 177, no. 1–3, pp. 613–619, May 2010.

[102] F. Banat, S. Al-Asheh, and M. Qtaishat, “Treatment of waters colored with methylene blue dye by vacuum membrane distillation,” *Desalination*, vol. 174, no. 1, pp. 87–96, Apr. 2005.

[103] V. Calabrò, E. Drioli, and F. Matera, “Membrane distillation in the textile wastewater treatment.,” *Desalination*, vol. 83, no. 1–3, pp. 209–224, Sep. 1991.

[104] A. Criscuoli, J. Zhong, A. Figoli, M. Carnevale, R. Huang, and E. Drioli, “Treatment of dye solutions by vacuum membrane distillation,” *Water Res.*, vol. 42, no. 20, pp. 5031–5037, Dec. 2008.

[105] C. Liu and A. R. Martin, “The use of membrane distillation in high-purity water production for the semiconductor industry,” *Ultrapure Water*, vol. 23, no. 3, pp. 32–38, 2006.

[106] A. K. Manna, M. Sen, A. R. Martin, and P. Pal, “Removal of arsenic from contaminated groundwater by solar-driven membrane distillation.,” *Environ. Pollut.*, vol. 158, no. 3, pp. 805–11, Mar. 2010.

[107] D. Singh, P. Prakash, and K. K. Sirkar, “Deoiled Produced Water Treatment Using Direct-Contact Membrane Distillation,” *Ind. Eng. Chem. Res.*, vol. 52, no. 37, pp. 13439–13448, 2013.

[108] A. Alkhudhiri, N. Darwish, and N. Hilal, “Produced water treatment: Application of Air Gap Membrane Distillation,” *Desalination*, vol. 309, pp. 46–51, Jan. 2013.

[109] V. D. Alves and I. M. Coelhoso, “Orange juice concentration by osmotic evaporation and membrane distillation: A comparative study,” *J. Food Eng.*, vol. 74, no. 1, pp. 125–133, May 2006.

[110] L. Eykens, K. De Sitter, C. Dotremont, L. Pinoy, and B. Van Der Bruggen, “How to Optimize the Membrane Properties for Membrane Distillation: A Review,” *Ind. Eng. Chem. Res.*, vol. 55, no. 35, pp. 9333–9343, 2016.

[111] M. Gryta, “Membrane distillation of NaCl solution containing natural organic matter,” *J. Memb. Sci.*, vol. 181, no. 2, pp. 279–287, 2001.

[112] Z. Xie *et al.*, “Effect of Membrane Properties on Performance of Membrane Distillation for Ammonia Removal,” *J. Mater. Sci. Res.*, vol. 1, no. 1, pp. 37–44, Dec. 2011.

[113] A. Hausmann, P. Sanciolo, T. Vasiljevic, U. Kulozik, and M. Duke, “Performance assessment of membrane distillation for skim milk and whey processing,” *J. Dairy Sci.*, vol. 97, no. 1, pp. 56–71, Jan. 2014.

[114] A. Hausmann *et al.*, “Fouling mechanisms of dairy streams during membrane distillation,” *J. Memb. Sci.*, vol. 441, pp. 102–111, Aug. 2013.

[115] Á. Kozák, E. Békássy-Molnár, and G. Vatai, “Production of black-currant juice concentrate by using membrane distillation,” *Desalination*, vol. 241, no. 1–3, pp. 309–314, May 2009.

[116] M. Tomaszewska, “Membrane distillation-examples of applications in technology and environmental protection,” *Polish J. Environ. Stud.*, vol. 9, no. 1, pp. 27–36, 2000.

[117] G. Lewandowicz, W. Białas, B. Marczewski, and D. Szymanowska, “Application of membrane distillation for ethanol recovery during fuel ethanol production,” *J. Memb. Sci.*, vol. 375, no. 1–2, pp. 212–219, Jun. 2011.

[118] M. Gryta, A. W. Morawski, and M. Tomaszewska, “Ethanol production in membrane distillation bioreactor,” *Catal. Today*, vol. 56, no. 1–3, pp. 159–165, Feb. 2000.

[119] X. Li, Y. Qin, R. Liu, Y. Zhang, and K. Yao, “Study on concentration of aqueous sulfuric acid solution by multiple-effect membrane distillation,” *Desalination*, vol. 307, pp. 34–41, Dec. 2012.

[120] M. Khayet and J. I. Mengual, “Effect of salt concentration during the treatment of humic acid solutions by membrane distillation,” *Desalination*, vol. 168, pp. 373–381, Aug. 2004.

[121] J. Tang and K. Zhou, “Hydrochloric acid recovery from rare earth chloride solutions by vacuum membrane distillation,” *Rare Met.*, vol. 25, no. 3, pp. 287–292, Jun. 2006.

[122] “Membrane distillation process with modules “memDist“.” [Online]. Available: http://www.memsys.eu/technology.html. [Accessed: 12-Sep-2016].

[123] D. Winter, “Membrane Distillation - a Thermodynamic , Technological and Economic Analysis, PhD Thesis, University of Kaiserslautern,” Shaker Verlag,

Aechen, Germany., 2015.

[124] J. H. Hanemaaijer *et al.*, “Memstill membrane distillation – a future desalination technology,” *Desalination*, vol. 199, no. 1–3, pp. 175–176, Nov. 2006.

[125] R. Schwantes *et al.*, “Membrane distillation: Solar and waste heat driven demonstration plants for desalination,” *Desalination*, vol. 323, pp. 93–106, Aug. 2013.

[126] A. Jansen, J. Hanemaaijer, J. Assink, E. van Sonsbeek, C. Dotremont, and M. J Van, “Pilot plants prove feasibility of a new desalination technique,” *Asian Water*, no. March, pp. 22–26, 2010.

[127] A. Ali, C. A. A. Quist-Jensen, F. Macedonio, and E. Drioli, “Optimization of module length for continuous direct contact membrane distillation process,” *Chem. Eng. Process. Process Intensif.*, vol. 110, pp. 188–200, Dec. 2016.

[128] S. Ben Abdallah, N. Frikha, and S. Gabsi, “Design of an autonomous solar desalination plant using vacuum membrane distillation, the MEDINA project,” *Chem. Eng. Res. Des.*, vol. 91, no. 12, pp. 2782–2788, Dec. 2013.

[129] Memsys, “Waste heat and membrane distillation help Maldives produce drinking water,” *Membr. Technol.*, vol. 2014, no. 4, p. 7, 2014.

[130] A. Castillo, C. Panoutsou, and A. Bauen, “Biomass role in achieving the Climate Change & Renewables EU policy targets. Demand and Supply dynamics under the perspective of stakeholders,” *IEE/08/653 BIOMASS FUTURES*, 2011. [Online]. Available: http://www.biomassfutures.eu/work_packages/work_packages.php. [Accessed: 12-Jun-2014].

[131] K. Ericsson and P. Svenningsson, “Introduction and development of the Swedish district heating systems-Critical factors and lessons learned,” Lund University, 2009.

[132] H. Sköldberg and B. Rydén, “The heating market in Sweden -an overall view,”Sverige Värmemarknad, 2014. [Online] Available. http://www.varmemarknad.se/pdf/Varmemarknad_Sverige_sammanfattning.pdf. [Accessed 12-Dec.-2015].

[133] D. Kulin and S. Enmalm, “Electricity supply, district heating and supply of natural

gas 2015," *Sveriges Off. Stat.*, vol. EN 11 SM 1, no. November, 2016.

[134] H. Sköldberg *et al.*, "Fjärrvärmen i framtiden," Svensk Fjärrvärme AB, Stockholm, 2011. [Online] Available. http://www.svenskfjarrvarme.se/Fjarrsyn/Forskning--Resultat/Ny-kunskapresultat/Rapporter/Omvarld/Fjarrvarmen-i-framtiden/ [Accessed 15-Dec.-2014].

[135] K.-M. Steen, U. Sagebrand, and H. Walletun, "Att använda fjärrvärme i industriprocesser," 2015. [Online] Available. http://www.energiforsk.se/program/-fjarrsyn/rapporter/att-anvanda-fjarrvarme-i-industriprocesser-2015-155/. [Accessed 10-Jan.-2016].

[136] L. Trygg, K. Difs, E. Wetterlund, P. Thollander, and I. Svensson, "Optimala fjärrvärmesystem i symbios med industri och samhälle," 2009. [Online] Available. http://www.svenskfjarrvarme.se/Om-oss/Forskning-och-utveckling/Fjarrsyn/Ny-kunskapresultat/Omvarld/200913-Optimala-fjarrvarmesystem/.[Accessed 21-Nov.-2014].

[137] M. Åslund, "Bra affär att torka spannmål med fjärrvärme," *Fjärrvärmetidningen*, pp. 12–13, Oct-2016.

[138] H. Gadd and S. Werner, "Achieving low return temperatures from district heating substations," *Appl. Energy*, vol. 136, pp. 59–67, Dec. 2014.

[139] S. Werner, "District heating and cooling in Sweden," *Energy*, vol. 126, pp. 419–429, May 2017.

[140] U. Fortkamp, H. Royen, M. Klingspor, Ö. Ekengren, A. Martin, and D. M. Woldemariam, "Membrane Distillation pilot tests for different wastewaters," IVL Swedish Environmental Research Institute, Stockholm, Report B 2236, 2015.

[141] A. Sääsk, "Removal of nanoparticles from semiconductor water," *Ultrapure Water*, no. May/June, pp. 1–5, 2013.

[142] D. Woldemariam, E. Khan, A. Kullab, and A. Martin, "District heat-driven water purification via membrane distillation," Energiforsk AB., Stockholm, Rapport 2016:229, 2016.

[143] G. Tsatsaronis, "Definitions and nomenclature in exergy analysis and exergoeconomics," *Energy*, vol. 32, no. 4, pp. 249–253, Apr. 2007.

[144] D. Elsevier, D. Elsevier, A. Criscuoli, A. Criscuoli, E. Drioli, and E. Drioli, “Energetic and exergetic analysis of an integrated membrane desalination system,” *Desalination*, vol. 124, no. 1–3, pp. 243–249, Nov. 1999.

[145] F. Macedonio and E. Drioli, “An exergetic analysis of a membrane desalination system,” *Desalination*, vol. 261, no. 3, pp. 293–299, Oct. 2010.

[146] E. Querol, B. Gonzalez-Regueral, and J. L. Perez-Benedito, “Exergy Concept and Determination,” in *Practical Approach to Exergy and Thermoeconomic Analyses of Industrial Processes*, 2013, pp. 9–28.

[147] I. Dincer and M. A. Rosen, *Exergy:Energy Environment and Sustainable Development*, 1st ed. Oxford, UK: Elsevier, 2007.

[148] G. de Koeijer and R. Rivero, “Entropy production and exergy loss in experimental distillation columns,” *Chem. Eng. Sci.*, vol. 58, no. 8, pp. 1587–1597, Apr. 2003.

[149] A. Ali, P. Aimar, and E. Drioli, “Effect of module design and flow patterns on performance of membrane distillation process,” *Chem. Eng. J.*, vol. 277, pp. 368–377, Oct. 2015.

[150] T. Brodin, J. Fick, M. Jonsson, and J. Klaminder, “Dilute Concentrations of a Psychiatric Drug Alter Behavior of Fish from Natural Populations,” *Science (80-.).*, vol. 339, no. 6121, pp. 814–815, Feb. 2013.

[151] M. S. Kostich, A. L. Batt, and J. M. Lazorchak, “Concentrations of prioritized pharmaceuticals in effluents from 50 large wastewater treatment plants in the US and implications for risk estimation,” *Environ. Pollut.*, vol. 184, pp. 354–359, Jan. 2014.

[152] J. Radjenović, M. Petrović, F. Ventura, and D. Barceló, “Rejection of pharmaceuticals in nanofiltration and reverse osmosis membrane drinking water treatment.,” *Water Res.*, vol. 42, no. 14, pp. 3601–10, Aug. 2008.

[153] M. Maurer, B. Escher, P. Richle, C. Schaffner, and A. Alder, “Elimination of β-blockers in sewage treatment plants,” *Water Res.*, vol. 41, no. 7, pp. 1614–1622, Apr. 2007.

[154] T. A. Ternes, “Occurrence of drugs in German sewage treatment plants and rivers,” *Water Res.*, vol. 32, no. 11, pp. 3245–3260, Nov. 1998.

[155] J. Fick, R. H. Lindberg, L. Kaj, and E. Brorström-Lundén, “Results from the Swedish National Screening Programme 2010,” IVL Swedish Environmental Research Institute, C 56, 2011.

[156] L. D. Nghiem, A. I. Schäfer, and M. Elimelech, “Pharmaceutical retention mechanisms by nanofiltration membranes,” *Environ. Sci. Technol.*, vol. 39, no. 19, pp. 7698–7705, Oct. 2005.

[157] K. Kimura, T. Iwase, S. Kita, and Y. Watanabe, “Influence of residual organic macromolecules produced in biological wastewater treatment processes on removal of pharmaceuticals by NF/RO membranes,” *Water Res.*, vol. 43, no. 15, pp. 3751–3758, 2009.

[158] B. Van Der Bruggen, G. Cornelis, C. Vandecasteele, and I. Devreese, “Fouling of nanofiltration and ultrafiltration membranes applied for wastewater regeneration in the textile industry,” *Desalination*, vol. 175, no. 1, pp. 111–119, May 2005.

[159] M. M. M. Nederlof, J. A. M. A. M. van Paassen, and R. Jong, “Nanofiltration concentrate disposal: experiences in The Netherlands,” *Desalination*, vol. 178, no. 1–3, pp. 303–312, Jul. 2005.

[160] M. Carballa *et al.*, “Behavior of pharmaceuticals, cosmetics and hormones in a sewage treatment plant.,” *Water Res.*, vol. 38, no. 12, pp. 2918–26, Jul. 2004.

[161] M. Clara, B. Strenn, O. Gans, E. Martinez, N. Kreuzinger, and H. Kroiss, “Removal of selected pharmaceuticals, fragrances and endocrine disrupting compounds in a membrane bioreactor and conventional wastewater treatment plants.,” *Water Res.*, vol. 39, no. 19, pp. 4797–807, Nov. 2005.

[162] A. Joss *et al.*, “Removal of pharmaceuticals and fragrances in biological wastewater treatment,” *Water Res.*, vol. 39, no. 14, pp. 3139–52, Sep. 2005.

[163] J. Sipma *et al.*, “Comparison of removal of pharmaceuticals in MBR and activated sludge systems,” *Desalination*, vol. 250, no. 2, pp. 653–659, Jan. 2010.

[164] S. Zorita, L. Mårtensson, and L. Mathiasson, “Occurrence and removal of pharmaceuticals in a municipal sewage treatment system in the south of Sweden.,” *Sci. Total Environ.*, vol. 407, no. 8, pp. 2760–70, Apr. 2009.

[165] F. Yuan, C. Hu, X. Hu, J. Qu, and M. Yang, “Degradation of selected

pharmaceuticals in aqueous solution with UV and UV/H(2)O(2).," *Water Res.*, vol. 43, no. 6, pp. 1766–74, Apr. 2009.

[166] C. Baresel, M. Ek, M. Harding, and R. Bergström, "Behandling av biologiskt renat avloppsvatten med ozon eller aktivt kol," IVL Swedish Environmental Research Institute, Stockholm, B 2203, 2014.

[167] Y. Yoon, P. Westerhoff, S. a. Snyder, E. C. Wert, and J. Yoon, "Removal of endocrine disrupting compounds and pharmaceuticals by nanofiltration and ultrafiltration membranes," *Desalination*, vol. 202, no. 1–3, pp. 16–23, Jan. 2007.

[168] X. Jin, J. Shan, C. Wang, J. Wei, and C. Y. Tang, "Rejection of pharmaceuticals by forward osmosis membranes.," *J. Hazard. Mater.*, vol. 227–228, no. 2012, pp. 55–61, Aug. 2012.

[169] L. Martínez and F. J. Florido-Díaz, "Theoretical and experimental studies on desalination using membrane distillation," *Desalination*, vol. 139, no. 1–3, pp. 373–379, Sep. 2001.

[170] A. Kullab and A. Martin, "Membrane Distillation and Applications for Water Purification in Thermal Cogeneration – Pilot Plant Trials," Värmeforsk, Stockholm, Dec. 2007.

[171] K. Byman, "Energy future of the Stockholm region 2010-2050," Stockholm County Council, Stockholm, 2010.

[172] Stockholmdataparks.com, "A Brief Introduction to District Heating and District Cooling," 2017. [Online]. Available: https://stockholmdataparks.com/wp-content/uploads/a-brief-introduction-to-district-heating-and-district-cooling_jan-2017.pdf. [Accessed: 17-Apr-2017].

[173] R. Guedes-Alonso, C. Afonso-Olivares, S. Montesdeoca-Esponda, Z. Sosa-Ferrera, and J. J. Santana-Rodríguez, "An assessment of the concentrations of pharmaceutical compounds in wastewater treatment plants on the island of Gran Canaria (Spain).," *Springerplus*, vol. 2, no. 1, p. 24, 2013.

[174] C. Gadipelly *et al.*, "Pharmaceutical Industry Wastewater: Review of the Technologies for Water Treatment and Reuse," *Ind. Eng. Chem. Res.*, vol. 53, no. 29, pp. 11571–11592, Jul. 2014.

[175] S. Daouk, N. Chèvre, N. Vernaz, C. Widmer, Y. Daali, and S. Fleury-Souverain, "Dynamics of active pharmaceutical ingredients loads in a Swiss university hospital wastewaters and prediction of the related environmental risk for the aquatic ecosystems," *Sci. Total Environ.*, vol. 547, pp. 244–253, 2016.

[176] P. Houeto *et al.*, "Assessment of the health risks related to the presence of drug residues in water for human consumption: Application to carbamazepine," *Regul. Toxicol. Pharmacol.*, vol. 62, no. 1, pp. 41–48, Feb. 2012.

[177] B. S. Oh *et al.*, "Effect of ozone on microfiltration as a pretreatment of seawater reverse osmosis," *Desalination*, vol. 238, no. 1–3, pp. 90–97, 2009.

[178] G. R. Pophali, S. Hedau, N. Gedam, N. N. N. Rao, and T. Nandy, "Treatment of refractory organics from membrane rejects using ozonation," *J. Hazard. Mater.*, vol. 189, no. 1–2, pp. 273–277, May 2011.

[179] L. A. Ioannou *et al.*, "Winery wastewater purification by reverse osmosis and oxidation of the concentrate by solar photo-Fenton," *Sep. Purif. Technol.*, vol. 118, pp. 659–669, 2013.

[180] C. Sheng, A. G. A. Nnanna, Y. Liu, and J. D. Vargo, "Removal of Trace Pharmaceuticals from Water using coagulation and powdered activated carbon as pretreatment to ultrafiltration membrane system," *Sci. Total Environ.*, vol. 550, pp. 1075–1083, 2016.

[181] Z. Yu, S. Peldszus, and P. M. Huck, "Adsorption characteristics of selected pharmaceuticals and an endocrine disrupting compound-Naproxen, carbamazepine and nonylphenol-on activated carbon," *Water Res.*, vol. 42, no. 12, pp. 2873–2882, 2008.

[182] "Analytical data obtained from AstraZeneca pharmaceutical WWTP Gärtuna, Södertalje," 2015.

[183] European Commission, "Proposal for a Directive of the European Parliament and of the Council on the promotion of the use of energy from renewable sources," Brussels, COM(2016) 767 final, 2016.

[184] European Parliament, "Directive 2009/28/EC of the European Parliament and of the Council of 23 April 2009," *Off. J. Eur. Union*, vol. 140, pp. 16–62, 2009.

[185] AFDS, “Global ethanol production,” 2016. [Online]. Available: http://www.afdc.energy.gov/data/10331. [Accessed: 15-May-2016].

[186] M. Balat, H. Balat, and C. Öz, “Progress in bioethanol processing,” *Prog. Energy Combust. Sci.*, vol. 34, no. 5, pp. 551–573, Oct. 2008.

[187] A. Demirbas, *Biohydrogen*, vol. 53, no. 9. London: Springer-Verlag London, 2009.

[188] J. D. Murphy and K. McCarthy, “Ethanol production from energy crops and wastes for use as a transport fuel in Ireland,” *Appl. Energy*, vol. 82, no. 2, pp. 148–166, Oct. 2005.

[189] B. Benjaminsson, J., Goldschmidt and R. Uddgren, “Optimal integrering av energianvändningen vid energikombinatet i Norrköping,” Värmeforsk AB, Rapport 1149, 2010.

[190] R. Fornell, “Technical description of the Biorefinery Demonstration plant in Örnsköldsvik,” *SP Technical Research Institute of Sweden*, 2012. [Online]. Available: https://www.sp.se/sv/index/services/biorefinerydemoplant/Documents/Teknisk beskrivning.pdf. [Accessed: 03-Mar-2017].

[191] J. Gregg *et al.*, “Value Chain Structures that Define European Cellulosic Ethanol Production,” *Sustainability*, vol. 9, no. 1, p. 118, Jan. 2017.

[192] St1biofuels, “Creating New Business from Waste-Based Advanced Ethanol,” *Whitepaper*. [Online]. Available: http://www.st1biofuels.com/. [Accessed: 17-Mar-2017].

[193] F. A. Banat and M. Al-Shannag, “Recovery of dilute acetone–butanol–ethanol (ABE) solvents from aqueous solutions via membrane distillation,” *Bioprocess Eng.*, vol. 23, no. 6, pp. 643–649, Dec. 2000.

[194] M. Gryta, “The fermentation process integrated with membrane distillation,” *Sep. Purif. Technol.*, vol. 24, no. 1–2, pp. 283–296, Jun. 2001.

[195] P. Paulsson, “Energy analysis of ethanol production; A case study of Lantmännen Agroetanol’s production system in Norrköping,” M.S. thesis, Department of Biometry and Engineering, Sveriges lantbruksuniversitet, SLU, Uppsala, Sweden, 2007.

[196] "Normalprislista fjärrvärme företag," 2016. [Online]. Available: https://www.eon.se/content/dam/eon-se/swe-documents/swe-norrkoping-soderkoping-prislista-2016.pdf. [Accessed: 25-Jan-2016].

[197] D. J. O'Brien, L. H. Roth, and A. J. McAloon, "Ethanol production by continuous fermentation–pervaporation: a preliminary economic analysis," *J. Memb. Sci.*, vol. 166, no. 1, pp. 105–111, Feb. 2000.

[198] G. Tsatsaronis, "Thermoeconomic analysis and optimization of energy systems," *Prog. Energy Combust. Sci.*, vol. 19, no. 3, pp. 227–257, Jan. 1993.

[199] F. Banat and N. Jwaied, "Exergy analysis of desalination by solar-powered membrane distillation units," *Desalination*, vol. 230, no. 1–3, pp. 27–40, Sep. 2008.

[200] E. Querol, B. Gonzalez-Regueral, and J. L. Perez-Benedito, *Practical Approach to Exergy and Thermoeconomic Analyses of Industrial Processes*. London: Springer, 2013.

[201] Y. Cerci, "Exergy analysis of a reverse osmosis desalination plant in California," *Desalination*, vol. 142, no. 3, pp. 257–266, Mar. 2002.

[202] M. Ameri and M. S. Eshaghi, "A novel configuration of reverse osmosis, humidification–dehumidification and flat plate collector: Modeling and exergy analysis," *Appl. Therm. Eng.*, vol. 103, pp. 855–873, Jun. 2016.

[203] R. S. El-Emam, I. Dincer, R. Salah El-Emam, I. Dincer, R. S. El-Emam, and I. Dincer, "Thermodynamic and thermoeconomic analyses of seawater reverse osmosis desalination plant with energy recovery," *Energy*, vol. 64, pp. 154–163, Jan. 2014.

[204] E. Drioli, E. Curcio, G. Di Profio, F. Macedonio, and A. Criscuoli, "Integrating Membrane Contactors Technology and Pressure-Driven Membrane Operations for Seawater Desalination," *Chem. Eng. Res. Des.*, vol. 84, no. 3, pp. 209–220, Mar. 2006.

Appendices

Table A. 1 Log Kow and concentrations (ng/L) of pharmaceuticals from Trial-1

Substance:	*Log Kow*	*Feed*	*Permeate*			
			Modul 1a, 74°C	*Modul 1a, 52°C*	*Modul 1b, 73°C*	*Modul 1b, 54°C*
Amlodipine	3.00	38	*<8	<8	<8	<8
Atenolol	0.10	136	<1	<1	<1	<1
Bisoprolol	4.00	25	<3	<3	<3	<3
Caffeine	-0.13	<80	<3	<3	<3	<3
Carbamazepine	2.67	190	<1	<1	<1	<1
Ciprofloxacin	0.28	16	<10	<10	<10	<10
Citalopram	3.20	115	<2	<2	<2	<2
Diclofenac	4.06	336	<3	<3	<3	<3
Doxycycline	0.00	<70	<40	<40	<40	<40
Enalapril	2.43	<16	<7	<7	<7	<7
Estradiol	4.13	<100	<30	<30	<30	<30
Estriol	2.50	<80	<10	<10	<10	<10
Estrone	3.10	<75	<10	<10	<10	<10
Ethinylestradiol	4.52	<100	<28	<28	<28	<28
Finasteride	3.00	<10	<3	<3	<3	<3
Furosemide	3.00	592	<5	<5	<5	<5
Hydrochlorothiazide	-0.07	860	<7	<7	<7	<7
Ibuprofen	3.72	63	<3	<3	<3	<3
Ketoconazole	4.35	<25	<10	<10	<10	<10
Ketoprofen	2.81	53	<4	<4	<4	<4
Metoprolol	1.79	761	<1	<1	<1	<1
Naproxen	3.00	42	<5	<5	<5	<5
Norethindrone	3.38	<80	<10	<10	<10	<10
Norfloxacin	-1.00	<50	<20	<20	<20	<20
Oxazepam	2.31	187	<2	<2	<2	<2
Paracetamol	0.34	20	<8	<8	<8	<8
Progesterone	4.04	<60	<15	<15	<15	<15
Propranolol	3.10	50	<2	<2	<2	<2
Ramipril	1.40	<15	<5	<5	<5	<5
Ranitidine	1.23	46	<5	<5	<5	<5
Sertraline	5.70	3.7	2,4	<0.8	0.9	<0.8
Simvastatin	4.70	<20	<20	<20	<20	<20
Sulfamethoxazole	0.90	95	<5	<5	<5	<5
Terbutaline	0.48	<20	<10	<10	<10	<10
Tetracycline	-1.50	<30	<10	<10	<10	<10
Trimetoprim	0.90	15	<3	<3	<3	<3
Warfarin	2.70	12.8	<2	<2	<2	<2

*Less than (<) means below detection limit

Table A. 2. Concentrations (ng/L) of pharmaceuticals from Trial-2

Substance:	*Feed*	*Permeate from module*			
		5a, 57°C	*5a, 73°C*	*5b, 58°C*	*5b, 74°C*
Amlodipine	24	<8	<8	<8	<8
Atenolol	147	<1	<1	<1	<1
Bisoprolol	35	<3	<3	<3	<3
Caffeine	<71	<3	<3	<3	<3
Carbamazepine	256	<1	<1	<1	<1
Ciprofloxacin	22	<10	<10	<10	<10
Citalopram	146	<2	<2	<2	<2
Diclofenac	441	<3	<3	<3	<3
Doxycycline	<138	<40	<40	<40	<40
Enalapril	<15	<7	<7	<7	<7
Estradiol	<100	<30	<30	<30	<30
Estriol	<57	<10	<10	<10	<10
Estrone	<50	<10	<10	<10	<10
Ethinylestradiol	<100	<25	<25	<25	<25
Finasteride	<9	<3	<3	<3	<3
Furosemide	613	<5	<5	<5	<5
Hydrochlorothiazide	1155	<3	<3	<3	<3
Ibuprofen	58	<3	<3	<3	<3
Ketoconazole	<28	<10	<10	<10	<10
Ketoprofen	101	<4	<4	<4	<4
Metoprolol	963	<1	<1	<1	<1
Naproxen	76	<5	<5	<5	<5
Norethindrone	<70	<10	<10	<10	<10
Norfloxacin	<50	<20	<20	<20	<20
Oxazepam	282	<2	<2	<2	<2
Paracetamol	22	<8	<8	<8	<8
Progesterone	<63	<15	<15	<15	<15
Propranolol	53	<2	<2	<2	<2
Ramipril	<10	<6	<6	<6	<6
Ranitidine	88	<5	<5	<5	<5
Sertraline	<11	2.1	4.6	1.1	2.7
Simvastatin	<20	<20	<20	<20	<20
Sulfamethoxazole	91	<7	<7	<7	<7
Terbutaline	13	<10	<10	<10	<10
Tetracycline	<31	<10	<10	<10	<10
Trimetoprim	31	<3	<3	<3	<3
Warfarin	12	<2	<2	<2	<2

Table A. 3. Concentrations (ng/L) of pharmaceuticals from Trial-3

Substance:	*Feed*			*Permeate from module*			
	initial	*at half volume*	*at end*	*at start 4a*	*at half 4a*	*at end 4a*	*at end 5a*
Amlodipine	<15	<15	<15	<3	<3	<3	<3
Atenolol	515	740	2540	<2	<2	<2	<2
Bisoprolol	114	152	405	<2	<2	<2	<2
Caffeine	190	424	1413	<7	<7	<7	<7
Carbamazepine	562	702	1644	<1	<1	<1	<1
Ciprofloxacin	73	121	633	<8	<8	<8	<8
Citalopram	439	513	692	<1	1.7	3.2	2.1
Diclofenac	481	496	795	<3	<3	<3	<3
Doxycycline	<98	<98	<98	<21	<21	<21	<21
Enalapril	<7	<7	<7	<2	<2	<2	<2
Estradiol	<100	<100	<100	<21	<21	<21	<21
Estriol	<62	<62	<62	<15	<15	<15	<15
Estrone	<50	<50	<50	<10	<10	<10	<10
Ethinylestradiol	<100	<100	<100	<18	<18	<18	<18
Finasteride	<8	<8	<8	<1	<1	<1	<1
Furosemide	966	780	1683	<6	<6	<6	<6
Hydrochlorothiazide	612	124	115	<2	<2	<2	<2
Ibuprofen	112	130	52	<2	<2	<2	<2
Ketoconazole	<30	<30	<30	<10	<10	<10	<10
Ketoprofen	68	29	136	<4	<4	<4	<4
Metoprolol	3403	4861	13787	<1	1.4	4.4	2.4
Naproxen	66	50	82	<3	<3	<3	<3
Norethindrone	<75	<75	<75	<8	<8	<8	<8
Norfloxacin	<50	<50	<50	<8	<8	<8	<8
Oxazepam	124	56	75	<1	<1	<1	<1
Paracetamol	66	77	218	<3	<3	<3	<3
Progesterone	<58	<58	<58	<10	<10	<10	<10
Propranolol	174	198	374	<2	<2	<2	<2
Ramipril	<10	<10	<10	<5	<5	<5	<5
Ranitidine	286	260	1405	<6	<6	<6	<6
Sertraline	8.7	<7	<7	<3	<3	<3	<3
Simvastatin	<25	<25	<25	<20	<20	<20	<20
Sulfamethoxazole	164	185	284	<1	<1	<1	<1
Terbutaline	15	<10	<10	<5	<5	<5	<5
Tetracycline	33	<25	<25	<7	<7	<7	<7
Trimetoprim	137	201	648	<2	<2	<2	<2
Warfarin	<2	<2	<2	<2	<2	<2	<2

Table A. 4. Concentrations (ng/L) of pharmaceuticals from Trial-4 (Initial)

Substans:	Feed	Permeate from module								
		1a	1b	2a	2b	3a	3b	4a	4b	5a
Amlodipine	<200	<100	<100	<100	<100	<100	<100	<100	<100	<100
Atenolol	189	<10	<10	<10	<10	<10	<10	<10	<10	<10
Bisoprolol	<50	<10	<10	<10	<10	<10	<10	<10	<10	<10
Caffeine	119	<20	<20	<20	<20	<20	<20	<20	<20	<20
Carbamazepine	299	<15	<15	<15	<15	<15	<15	<15	<15	<15
Ciprofloxacin	158	<25	<25	<25	<25	<25	<25	<25	<25	<25
Citalopram	292	<3	<3	<3	<3	<3	<3	<3	<3	<3
Diclofenac	271	<25	<25	<25	<25	<25	<25	<25	<25	<25
Doxycycline	<120	<75	<75	<75	<75	<75	<75	<75	<75	<75
Enalapril	<50	<50	<50	<50	<50	<50	<50	<50	<50	<50
Estradiol	<200	<100	<100	<100	<100	<100	<100	<100	<100	<100
Estriol	<150	<100	<100	<100	<100	<100	<100	<100	<100	<100
Estrone	<150	<50	<50	<50	<50	<50	<50	<50	<50	<50
Ethinylestradiol	<200	<200	<200	<200	<200	<200	<200	<200	<200	<200
Finasteride	<40	<20	<20	<20	<20	<20	<20	<20	<20	<20
Furosemide	1040	<100	<100	<100	<100	<100	<100	<100	<100	<100
Hydrochlorothiazide	559	<25	<25	<25	<25	<25	<25	<25	<25	<25
Ibuprofen	115	<40	<40	<40	<40	<40	<40	<40	<40	<40
Ketoconazole	172	<20	<20	<20	<20	<20	<20	<20	<20	<20
Ketoprofen	96	<20	<20	<20	<20	<20	<20	<20	<20	<20
Metoprolol	1330	<5	<5	<5	<5	<5	<5	<5	<5	<5
Naproxen	133	<80	<80	<80	<80	<80	<80	<80	<80	<80
Norethindrone	<150	<50	<50	<50	<50	<50	<50	<50	<50	<50
Norfloxacin	118	<25	<25	<25	<25	<25	<25	<25	<25	<25
Oxazepam	283	<5	<5	<5	<5	<5	<5	<5	<5	<5
Paracetamol	57	<25	<25	<25	<25	<25	<25	<25	<25	<25
Progesterone	<300	<100	<100	<100	<100	<100	<100	<100	<100	<100
Propranolol	95	<3	<3	<3	<3	<3	<3	<3	<3	<3
Ramipril	<100	<50	<50	<50	<50	<50	<50	<50	<50	<50
Ranitidine	490	<10	<10	<10	<10	<10	<10	<10	<10	<10
Sertraline	43	1.7	2.4	1.4	<1	2.9	2.7	4.2	9.3	7.8
Simvastatin	<100	<50	<50	<50	<50	<50	<50	<50	<50	<50
Sulfamethoxazole	<50	<15	<15	<15	<15	<15	<15	<15	<15	<15
Terbutaline	<30	<25	<25	<25	<25	<25	<25	<25	<25	<25
Tetracycline	<50	<25	<25	<25	<25	<25	<25	<25	<25	<25
Trimetoprim	73	<10	<10	<10	<10	<10	<10	<10	<10	<10
Warfarin	<10	<4	<4	<4	<4	<4	<4	<4	<4	<4

Table A. 5. Concentrations (ng/L) of pharmaceuticals from Trial-4 (step-1)

Substance:	Feed	Permeate from module:									
		1a	1b	2a	2b	3a	3b	4a	4b	5a	5b
Amlodipine	<200	<100	<100	<100	<100	<100	<100	<100	<100	<100	<100
Atenolol	329	<10	<10	<10	<10	<10	<10	<10	<10	<10	<10
Bisoprolol	69	<10	<10	<10	<10	<10	<10	<10	<10	<10	<10
Caffeine	262	25	<20	<20	<20	<20	<20	127	<20	<20	<20
Carbamazepine	512	<15	<15	<15	<15	<15	<15	<15	<15	<15	<15
Ciprofloxacin	335	<25	<25	<25	<25	<25	<25	<25	<25	<25	<25
Citalopram	202	<3	<3	<3	<3	<3	<3	<3	<3	<3	<3
Diclofenac	426	<25	<25	<25	<25	<25	<25	<25	<25	<25	<25
Doxycycline	<120	<75	<75	<75	<75	<75	<75	<75	<75	<75	<75
Enalapril	<50	<50	<50	<50	<50	<50	<50	<50	<50	<50	<50
Estradiol	<200	<100	<100	<100	<100	<100	<100	<100	<100	<100	<100
Estriol	<150	<100	<100	<100	<100	<100	<100	<100	<100	<100	<100
Estrone	<150	<50	<50	<50	<50	<50	<50	<50	<50	<50	<50
Ethinylestradiol	<200	<200	<200	<200	<200	<200	<200	<200	<200	<200	<200
Finasteride	<40	<20	<20	<20	<20	<20	<20	<20	<20	<20	<20
Furosemide	1450	<100	<100	<100	<100	<100	<100	<100	<100	<100	<100
Hydrochlorothiazide	461	<25	<25	<25	<25	<25	<25	<25	<25	<25	<25
Ibuprofen	196	<40	<40	<40	<40	<40	<40	<40	<40	<40	<40
Ketoconazole	98	<20	<20	<20	<20	<20	<20	<20	<20	<20	<20
Ketoprofen	137	<20	<20	<20	<20	<20	<20	<20	<20	<20	<20
Metoprolol	2280	<5	<5	<5	<5	<5	<5	<5	<5	<5	<5
Naproxen	148	<80	<80	<80	<80	<80	<80	<80	<80	<80	<80
Norethindrone	<150	<50	<50	<50	<50	<50	<50	<50	<50	<50	<50
Norfloxacin	309	<25	<25	<25	<25	<25	<25	<25	<25	<25	<25
Oxazepam	356	<5	<5	<5	<5	<5	<5	<5	<5	<5	<5
Paracetamol	81	<25	<25	<25	<25	<25	<25	<25	<25	<25	<25
Progesterone	<300	<100	<100	<100	<100	<100	<100	<100	<100	<100	<100
Propranolol	137	<3	<3	<3	<3	<3	<3	<3	<3	<3	<3
Ramipril	<100	<50	<50	<50	<50	<50	<50	<50	<50	<50	<50
Ranitidine	825	<10	<10	<10	<10	<10	<10	<10	<10	<10	<10
Sertraline	13	<1	<1	<1	<1	1.2	<1	<1	<1	<1	<1
Simvastatin	<100	<50	<50	<50	<50	<50	<50	<50	<50	<50	<50
Sulfamethoxazole	131	<15	<15	<15	<15	<15	<15	<15	<15	<15	<15
Terbutaline	<30	<25	<25	<25	<25	<25	<25	<25	<25	<25	<25
Tetracycline	<50	<25	<25	<25	<25	<25	<25	<25	<25	<25	<25
Trimetoprim	131	<10	<10	<10	<10	<10	<10	<10	<10	<10	<10
Warfarin	<10	<4	<4	<4	<4	<4	<4	<4	<4	<4	<4

Table A. 6. Concentrations (ng/L) of pharmaceuticals from Trial-4 (step-2)

Substance:	Tank	1a	1b	2a	2b	3a	3b	4a	4b	5a	5b
Amlodipine	<200	<100	<100	<100	<100	<100	<100	<100	<100	<100	<100
Atenolol	1300	<10	<10	<10	<10	<10	<10	<10	<10	<10	<10
Bisoprolol	200	<10	<10	<10	<10	<10	<10	<10	<10	<10	<10
Caffeine	640	<20	<20	<20	<20	<20	<20	<20	<20	<20	<20
Carbamazepine	1600	<15	<15	<15	<15	<15	<15	<15	<15	<15	<15
Ciprofloxacin	2000	<25	<25	<25	<25	<25	<25	<25	<25	<25	<25
Citalopram	700	<3	<3	<3	<3	<3	<3	<3	<3	<3	<3
Diclofenac	1100	<25	<25	<25	<25	<25	<25	<25	<25	<25	<25
Doxycycline	<120	<75	<75	<75	<75	<75	<75	<75	<75	<75	<75
Enalapril	<50	<50	<50	<50	<50	<50	<50	<50	<50	<50	<50
Estradiol	1600	<100	<100	<100	<100	<100	<100	<100	<100	<100	<100
Estriol	280	<100	<100	<100	<100	<100	<100	<100	<100	<100	<100
Estrone	<150	<50	<50	<50	<50	<50	<50	<50	<50	<50	<50
Ethinylestradiol	770	<200	<200	<200	<200	<200	<200	<200	<200	<200	<200
Finasteride	<40	<20	<20	<20	<20	<20	<20	<20	<20	<20	<20
Furosemide	5100	<100	<100	<100	<100	<100	<100	<100	<100	<100	<100
Hydrochlorothiazide	1200	<25	<25	<25	<25	<25	<25	<25	<25	<25	<25
Ibuprofen	480	<40	<40	<40	<40	<40	<40	<40	<40	<40	<40
Ketoconazole	<50	<20	<20	<20	<20	<20	<20	<20	<20	<20	<20
Ketoprofen	290	<20	<20	<20	<20	<20	<20	<20	<20	<20	<20
Metoprolol	7200	<5	<5	<5	<5	<5	<5	<5	<5	<5	<5
Naproxen	190	<80	<80	<80	<80	<80	<80	<80	<80	<80	<80
Norethindrone	<150	<50	<50	<50	<50	<50	<50	<50	<50	<50	<50
Norfloxacin	530	<25	<25	<25	<25	<25	<25	<25	<25	<25	<25
Oxazepam	870	<5	<5	<5	<5	<5	<5	<5	<5	<5	<5
Paracetamol	320	<25	<25	<25	<25	<25	<25	<25	<25	<25	<25
Progesterone	<300	<100	<100	<100	<100	<100	<100	<100	<100	<100	<100
Propranolol	340	<3	<3	<3	<3	<3	<3	<3	<3	<3	<3
Ramipril	<100	<50	<50	<50	<50	<50	<50	<50	<50	<50	<50
Ranitidine	2500	<10	<10	<10	<10	<10	<10	<10	<10	<10	<10
Sertraline	4.3	5.9	4.2	5.2	6.3	7.3	3.4	6.7	4.5	6.5	3.2
Simvastatin	<100	<50	<50	<50	<50	<50	<50	<50	<50	<50	<50
Sulfamethoxazole	360	<15	<15	<15	<15	<15	<15	<15	<15	<15	<15
Terbutaline	<30	<25	<25	<25	<25	<25	<25	<25	<25	<25	<25
Tetracycline	84	<25	<25	<25	<25	<25	<25	<25	<25	<25	<25
Trimetoprim	330	<10	<10	<10	<10	<10	<10	<10	<10	<10	<10
Warfarin	21	<4	<4	<4	<4	<4	<4	<4	<4	<4	<4

Table A. 7. Concentrations (ng/L) of pharmaceuticals from Trial-4 (step-3)

		Permeate									
Substance:	*Feed*	*1a*	*1b*	*2a*	*2b*	*3a*	*3b*	*4a*	*4b*	*5a*	*5b*
Amlodipine	<200	<100	<100	<100	<100	<100	<100	<100	<100	<100	<100
Atenolol	3600	<10	<10	<10	<10	<10	<10	<10	<10	<10	<10
Bisoprolol	550	<10	<10	<10	<10	<10	<10	<10	<10	<10	<10
Caffeine	1500	<20	<20	<20	<20	<20	<20	<20	<20	<20	<20
Carbamazepine	4300	<15	<15	<15	<15	<15	<15	<15	<15	<15	<15
Ciprofloxacin	3800	<25	<25	<25	<25	<25	<25	<25	<25	<25	<25
Citalopram	1400	<3	<3	<3	<3	<3	<3	<3	<3	<3	<3
Diclofenac	2600	<25	<25	<25	<25	<25	<25	<25	<25	<25	<25
Doxycycline	<120	<75	<75	<75	<75	<75	<75	<75	<75	<75	<75
Enalapril	<50	<50	<50	<50	<50	<50	<50	<50	<50	<50	<50
Estradiol	5500	<100	<100	<100	<100	<100	<100	<100	<100	<100	<100
Estriol	510	<100	<100	<100	<100	<100	<100	<100	<100	<100	<100
Estrone	<150	<50	<50	<50	<50	<50	<50	<50	<50	<50	<50
Ethinylestradiol	2000	<200	<200	<200	<200	<200	<200	<200	<200	<200	<200
Finasteride	<40	<20	<20	<20	<20	<20	<20	<20	<20	<20	<20
Furosemide	10000	<100	<100	<100	<100	<100	<100	<100	<100	<100	<100
Hydrochlorothiazide	3200	<25	<25	<25	<25	<25	<25	<25	<25	<25	<25
Ibuprofen	980	<40	<40	<40	<40	<40	<40	<40	<40	<40	<40
Ketoconazole	99	<20	<20	<20	<20	<20	<20	<20	<20	<20	<20
Ketoprofen	790	<20	<20	<20	<20	<20	<20	<20	<20	<20	<20
Metoprolol	20000	<5	<5	<5	<5	<5	<5	<5	<5	<5	<5
Naproxen	210	<80	<80	<80	<80	<80	<80	<80	<80	<80	<80
Norethindrone	<150	<50	<50	<50	<50	<50	<50	<50	<50	<50	<50
Norfloxacin	1200	<25	<25	<25	<25	<25	<25	<25	<25	<25	<25
Oxazepam	2300	<5	<5	<5	<5	<5	<5	<5	<5	<5	<5
Paracetamol	1400	<25	<25	<25	<25	<25	<25	<25	<25	<25	<25
Progesterone	<300	<100	<100	<100	<100	<100	<100	<100	<100	<100	<100
Propranolol	810	<3	<3	<3	<3	<3	<3	<3	<3	<3	<3
Ramipril	<100	<50	<50	<50	<50	<50	<50	<50	<50	<50	<50
Ranitidine	7200	<10	<10	<10	<10	<10	<10	<10	<10	<10	<10
Sertraline	10	5.9	5.4	5.7	8.7	9.4	5.6	7.6	5.6	6.7	6.6
Simvastatin	<100	<50	<50	<50	<50	<50	<50	<50	<50	<50	<50
Sulfamethoxazole	840	<15	<15	<15	<15	<15	<15	<15	<15	<15	<15
Terbutaline	99	<25	<25	<25	<25	<25	<25	<25	<25	<25	<25
Tetracycline	180	<25	<25	<25	<25	<25	<25	<25	<25	<25	<25
Trimetoprim	770	<10	<10	<10	<10	<10	<10	<10	<10	<10	<10
Warfarin	49	<4	<4	<4	<4	<4	<4	<4	<4	<4	<4